University of Alberta

Abrasive Wear Assessment of X-70 Steel and Polyurethane Coupons on a Modified Dry/Sand Rubber Wheel Apparatus

by
Victor Jaimes

A thesis submitted to the Faculty of Graduate Studies and Research
in partial fulfillment of the requirements for the degree of

Master of Science
In
Engineering Management

Department of Mechanical Engineering

Fall 2013
Edmonton, Alberta

Abstract

An experimental study was conducted to assess the scratching abrasion in dry and wet environments on X-70 steel and five different types of titanium carbide particulate polyurethane composites (PU). A testing apparatus was constructed based on the dry sand rubber wheel test method standardized by the American Society of Testing and Materials (ASTM). The major focus of attention was given to wet abrasion testing of these materials with either a rubber wheel or a steel wheel. The influence in wear behavior of PU due to their moisture content and steel wheel roughness was also addressed. In addition, wet abrasion experiments under low dissolved oxygen conditions were conducted on X-70 steel to isolate erosion effects under wet conditions. Wear mechanisms in the materials under study were assessed through scanning electron microscopy analysis. In general, wear mechanisms such as cracking, pluck-out and indentations were observed with more or less severity.

Acknowledgements

This research was possible thanks to the guidance and support from beginning to end of my supervisor Dr. Michael Lipsett from Mechanical Engineering, and Dr. John Wolodko from Alberta Innovates Technology Futures. Their continuous feedback and support was of great importance. John gave me the opportunity to work in the field of abrasion testing with a modified apparatus, this was a key for the development of this research. To both of my supervisors my sincere gratitude. I also want to thank Dr. Gary Fisher and Hoa Dang from Alberta Innovates Technology Futures. Their input contributed significantly with this research work.

Family and friends also played a remarkable role during the development of this research. I extend my gratitude to my girlfriend Anna Marie Cruz, for her sacrifices and continuous inspiration. She always gave me strength to continue with my research work. My sincere gratitude goes also to my mother and sister, Ana Diaz and Sherlyne Jaimes, who always from the distance supported and guided me all this time. Significant gratitude is given to my friends and colleagues from mechanical engineering, specially: Jason Luk and Ahmed Fotouh. My friends in Edmonton: Edwin Zerpa, Manuel Diaz, Roberto Cuadros and Daniel Petrash, your friendship and ongoing support was very important to me.

Table of Contents

List of Tables

List of Figures

Nomenclature

β	Angle between bed layer and bulk fluid (radians)
ρf	Density of the fluid (kg/m^3)
ρl	Density of liquid (kg/m^3)
ρs	Density of solid particles (kg/m^3)
ρm	Density of the slurry (kg/m^3)
C_D	Drag coefficient of particles (dimensionless)
C_l	Concentration of slurry bed (%)
C_u	Concentration of the bulk (%)
C_v	Volume fraction of solids (%)
C_w	Volume fraction of water
d	Particle size (mm)
D	Pipeline inner diameter (mm)
Ew	Erosion rate (mm/year)
FL	Froude number (dimensionless)
f	Darcy-Weisbach friction factor for water (dimensionless)
g	Gravity acceleration (m/s^2)
H	Hardness of a surface (Mohs' scale)
h	Head (m of water)
i	Friction loss in the pipeline (m of water)
i_w	Friction loss for water (m of water)
k	Wear coefficient (dimensionless)
$n\rho$	Pump efficiency (%)
η_s	Sliding friction coefficient (dimensionless)
P	Pressure gradient (Pa/m)
Pw	Pump power (Kw)
Q	Flow rate (m^3/s)
Re	Reynolds number (dimensionless)
S	Specific gravity of solid particles (dimensionless)
Sm	Geometry factor for pipelines (dimensionless)
τ	Shear stress due to contact of particles (units of force per area)
T_0	Threshold of wall damage (dimensionless)
Vm	Mixture (slurry) velocity (m/s)
W	Normal load (N)

Chapter 1

1. Introduction

This research work presents a testing methodology for assessing dry and wet abrasion on a defined set of materials. The introductory chapter describes the background and motivation for conducting more iterative wear abrasive testing on service materials. Research objectives and limitations are described, and an overview of the remaining chapters in this work is also provided.

1.1. Background and Motivation

Slurry transport of materials is a very common method used in different types of industries (Schaan and Sanders 2007). For example, in oil sands mining operations in Alberta, extensive pipeline systems are used to transport ore-water mixtures prior to extraction (hydro transport), and for tailings slurry transport. Hydro transport slurry comprises bitumen mixture, sharp silica sand solids (with diameters between 50 to 100 microns or more), clay, silt, and water; and tailings is a similar slurry with almost all of the bitumen removed (Wilson et al. 2006). Crushed rock may also be present. These slurries have an average density of approximately 1500 to 1600 kg/m^3, and travel at average velocities between 4 to 7 m/s. Severe wear conditions arise in these pipelines due to velocity, concentration and nature of sand particles. Wear is of great concern for reliability and

maintenance; and wear has been the subject of significant effort in maintenance improvement, and research into material selection for slurry service. There is now some understanding of the relationship between process variables and damage accumulation, such as: particle size, solids concentration, flow rate (and its variation across the pipe), and material properties of the pipe such as hardness. This relationship is qualitative, because there is yet no accurate model or absolute testing methods to predict abrasive wear rates in a given type of service (El Sayed and Lipsett 2009).

Taking in consideration the great presence of slurry pipeline systems in the Alberta oil sands within the four operating plants in the Athabasca region (Syncrude, Suncor, Shell and CNRL), which produce approximately 3.5 million cubic meters of bitumen per year. A slurry flow associated to these production levels reaches 1/2 million tonnes daily (Sanders 2004). According to these figures; there is a considerable economic impact in operations due to frequent failures of critical components and plant downtime. As such, there is a need of more wear resistant materials for the handling and transporting slurries for mining and processing operations. Due to the importance of slurry transport (either in hydro transport or in tailings lines), the industry has monitored pipeline performance and begun to invest in research related to wear rate assessment over the past number of years (Sanders 2004).

The impact on bitumen production operations is of great significance when failures occur during slurry transport along extensive sections of steel pipelines (Sanders 2004). The main concern is centered on when to conduct maintenance activities on these pipelines. Pipeline sections are rotated so that partially worn sections of the pipe circumference are moved away from regions of high wear. Timing for rotations is based on prior operational experience, but it does necessarily consider the variability of wear rates that occur as a consequence of complex operational conditions, including variable flow rates, concentrations and average particle size (Schaan and Sanders 2007). Furthermore, wear profiles may vary depending on type of condition which negates the ability to rotate pipes.

Previous research on erosive wear prediction and monitoring reveals the ambiguity in different interpretations of wear tests, patterns and results. The lack of understanding of the effect of process conditions on damage accumulation present in slurry pipeline applications suggests that more experimental iterative work needs to be done to accurately address this need and guide us to better ways of monitoring the wear process. Improved prediction of the expected wear rate under a range of operating conditions, and improved understanding of the physics of failure for damage mechanisms of interest, will allow reliability and maintenance personnel to conduct more effective predictive maintenance. This will lead to improved reliability and reduced downtime in slurry transport systems (Lipsett. 2004).

1.2. Objectives

The main objective of the present work is to develop testing methods that can be used to measure wear rates in ways that emulate actual operating conditions. Higher fidelity testing methods can be used to predict the expected performance of a material in a particular operating service, and give insights into predictive modeling of damage in slurry equipment.

The guideline of the present study is based on providing better understanding of dry and wet abrasive wear assessment on a set of different materials. In order to accomplish this goal, a standard testing method was modified to better simulate erosive wear conditions present in slurry transport applications.

1.3. Scope

The scope of this thesis is to develop a wear test method that may be used to emulate the damage mechanism in a slurry pipeline, and to conduct dry and wet abrasive tests of different materials. Two pieces of experimental apparatus were designed and developed. A laboratory-scale pipeline loop was designed and built using 2-inch diameter carbon steel pipe for slurry pipeline system reference tests.

A second wear test apparatus was designed and built for wet rubber-wheel testing of coupons. This design was inspired by the Dry Sand Rubber Wheel test method (DSRW), standardized by the American Society for Testing and Materials (ASTM) under the designation G65. This modified version of the test rig was developed for conducting dry and wet abrasion testing on different materials in which the pipeline slurry system's conditions were imitated.

All of the experiments conducted in the present study were limited in the type of abrasive material used (one size of silica sand only), and fluid (only water was used as the carrying fluid for the slurry mix tests). A limited number of specimens were available for each of the six materials tested for wear abrasion, and the wear characterization used was limited to mass loss and qualitative visual assessment using scanning electron microscopy (SEM). For both the pipeline loop and the modified version of the G65 wear test rig, X-70 steel alloy was the "control material" under study. Five different types of polyurethane coupons with Titanium Carbide particulate composition were also tested for abrasive wear resistance under the same conditions as the X-70 steel alloy material.

In this study, both dry and wet abrasive conditions were investigated. In addition, the effect of dissolved oxygen in water as a major contributor to corrosion damage in pipeline steel was also studied. For this purpose, a set of experiments was conducted on X-70 steel samples with low levels of dissolved

oxygen in water. Another addition to the experiments was the wet abrasion testing of reinforced polyurethane samples previously saturated in water.

1.4. Organization of the Thesis

This thesis contains six chapters: this introductory chapter, literature review, equipment design & development, experiments and commissioning of the apparatus, test results and wear characterization, and conclusions and recommendations for future work.

The literature review describes previous research conducted in dry and wet abrasive testing. Different test options for various types of wear assessment needs and applications are described. Some particular dry scratching abrasion and erosion wear test rigs are described. A rationale regarding the testing method chosen for the experimental purposes of this research is also discussed.

Chapter three summarizes the conceptual and practical design aspects of the Wet G65 apparatus, the slurry pipeline loop as the reference testing apparatus, and the relationship between these two experimental setups.

Chapter four explains in detail the methodology followed for the wear abrasion testing, and the commissioning and calibration process of the Wet G65 apparatus.

Chapter five presents the wear rate results of dry and wet abrasive testing, and characterization of the wear scars obtained on six different types of test materials. Wear characterization is assessed on worn test pieces by means of scanning electron microscopy (SEM).

The final chapter presents the conclusions obtained from the present research work and recommendations for future work in the field of slurry erosion testing and wear assessment.

Chapter 2

2. Literature Review

This chapter reviews the literature related to tribology and wear. Different types of wear are described along with their associated damage mechanisms and modes. Different factors that identify an appropriate wear test method for a given application to be simulated is discussed. Similar testing methods for assessing abrasive wear and erosion are described in terms of advantages and disadvantages. The need for further research in predicting damage accumulation in slurry transport applications is highlighted. The concept of the dry sand rubber wheel apparatus is presented in this study as the testing tool that offers the possibility to simulate slurry erosion conditions in sections of pipe.

2.1. Tribology and Wear

Wear is damage to a solid surface that involves progressive loss of material (Davim 2011). This loss is due to relative motion between that surface and another contacting material or substance. Usually, wear can be determined as the volume loss from solid surfaces in moving contact.

Tribology is the science and technology put into practice for studying the interaction between surfaces in relative motion. This term derives from the greek term “tribos”, meaning rubbing or sliding. Moreover, tribology focuses on applications that involve principles of friction, wear and lubrication (Davim 2011) (Stachowiak and Batchelor 2005).

Wear is the major cause of material loss and an important factor that reduces reliability and mechanical performance of many industrial applications (Stachowiak and Batchelor 2005). In order to reduce wear, as much as possible, an understanding of its damage mechanisms is required. Wear is a complex process that has been studied extensively and is one of the most difficult aspects of tribology. Despite many technological and experimental efforts, no simple and universal solution has been developed in order to explain it (Davim 2011).

Many authors have contributed to the field of tribology in analyzing the different types of wear and their damage mechanisms. An important starting effort came from the basic concept of wear where it is produced by means of two solid surfaces sliding over each other known as sliding wear (Hutchings 1992). A pioneer approach was done by Archard in 1953, with his wear model. The starting point of this model was based on the premise that contact between two surfaces will occur where asperities touch, and the true area of contact will be equal to the

sum of each individual asperity contact areas (Hutchings 1992). This model is represented by the Archard's wear equation.

From the following equation, it can be assumed that the wear rate (known as the volume of material removed in cubic millimeters per unit of distance slid in meters) depends on the normal load (in newtons) and on the hardness or yield strength of the softer material. (Hutchings 1992).

$$Q = \frac{kW}{H} \qquad (1)$$

where Q is the volume worn per unit sliding distance (in cubic millimeters per meter). W is the normal load. H is the hardness or yield strength of the softer surface, and k is the dimensionless wear coefficient.

The Archard wear equation implies that k is a constant for a given sliding system in which the volume loss of material produced by wear should be proportional to the distance slid (i.e. Q should be constant), meaning that if the normal load W varies, then the wear rate should vary proportionally (Hutchings 1992).

In the real world it is confirmed for many sliding systems that the loss of material by wear is proportional to the sliding distance. This also applies in sliding systems subjected to constant velocity in time (Hutchings 1992) (Stachowiak and Batchelor 2005). However, transient behavior can be observed at the beginning of a wear process in several applications depending on the nature of the initial running conditions. Until equilibrium surface conditions or steady state conditions have been reached, the wear rate could be lower or higher (Hutchings 1992).

Proportionality between wear rate and normal load W is more difficult to find in many sliding applications. Despite the fact that for many systems the wear rate varies directly in accordance to the load applied within limited ranges, some abrupt changes can be observed from low to high wear rate or vice-versa. This suggests that the nature of the material being subject to wear or the wear mechanisms present for a particular application may be influenced by many other factors (Hutchings 1992). The study of all the set of factors that impact the behavior of the wear process happening between two or more sliding materials or present in many industrial applications is the reason of existence of tribology.

2.2. Types of Wear

The extensive tribology literature available that studies the different types of wear shows diverse ways to interpret wear and its mechanisms. Many authors classify wear according to different principles. The most important principle is the nature of the contact interaction of solid surfaces (Bharat 2001). However, in our daily basis we encounter more types of wear depending on the type of system or application in which wear develops. The different types of wear according to Bharat 2001 that depend on the type of application are illustrated in Figure 1.

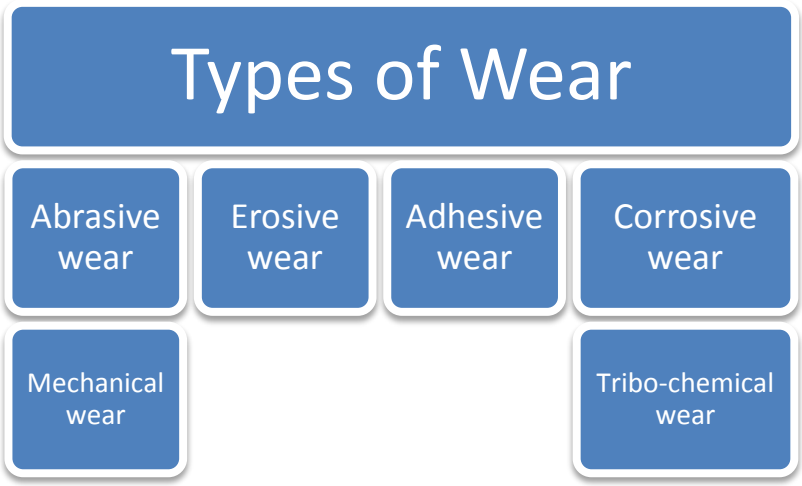

Figure 1 - Wear types and their interactions

(Modified from Bharat 2001)

The wear classification schematic shows four main wear types: adhesive wear, fatigue wear, abrasive wear and corrosive wear. Special attention will be given to abrasive and erosive wear in this work, since their damaging mechanisms

are analyzed in this study. However, the other two types of wear are also related to abrasion and the different interacting mechanisms found in the literature regarding types of wear.

Wear by abrasion and by erosion are the most common forms of wear caused by contact between a particle and a solid material. Abrasive wear occurs when a solid object or surface is loaded against particles of material with equal or greater hardness. A good example of this is the wear that shovel and machinery experience when moving rocks, sand and debris (Stachowiak and Batchelor 2005).

In situations in which wear is caused by the striking of hard particles either carried by a gas or a liquid (usually water), it is defined as erosion. In the second case where a liquid is the particle carrier, the terminology used is slurry erosion (Hutchings 1992) (Kajdas et al. 1990). Other definitions for this phenomenon are also solid particle erosion or solid impingement erosion. In these cases, the term used will depend on the type of damage caused to the surface by the stream of particles carried by the fluid (Hutchings 1992).

Adhesive wear occurs by the action of junctions between the surfaces that are exposed to friction. When these junctions are strong, the softer material is

subject to shearing and, as a consequence, is transferred onto the harder material (Takadoum 2008).

Corrosive wear occurs as a consequence of chemical reactions between the worn material and a corroding medium, which can be a chemical reagent, reactive lubricant or even air (Stachowiak and Batchelor 2005). This type of wear can easily be mistaken with oxidative wear, which is the process in which wear is caused by the action of atmospheric oxygen (Stachowiak and Batchelor 2005).

Another principle that is used to classify abrasive wear is related to the stresses found in the process and how they impact the abrasive particles (Gant et al. 2004). Abrasive wear can be high stress when the abradant particles are fractured in the process. Whereas, when this doesn't happen, it is considered low stress abrasion (Gant et al. 2004). Low stress abrasion is normally associated with applications such as earth tilling, sliding coal down a chute, and also walking on a floor with dirt particles in our shoes. Conversely, examples of high stress abrasion are a coal crusher or dirt particles trapped between hard steel gear teeth. This latter type of abrasion produces scratching with more evidence of indentations due to the fracture of grit particles (Budinski 2007). Both stress states are important in oil sands mining and extraction operations.

2.3. Mechanisms for Abrasive and Erosive Wear

2.3.1. Mechanisms of Abrasive Wear

In the process of abrasive wear, four main mechanisms can be identified:

1. Cutting: This mechanism of wear occurs in a sliding contact system of a hard surface with a softer material (Kajdas et al. 1990). It can be represented by the classic model in which a sharp grit or hard asperity cuts the softer surface. The material that is cut is removed as wear debris (Stachowiak and Batchelor 2005). When the abraded material is brittle (e.g. ceramic), fracture of the worn surface is most likely to occur.

   According to experimental work on abrasive wear, cutting of worn surfaces may be affected by two main factors; the presence of a lubricant and the geometry of the grit (Stachowiak and Batchelor 2005). When a lubricant is present in the wear process, cutting occurs for a smaller ratio of grit penetration to grit diameter than in the counterpart case. The geometry of the grit also affects the cutting mechanism, since it has been observed that a stylus with a fractured surface containing many micro cutting edges removes far more

material than un-fractured pyramidal or spheroidal styluses (Stachowiak and Batchelor 2005).

2. Fracture: Is the visual evidence of material removal from a surface by action of cracks caused by a sharp indenter on a brittle solid (Stachowiak and Batchelor 2005). Brittle fracture is favored by high loads acting on each grit and sharp edges on the grit, as well as brittleness of the substrate (Stachowiak 1993). When grit moves successively across the surface, accumulation of cracks normally results in the release of large quantities of material.

3. Fatigue: Occurs as a consequence of loss of material when fatigue cracks in the surface produce loose particles, mainly due to contact stress or thermal stress fatigue mechanisms (Neale and Gee 2001). This wear mechanism leads to separation of particles from a surface in the form of flakes. The name associated to this particular type of wear fatigue is spalling (Kajdas 1990). This last mechanism is commonly found in the wear of rolling element bearings and gear teeth (Kajdas 1990).

4. Grain Pull-out: Is a mode of wear consisting in primarily intergranular fracture where one or two grains are removed at a time (Kajdas 1990). This is a relatively rare form of wear, mainly found in ceramics. It can be extremely fast when inter-grain bonding is weak and grain size is large (Stachowiak and Batchelor 2005).

2.3.2. Modes of Abrasive Wear

The way the particles or grit pass over the worn surface determines the nature of the abrasive wear (Stachowiak and Batchelor 2005). This plays an important role in identifying the type of wear mechanism to expect in a particular testing set up or sliding application. According to the literature there are two abrasive modes:

1. Two-body abrasion: This mode of abrasive wear is caused by hard protuberances on the counter face (Hutchings 1992). A good example is the action of sandpaper on a surface (Stachowiak and Batchelor 2005). Hard asperities or rigid grit pass over the surface like a cutting tool (Stachowiak and Batchelor 2005).

2. Three-body abrasion: In this abrasive mode, hard particles are free to roll and slide between two sliding surfaces (Hutchings 1992).

The two and three-body modes of abrasive wear are illustrated schematically in Figure 2.

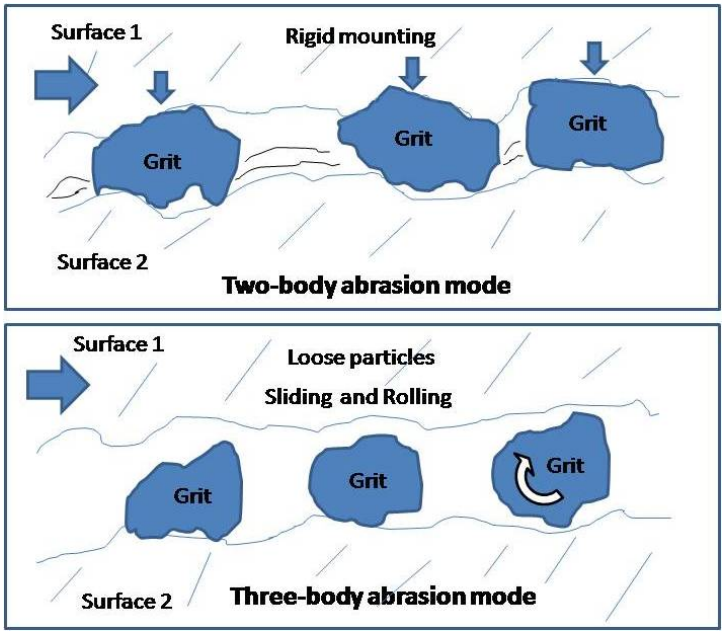

Figure 2- Two and three-body modes of abrasive wear

(Modified from Stachowiak and Batchelor 2005)

These two modes of abrasive wear have been considered to be similar in early tribology literature (early 1960s). However, significant differences have been revealed over the past few decades (Stachowiak and Batchelor 2005). It was found that three body wear is ten times slower than two body wear since it has to compete with other mechanisms involved i.e. adhesive wear (Sasada et al. 1984). Two-body wear corresponds closely to the cutting tool model of material removal,

while in three-body wear, slower mechanisms of material removal occur (Johnson, R. 1968). It seems that the worn material on a surface is not removed by a series of scratches as in the two-body case. Worn surfaces display a random topography that suggests gradual removal of surface layers by successive contact of grit (Sasada et al. 1984) (Misra and Finnie 1979).

Most of the abrasive wear problems that arise in agricultural and industrial equipment are three-body, i.e. sleeve bearing and bushes operating in abrasive environment, lower sleeve bearing in vertical sewage pumps, chain wear strips, among others (Harsha and Tewari 2003). While two-body abrasion is usually found in material removal operations, i.e. rotors of powder mixers, pivot pins in construction machinery, blades and components in agricultural and earth moving machinery. Despite the importance of three-body abrasion, the vast majority of abrasive wear in the literature is focused on two-body abrasion (Harsha and Tewari 2003).

When analyzing the three-body mode of wear in slurry erosion applications, four steps are present and can at times occur simultaneously (Wirojanupatump and Shipway 1999):

1. Particle Detachment: Occurs when particles are detached from the first bodies (i.e. from the original surfaces being in contact), by means of any of the following types of wear: adhesion, abrasion, corrosion or surface fatigue.

2. Third Body Life: Once the particles are detached, they can remain trapped in the tribological dynamics of the application or setting, becoming part of the third body and changing in morphology and composition. This is the case of silica sand particles used as abrasive material in several abrasion testers, i.e. the dry sand rubber wheel (DSRW) or the wet sand rubber wheel apparatuses (WSRW).

3. Debris Circuit: This refers to the mechanism existing when a trapped particle is re-circulated in the system. This depends on the nature of the contact with the first bodies, and experimental factors such as humidity and vibration.

4. Particle Expulsion: This happens when the particles are ejected from both the contact area and the wear track. In this case re-circulation is avoided.

2.3.3. Mechanisms of Erosive Wear

Erosion is a process that involves the removal of material from the surface of a component due to the action of high speed impact of a stream of solid particles in a carrying liquid flow (Neale and Gee 2001). The two common types of erosion are cavitation and particle erosion. The first occurs on components subject to low transient fluid pressures, normally seen in ships' propellers when these component surfaces are impacted by low pressure vapor bubbles. The second type of erosion (and the one we will be mostly interested in) is mainly explained as the stream of particles directed against a surface in a fluid. This can occur intentionally for shot blasting applications, or accidentally like in the pipelines that carry slurries or crude oil (Neale and Gee 2001).

Erosive wear is a damage process that involves an unspecified number of wear mechanisms which occur when relatively small particles impact against mechanical components (Stachowiak and Batchelor 2005). This type of wear occurs in a wide variety of equipment and fluid systems in different industries. Typical examples are the damage to gas turbine blades when an aircraft flies through dust clouds, or the wear found on pump impellers in mineral slurry processing systems (Stachowiak and Batchelor 2005).

There are several damaging mechanisms involved in erosive wear, which have been extensively studied since the Second World War. Unfortunately, a simple model for predicting this mode is far from complete (Finnie 1995). Many authors have contributed in the literature with studies that relate different elements of the erosive process. The set of elements can be divided in three main groups: 1) particle properties (size, shape and hardness), 2) fluid flow conditions (density of the fluid, angle of impingement, particle velocity, particle concentration in the fluid, nature of the fluid and temperature of the fluid), and 3) surface properties (hardness and microstructure, geometry component, fatigue, melting point) (Finnie 1995). (Hutchings 1992) (Stachowiak and Batchelor 2005) (Budinski 2007).

From this classification of parameters which affects the erosive wear process, it is possible to infer that there are multiple combinations of factors and conditions in which wear can occur. This makes the characterization process very challenging and difficult to explain. Some of the main parameters that have been investigated include the angle of impingement, the speed of erosive particles, the size of the particles, the temperature and the fluid medium.

The angle of impingement is the angle between the eroded surface and the trajectory of the particle before the impact (Stachowiak and Batchelor 2005). A low angle of impingement (less than 45°) may produce severe wear if the particles

are harder than the surface of impact. Abrasive wear signs are often found under these conditions (Hutchings 1992). Whereas, high angles of impingement (closer to 90°) produce typical erosive wear mechanisms (Stachowiak and Batchelor 2005).

The speed of the erosive particles has a strong influence on wear. If the erosion process occurs in a slow velocities, the stresses at impact are insufficient for plastic deformation to occur. In this case, wear will mostly occur by surface fatigue. Conversely, at higher velocities (about 20 m/s), it is possible for the particles to erode the surface by plastic deformation (Stachowiak 2004; Goodwin et al. 1970). This is a very common scenario in engineering components and applications (Hutchings 1992). If the eroding particles are blunt or spherical, the formation of thin plates of worn material on the surface is likely to happen. If the particles are sharp, then cutting or brittle fragmentation is more likely to occur (Stachowiak and Batchelor 2004).

The size of the particles is also an important parameter when predicting wear. Most industrial applications related to erosive wear involve particles between 5 and 500 μm in size. However, there is no fundamental reason to limit eroding particles to this size range (Stachowiak and Batchelor 2005).

The effect of temperature on erosive wear mechanisms are related to the fact that temperature softens the eroded material and increases wear rates (Studt 1987) (Shida and Fujikawa. 1985). However, for the objectives of the present study, temperatures will not be investigated. When high temperature erosion of metals occurs in an oxidizing medium, corrosion can take place and accelerate the wear. It is not until temperatures of 600°C are reached that erosion rate will increase significantly (this is the softening point of steel) (Studt 1987).

When considering the fluid medium in which erosive particles travel during a slurry transport process, studies have shown that some important factors such us viscosity, density and turbulence of the stream, can significantly influence wear rate results (Levy et al. 1987). The ability of a liquid or medium to provide cooling during particle impingement is also an important parameter in wear rates. In terms of bulk properties, the forces present in the slurry, by the action of a viscous medium on the erosive particles, can affect wear by altering the impingement angle of these particles (Levy and Hickey 1987).

2.4. Review of Testing Methods

In this section, a series of testing options available to characterize wear are reviewed. Testing options are presented in two groups, abrasive and erosive wear.

For the purposes of the present study, wear mechanisms occurring in metals and in polymers are of particular importance.

Laboratory scale friction and wear testing is usually performed in order to accomplish two main goals: either to rank the performance of candidate materials for a particular application, or to investigate wear processes and their mechanisms (Anderson 1986). For both purposes, control and measurement of all variables that might influence wear results is of great importance. In laboratory experimental set ups, it is vital to appreciate that wear rate and friction are often dependent on the sliding conditions. Moreover, any minor changes in the tribological interaction of materials may lead to radical changes in dominant wear mechanisms occurring, and will affect wear rate results (Hutchings 1992).

The word tribometer was first introduced in 1774, referring to an instrument intended to measure friction between two interacting surfaces (Hutchings 1992). The evolution of these instruments or machines has experienced a significant development until present day, with a great variety of systems which simulate different types of wear in a safe laboratory environment.

The diversity of tribometers or tribological tests available can operate in air or in a controlled atmosphere under certain experimental conditions

(Takadoum 2007). The set of parameters usually imposed are the applied load, the sliding speed and the environmental conditions (humidity and controlled atmosphere). The variables measured are usually the friction force, the surface temperature, the contact resistance and wear produced (Takadoum 2007).

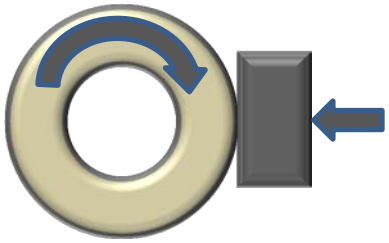

Figure 3- Plane/cylinder geometry interaction for tribometer

2.4.1. Testing Methods for Abrasive Wear

Depending on the particular application to be simulated, tests can be performed using different types of contact geometries: sphere on plane, pin on disk, plane on plane, plane on cylinder, or cylinder on cylinder. This study will only focus on the plane and cylinder geometric interaction between two sliding surfaces. This concept in shown in figure 3.

The previous mentioned geometric surface interactions for tribometers can be divided in two types: 1) those where the sliding surfaces are symmetrically disposed, in which the wear rates of two surfaces of identical material should be the same, and 2) the common arrangement where the system is asymmetric in

which the two sliding bodies will almost certainly experience different rates of wear. In asymmetric arrangements, one component of the mating pair, in most cases the pin or block, is usually treated as the specimen, and is the component for which the wear rate is measured, while the other component, usually the disc, plane or ring is called the counterface (Hutchings 1992).

From the variety of contact geometries available for sliding wear testing previously illustrated, the set up commonly used for abrasive wear testing involves a pin shaped specimen sliding against fixed abrasive. Another testing method commonly used involves a rotating wheel sliding against a plane specimen with loose abrasive particles being continuously fed between the two surfaces (Hutchings 1992).

Four common test methods used to measure abrasive wear rates are illustrated in figure 4.

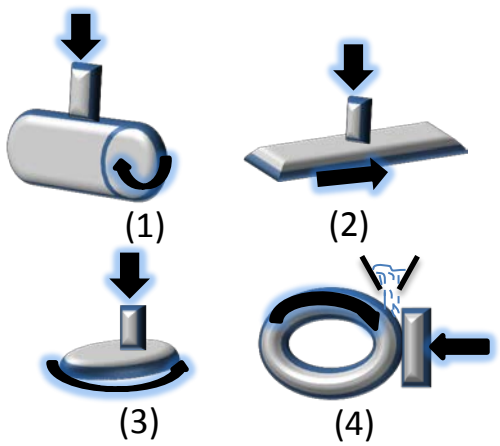

Figure 4 - Schematic of common testing methods for abrasive wear.

(Modified from Hutchings 1992).

(1 -3) pin on abrasive disc, on a plate, and on abrasive drum; (4) rubber wheel abrasion test.

The first 3 systems shown in figure 4 (1-3) are three common variations of the method in which a specimen pin slides against fixed abrasive. This type of test method simulates a two-body wear mechanism. Commercially available, bonded abrasive paper or cloth is usually used for the counterface, carrying evenly distributed grit particles of narrow size distribution bonded to the substrate by a strong resin. The wear rate produced by these fixed abrasive particles decreases with repeated passes of the specimen over the same track (Hutchings 1992). There have been several mechanisms identified that cause this progressive reduction in abrasivity: fracture of particles that lead to a decrease in the number of cutting points; removal of the whole particles from the binder resin (shelling), rounding of the contacting areas of particles by mechanical, chemical or thermal mechanisms (attrition); adhesion of wear debris to the tips of particles (capping); and accumulation of wear debris in the spaces between particles carrying part of the applied load (clogging) (Hutchings 1992) (Hutchings and Trezona 1999). The

rates and relative importance of these mechanisms vary according to the testing material, the load applied, sliding speed, atmosphere and other factors (Hutchings and Trezona 1999). In order to ensure consistent conditions and wear rates, it is recommended that the testing specimen is always sliding against fresh abrasive (Hutchings 1992).

The second common type of abrasive wear test is illustrated in figure 4 (4). In this set up, the specimen is in form of a plate or block, pressed under constant load against the rim of a rotating wheel (Hutchings 1992) (Budinski 2007). The working mechanism of this particular abrasive tribometer was adopted as a US standard under the designation ASTM G-65.

The dry sand rubber wheel (DSRW) abrasion test (ASTM G65) is one of the most popular abrasion tests known in modern tribology. A schematic of the system is shown in figure 5. It consists of a testing machine in which the specimen is cut in the form of a rectangular block. This specimen is pressed against a rotating rubber rim of defined hardness, molded on to the surface of a steel disc. This standard specifies the thickness of the rubber rim (12.7 mm), and the width of the wheel (12.7 mm) with an overall diameter of 228.6 mm. The wheel rotates at 200 revolutions per minute (rpm).

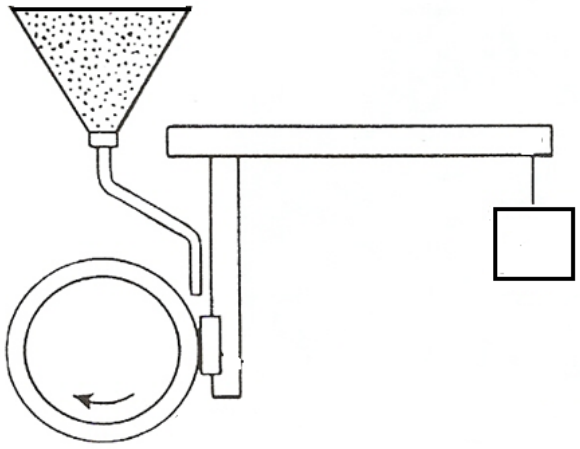

Figure 5 - Schematic of the dry sand rubber wheel abrasion test.
(Modified from ASTM G-65 2004)

The force pressing the specimen against the wheel is set at 130 Newton (N). Silica (quartz) particles of a narrow size distribution (50-70 US Mesh) and from a specified source are continuously fed at a constant rate range of 300-400 grams per minute (gpm) into the gap between the rubber rim and the specimen's surface. Wear is measured gravimetrical by weighing the specimen before and after the test in order to determine the mass loss of material. This mass loss is later converted to volume loss (in mm^3) in order to avoid confusions in wear results due to variation in density. The conversion to volume loss for reporting wear results is done according to the following equation:

$$Volume\ loss = \frac{mass\ loss\ (g)}{density\ (\frac{g}{cm^3})}\ x\ 1000 \qquad (2)$$

The DSRW test involves loose particles of abrasives which indent the compliant wheel during abrasion. Although the particles most probably do not roll during contact, they can rotate significantly. When doing so, they tend to move away from cutting orientations in order to minimize the frictional energy dissipation. The conditions in this set up are considered closer to the three-body abrasion mode than to the two-body mode (Hutchings 1992) (Hutchings and Stevenson 1996).

2.4. 2. Testing Methods for Erosive Wear

Similar to abrasive wear, laboratory scaled erosion testing is conducted in order to accomplish certain specific goals: to provide data on wear rates under certain conditions, to validate theoretical models, and to study the different mechanism involved in erosive wear (Hutchings and Stevenson 1996).

The methods commonly used for laboratory erosion testing can be divided into two groups according to Hutchings 1992: 1) those where circular motion is used in order to achieve impact velocity, and 2) those in which the particles are accelerated in a fluid (gas or liquid). An example for the former group of erosion testing methods is the recirculating slurry loop pipeline. In this set up a two-phase flow of particles and fluid (usually water) is driven around a pipeline loop. This

method is very useful for evaluating wear rates in pipeline components such as bends or valves. This method is also used to examine the wear behavior of certain materials by completely immersing the specimens in the flow. One of the drawbacks of this testing method is the fact that the erosive particles eventually suffer degradation by the continuous impact with the pipeline elements (Hutchings 1992) (Budinski 2007). More details about the functioning concept and the type of pipeline elements commonly used in a slurry pipeline set up are describe in chapter 3 of this thesis.

A good example of the latter group of test methods is the slurry jet impingement test, in which particles are accelerated in a fluid stream through a nozzle. The target material is held at some distance from the end of the nozzle at a desirable fixed angle, and is impacted by the stream of impinging particles (Hutchings 1992). A volume of fluid is circulated around a close loop with a pumping system in order to provide the slurry jet fluid over the surface of the testing specimen. The specimen is located at an appropriate angle and distance from the ejecting nozzle that sends the jet fluid with the erodent particles onto the sample. This fluid is caught and re-circulated within the system (Neale and Gee 2001).

The essential controlling parameters in this type of test are the angle and position of the sample with respect to the nozzle, the shape of the fluid provided,

depending on the nozzle used, fluid pressure, the abrasive loading, and its shape and size (Neale and Gee 2001). In addition, chemistry of the fluid is important due to potential erosion-corrosion effects. Synergy between erosion and corrosion can sometimes generate dramatic changes in material loss. Another testing parameter to evaluate could be the reuse of the erodent by re-circulation through the pumping system (Neale and Gee 2001).

Wear is characterized by volume loss of the testing material and the visual examination of the worn surface of specimens. The impact angle can be adjusted in a range of approximately 20-90 degrees. Many types of erodent can be used, however, silica sand is the most common option. The jet impact velocity can vary from 2-30 m/s (Neale and Gee 2001).

2.5. Slurry Erosion and Wet Abrasion Testing

"Slurry erosion" is one of the most common terms used in the present research interchangeably with "wet abrasion." However, when talking about abrasion testing in wet conditions, technically the right term we are referring to would be slurry erosion, since erosion differs from wear abrasion in the fact that the first one has a contributing degenerating element attached to it, "water." A slurry is a mix of solid particles and a carrying fluid. The solids can vary in size,

type, and hardness while the carrying fluid normally can be any liquid that allows the mix to be pumped (Budinski, 2007). Normally in the oil sands industry slurries are mainly made of bitumen, water, silica sand and clay particles that vary drastically in size.

Models for estimating erosion wear in slurry pipelines are typically based on empirical data collected at a set of operating conditions of interest. An empirical model developed by Salama (Salama. 2000) based on test data for predicting erosion wear rates in gas/liquid two phase well production pipelines is represented with the following equation:

$$Ew = \frac{1\ x\ W\ x\ Vm^2\ x\ d}{Sm\ x\ \rho m\ x\ D^2} \qquad (3)$$

where Ew is the erosion rate (mm/year), W is the sand production rate (Kg/day), Vm is the mixture velocity (m/s), d is the particle size (mm), D is the pipe inside diameter (mm), Sm is the geometry factor (found to be 5.5 for pipe bends), and ρm is the mixture density. This relationship between process operating variables and erosion rate is limited for very low concentrations of sand flow. Moreover, this relationship does not provide insight to specific wear mechanisms causing erosion such as random impacts and abrasion (Lipsett and Bhushan. 2011). For the purposes of this study, is of great importance to discuss about two testing methods adopted as American standards by the ASTM organization for assessing

abrasive wear in wet environment. These testing rigs have similar working principles to the dry sand rubber wheel test (DSRW). However, the stream of abrasive particles that abrade the specimen that is being pressed against the wheel is now being carried by a fluid (water), making it a dense slurry of abrading particles. These testing methods are known as the rubber wheel wet abrasive slurry test (ASTM G-105), and the test method for abrasive wear resistance of cemented carbides (ASTM B-611)

2.5.1. The Rubber Wheel Wet Abrasive Slurry Test (ASTM G105)

This test method has a similar working concept to the dry sand rubber wheel test (ASTM G-65). However, the fact that the abrasive particles are part of a recirculating slurry bath highlights the main difference between the two test rigs. The ASTM G-105 consists of a rotating steel wheel of 178 mm diameter with a neoprene rubber rim that is pressed against a testing specimen. This specimen is being held in a holder and subject to a normal load of 222 N that is applied by the lever arm mechanism. The sliding speed is 245 revolutions per minute. The wheel is partially immersed in a slurry mix bath. The sand water slurry is continuously agitated and recirculated towards the specimen's contact face (in the direction of wheel rotation) by the action of paddles located on the wheel. The abrasive wear generated is due to the action of the slurry mix on the specimen surface (ASTM G-105 2002) (Vite et al. 2003). Wear is characterized by the volume loss of

material, calculated from mass loss and material density measurements (similar to equation 2). More specific details regarding the testing set up can be found in the ASTM G 105-02 standard for conducting wet sand/rubber wheel abrasion tests.

The main downside found with this test apparatus is related to the continuous deterioration of the abrasiveness of the particles that are being carried in the slurry. Since the abrasive passes through the wear interface more than once, the particle size and sharpness degrade as it is contained in a closed bath and recirculated slurry mix. Another disadvantage is that the test requires constant supervision in order to ensure that adequate mixing is occurring (Vite et al. 2003). This test is not well suited for studying synergistic effects of erosion and corrosion in certain metals, due to the short testing time duration of less than 1 hour (Budinski 2007).

2.5.2. Method for Abrasive Wear Resistance of Cemented Carbides (ASTM B-611)

The ASTM B-611 test method is very similar in setup to the G-105 standard test, in that it consists of a rotating steel wheel of 165 mm of diameter, with vanes or baffles that are immersed in an abrasive slurry mix. The abrasive used according to the standard is alumina of about 600 μm in size. The first

noticeable difference between the G-105 and B-611 setup is mostly that the latter does not have a rubber rim at its periphery. This test method is used for assessing wet abrasive wear of ceramics used in mining operations. The slurry mix is picked up from the bottom of the reservoir and pushed towards the interface area between the test specimen and the steel wheel by the action of the baffles. The specimen is pressed against the steel wheel that rotates at a speed of 100 revolutions per minute. The lever arm mechanism applies a constant load of 20 N on the specimen (Gant et al. 2005). Wear characteristics is volume loss of material calculated from mass loss values and testing material density measurements. More details regarding the test method can be found in the standard ASTM B-611.

The B-611 testing rig has the same functioning mechanism of the G-105, in the sense that it reuses the grit slurry mix during the entire experiment, resulting in degradant of the abrasive sharpness. Moreover, the high stress wear mechanism occurring in this set up produces micro cracking of the abrasive particles from the constant sliding action with the steel wheel (Neale and Gee 2001).

2.6. Wear Mechanisms in Engineering Materials

2.6.1. Metals

Many different mechanisms have been identified in the literature for the severe wear of metals. In all cases, plastic deformation occurs, but differs in the details regarding the processes by which material removal happens (Hutchings 1992).

Early theories of sliding wear suggested the material removal occurring as lumps or fragments from asperities peaks by adhesive processes. Some evidence of this was the presence of some irregular debris particles with blocky shapes (Hutchings 1992) (Hutchings and Trezona 1999). Many mechanisms have been proposed by which asperity contacts can produce wear debris. In this case, plastic shearing of successive layers occurs in conjunction with the propagation of a shear crack, along which the particle detaches. Adhesive forces are not the reason by which material is removed, since this mechanism depends only on the mechanical interaction between two asperities (Hutchings 1992), but they must be invoked in process of explaining any subsequent transfer of debris to one of the sliding surfaces.

Another proposed model for wear supposes that the formation of a debris fragment by asperity rupture is followed by immediate adhesive transfer of material to the counterface, which forms a new asperity on that surface. Further sliding causes more fragments to be formed that eventually will adhere to the original fragment until a much larger conglomerate of wear particle becomes detached. This particle of debris may be roughly equiaxed, or it may be flattened and elongated in the direction of sliding by the action of further plastic deformation (Hutchings 1992).

Early measurements of sliding wear in metals were carried out mainly in dry conditions, partly because the interpretation of results was easier in the absence of hydrodynamic lubrication. In the ten years from 1955 to 1965, Archard, Hirst, Kerridge, Lancaster and Welsh demonstrated two conditions of dry wear which they called severe and mild (Childs 1980). In the former, rubbing caused surface roughening and the wear debris was metallic. In the latter, surfaces were smoothed by rubbing and debris was mainly flakes of oxide (Childs 1980).

When analyzing the wear mechanisms occurring in metals, one of the main factors to consider is the relationship existing between wear rate and hardness. According to many authors, the classic relationship for abrasive wear of metals is that wear is inversely proportional to the hardness of the metal (Rabinowicz 1966). The harder the metal, the lower the abrasion rate obtained

(Bundinski. 1997). This relationship can be evidenced in Archad's equation (1). However, the existence of transitions in wear rate in metals, in which wear can change by orders of magnitude, can make it risky to freely use any wear equation over a wide range of conditions (Rigney 1988). The coefficient k is a dimensionless wear coefficient that has been interpreted in different ways: the probability that an asperity contact event yields a wear particle, the fraction of asperities able to generate debris, the ratio of the volume worn away to the volume plastically deformed (Rigney 1988), or as a factor inversely proportional to the number of loading cycles needed to produce a wear particle. When k is in the range 10^{-6} to 10^{-8}, wear is considered mild. For k larger than 10^{-4} it is severe. Rabinowicz suggested an alternative range, with severe wear for k values of approximately 10^{-2} to 10^{-4}, moderate wear for k values of 10^{-4} to 10^{-6}, and burnishing wear for k values of 10^{-6} to 10^{-8} (Rabinowicz. 1984). While Challen et al. (Challen et al. 1986) proposed that mild wear (Rabinowicz's burnishing wear) can be analyzed by using a model of plastic waves in front of hard asperities that have small slopes. This model can also be used to explain transitions to severe wear at higher loads (Rigney 1988). Increased loads cause asperities to penetrate more deeply. Therefore, if the tips of asperities are rounded, the effective asperity slope increases with load, and wear rate increases (Rigney 1988).

Although many attempts have been made to model sliding wear of metals as a fatigue process, the validity of this approach is still not well established (Hutchings 1992). Models have been proposed for the propagation of subsurface

fatigue cracks under cyclic shear forces, while other have assumed that asperities are removed as a result of low-cycle (macroscopically plastic) fatigue (Hutchings 1992).

2.6.2. Polymers

The abrasive wear behavior of polymers and polymer based composites is currently the subject of large investigation efforts. Engineering polymers and polymer based composites are widely used in design (Harsha and Tewari 2003). Polymers and their composites are often required to move in contact with hard abrasive particles as counterfaces (Hutchings and Trezona 1999). Many authors have applied diverse test methods on polymers; both two-body and three-body abrasion modes have been examined. Two-body abrasion mechanisms have been studied by using abrasive papers and rough metal counterfaces (Shipway and Ngao 2003). Whereas, three-body abrasion studies have been done by means of the dry sand rubber wheel test (DSRW) by Harsha and Tewari (among other authors), who have conducted abrasive wear performance tests of different polymer composites under different loads and sliding distances.

Polymers in contrast to metals exhibit lower coefficients of friction with values between 0.1 and 0.5, whether self-mated or sliding against other materials (Hutchings 1992). Polymers are much more compliant than metals with values of

elastic modulus about one tenth or less, and having also lower strengths. For this reason it is considered that metallic or ceramic counterfaces always act as rigid bodies when sliding against polymers (Hutchings 1992). In most cases all the deformation due to contact or sliding in polymers will be greatly influenced by the wear mechanism occurring due to the nature of the hard counterface material (Hutchings 1992) (Harsha and Tewari 2003). If the counterface is smooth, wear may occur as a result of adhesion between the surfaces in contact and will involve deformation only in the surface layers of the polymer (Hutching 1992). By contrary, if the counterface is rough, then its asperities will cause deformation in the polymer to a significant depth. In this case, wear may result either from abrasion related to plastic deformation of the polymer, or from fatigue crack growth in the deformed area (Hutchings 1992) (Hutchings and Trezona 1999). These two classes of wear mechanisms that involve surface and subsurface deformation respectively, have been named by some authors as interfacial and cohesive wear processes. In general, susceptible polymers sliding on highly polished hard counterfaces will experience adhesive wear, whereas, turned or ground surfaces will produce cohesive wear mechanism (Hutchings and Trezona 1999). Cohesive wear is defined as subsurface or bulk wear when the interacting surfaces produce damage to the material far deeper into the material than only at the interface (Friedrich 1986). This type of wear is also referred to in the literature as plowing.

Abrasive wear properties of polymers can be strongly affected by additives such as fillers and plasticizers (Stachowiak and Batchelor 2005). Plasticizer has been found to be detrimental to the abrasive wear resistance of PVC since it softens the polymer (Bartenev and Laurentev. 1981).

Two and three-body modes of abrasive wear are also considered to be different in plastics relative to metals (Stachowiak and Batchelor 2005). With a two-body wear mode mechanism, the wear rate is linearly proportional to load, but with three-body abrasion the wear of plastics has a non-linear dependence on load (Bartenev and Laurentev. 1981). The reasons for the variation are still unclear until today in the literature.

Despite all the research efforts conducted on polymeric materials, the processes of wear in polymers are still not well understood. This is confirmed in a review of some of the early literature concerning abrasive wear of polymers by Evans and Lancaster (1979). In their review, the authors showed that in tests covering eighteen polymer types, low density polyethylene exhibited the lowest wear rate in abrasion against a rough mild steel, but the highest wear rate in abrasion with coarse carborundum paper. Therefore, it can be seen that abrasive wear behavior of polymers is complex (Shipway and Ngao 2003). In addition, (Budinski 1997) recognizes that most of the studies on the abrasion resistance of plastics are inconclusive and tend to recommend further iterative studies.

Among the extensive types of polymers, this study will only focus on Polyurethanes (PU). These polymers are one of today`s most versatile materials and are used in a variety of applications. Their many uses range from flexible foam in upholstered furniture, to rigid foam in wall insulation. They are also used in roofs and appliances. Thermoplastic polyurethanes are used in medical devices and footwear, also in coatings, adhesives and sealants; whereas, polyurethane elastomers are used on floors and automotive interiors (Khalid et al. 2007). Polyurethanes are widely used in the mining industry because of their moderate cost, excellent mechanical properties and high wear resistance compared with alternative polymeric materials (Hill et al. 1997).

2.7. Dry and Wet Abrasion Testing

Dry abrasive wear is one of the most common wear mechanisms studied in recent decades when it comes to ranking materials according to their resistance to scratching abrasion for certain types of industrial applications. On the other hand, investigating the effects of wear abrasion observed in wet environments or mediums for the same materials used for slurry transport applications is a field that still has room for research and development. However, some important comparative work has been conducted by diverse authors. For example, Wirojanupatump 2000 studied the wear behavior of mild steel using both rubber and steel wheel apparatus in dry and wet conditions. His study revealed that wear

rate is greater in wet conditions with a steel wheel than with a rubber wheel. It also provided insight regarding reduced abrasive particle embedment due to lubricating action of water over the abrasive particles. Whereas, when conducting comparative wear testing for dry and wet conditions on the same testing rig (a modified G-65 apparatus) allowed him to test mild steel in dry and aqueous environment with two types of abrasives. The results highlighted wear reduction in wet conditions with rounded silica particles (previously chosen). Conversely, evidence of indentation in test pieces was found in specimens in which larger alumina abrasives were used. It was also suggested that water not only has its lubricating factor, but also a corrosion effect in wear results. However, this variable was not analyzed in the test results (Wirojanupatump. 1999).

Previous studies that compared the G-65 and B-611 apparatus documented the difficulty of assessing accurately wear rate results due to challenging experimental conditions between the two setups; fracture of abrasive particles (high stress abrasion) reducing the abrasiveness effect in a re-circulating slurry mix on the B-611 test, while a pass through only once of sand mix used in the G-65 with the rubber wheel (Ness and Zibbell 1996). Some authors compared the two testing setups with the same experimental conditions (abrasive material and type of wheel used) in dry and wet environments, concluding that mild steel wore 2.5 times faster in dry abrasion with sub-angular silica sand when using a steel wheel instead of a rubber wheel (Chen and Hutchings. 1998). Other authors (Vite et al., 2005) worked on a comparative study of different parameters in abrasive

wear in dry and wet conditions of Inconel 600 and stellite. They used the B-611 and the G-105 testing methods with silica sand 50/70 US mesh size and same load of 222 N on both cases. Their results pointed to less weight loss in wet conditions. The lubricating effect of water was again confirmed in these studies.

All of these previous studies in abrasive wear testing in dry and wet conditions made a good contribution in indicating the way to follow when developing and testing for similar wear mechanisms and testing materials. Since these studies were conducted with diverse experimental purposes and different material applications were analyzed, there is still no uniformity in the understanding and reasoning of abrasive wear mechanisms present in the slurry erosion process in industrial slurry transport applications. The effect of water as a lubricant in scratching abrasion has been suggested in different studies; however, there is not much available in the literature related to erosion and corrosion synergetic effects.

2.8. Synergism between Corrosive and Abrasive Wear

Abrasive wear can accelerate corrosion by the action of repeated removal of passivating films formed over the worn surface, and a very rapid form of material loss may result (Stachowiak and Batchelor 2005). This synergism is particularly evident in mineral processing industries where slurries containing

corrosive fluids along with abrasive grits are pumped in large pipelining systems. This model is based on cyclic film formation and removal of material by corrosive and abrasive action, respectively (Stachowiak and Batchelor 2005). This mechanism of wear prevails when the rate of mechanical abrasion under dry conditions is less than the corrosion rate without abrasive wear (Stachowiak and Batchelor 1988). When mechanical is more intense, corrosive effects on the surface will become less significant (Stachowiak and Batchelor 1988). It is probable that when corrosion is slow compared to abrasive wear the grits remove underlying metal with very little interference from the corrosion film (Stachowiak and Batchelor 2005). Material resistance under corrosion-abrasion action will depend on the material's resistance to corrosion. It has been shown that a soft but non-corrodible organic polymer can be more long lasting as a lining of a slurry pipe than a hard but corrodible steel material (Hocke and Wilkinson 1978).

2.9. Literature Review Summary

The literature review introduced us into the world of tribology and wear. The different types of wear were described along with their mechanisms. Among all the different types of wear, four of them were identified as the most important for the purposes of this research: adhesive wear, fatigue wear, abrasive wear and corrosive wear. Great attention was given in this chapter to abrasive wear and erosive wear and their damaging mechanisms were identified in the literature. The

two modes of abrasive wear (two-body and three body abrasion) related to the way the abrasive particles pass over a worn surface were explained and associated to particular applications in industry and real world situations.

Many wear testing methods or tribometers were mentioned in the literature according to two main groups: testing methods for abrasive wear and for erosive wear. In the former group, great attention was given to the dry sand rubber wheel test method or the ASTM G-65, since this testing apparatus is the main focus of the present study.

Other testing methods with similar operating principles or similar wear acting mechanisms to the ASTM G-65 were described in the literature. This was the case of the rubber wheel wet abrasive slurry test or ASTM G-105, and the test method for abrasive wear resistance of cemented carbides or ASTM B-611which are popular standard testing methods for the dry and wet abrasive wear assessment of different testing materials. The second test rig is currently used for the erosive wear assessment of cemented carbides in high stress abrasion conditions, while the G-105 tester simulates wet abrasion conditions for different materials in a setup very similar to the G-65 machine.

Wear mechanisms found in certain engineering materials of interest for this research were described. It was found in early studies that metals and polymers have different ways in which abrasion and erosion wear occur depending on the nature of the testing materials and their resistance to particular types of wear. In this study, among all the polymers especial attention is given to polyurethanes due to their versatility and great wear resistance. Despite all the research contributions made in tribological studies of metals and plastics, it is recognized by many authors that there is still room for more experimental research to be done, and there is a need to clearly understand the way wear mechanisms occurring in these materials interact under diverse operating and wear conditions.

Comparative research conducted on ASTM G-65, B-611 and G-105 was also discussed in the literature for dry and wet abrasion testing evolution. These contributions were of capital importance in the analysis of wet abrasive wear testing methods used on mild steel with variations introduced to these tribometers as per experimental needs. It was observed that wear rate diminished significantly in wet conditions compared to its dry counterpart due to the lubricating action of water over the abrasive particles introducing a two-body wear mode mechanism, instead of the expected three-body wear mode. The corrosive action of water over the testing materials was suggested in the experimental results; however, it was not assessed and analyzed. The steel and rubber wheels also played an important role when interchanged in the experiments as they impacted in the level of

abrasive degradation process and consequently in the wear rate reduction. These previous experiments provided an important insight into the study of wet abrasive testing. However, since the testing methodologies were used for different experimental purposes and the analysis of wear mechanisms was done according to different practical objectives (i.e. material wear assessment, abrasive type used and testing material composition), a uniformity in test results as a reference for wet erosion assessment of different materials used in slurry applications has not been achieved yet.

The synergism between abrasive and corrosive wear was addressed in the literature as the introductory topic for further analyzing the wear behavior in X70 steel used in slurry transport applications in the present study.

In summary, many research efforts have been accomplished in tribology for the abrasive and erosive wear prediction of different engineering materials like metals and polymers. However, in some particular synergistic cases, such us in erosion-corrosion of materials used in slurry transport applications, the literature seems to be scarce or very divergent, suggesting that more work should be done on wet abrasive assessment for slurry pipeline applications on standardized testing techniques. This could facilitate to mimic, as accurate as possible, the wear mechanisms present in the real industrial applications.

Chapter 3

3. Equipment Development

This chapter describes the conceptual design of a modified G65 testing apparatus for dry and wet abrasion testing. The concept and design of the slurry pipeline loop is also described in this chapter. The common wear mechanism present in both testing apparatuses is discussed at the end of this chapter.

3.1. Tribometer Planning and Methodology

After surveying the testing methods available for dry and wet abrasion testing in chapter 2, and the damage mechanisms that can be simulated by means of different tribometers, the next step is to choose an appropriate option for the current application, that is, erosive wear in a slurry pipeline. This is not generally an easy step; however, in our specific research objective, the main purpose of using an abrasive setup like the ASTM G65 is based on the practical opportunity of introducing some modifications to an available, reliable and well known standard for abrasion testing. These modifications will allow to conduct abrasion tests in dry and wet environments. Moreover, it is important to identify the set of variables that will be controlled, and the ones that will be modified under the specific testing conditions that will be later discussed in chapter 4.

A key factor to consider when choosing the right tribometer is to simulate, as accurate as possible in the laboratory, the real operational conditions present in the industrial setting that is to be imitated. Many factors play a role in a wear experiment, such us: interactions of the surfaces involved in the mechanical contact, the testing conditions (normal and shear forces of load), hardness of material and abrasive, medium (dry or wet), time, and others. Based on this rationale, the testing methodology chosen matches the aim of the present study, which will be the evaluation of six different materials as for their scratching abrasion resistance in a dry and wet (slurry) environment; the required testing conditions are based on simulating low stress abrasive and erosive wear by means of a “three body” wear mechanism. Some of the identified limitations in the experimental methodology are: sample size, number of samples, amount and type of abrasive material, among other predetermined variables that will be identified in more details in chapter 4 of this study. A summary of the criteria followed for selecting the tribometer to use in this research project is given in the following table:

Table 1 - General Tribometer Selection Criteria

<table>
<tr><th colspan="2">Desired Characteristics</th><th>Concerns</th></tr>
<tr><th>Musts</th><th>Wants</th><td rowspan="2">Specimen alignment can be a problem</td></tr>
<tr><td>Fast Testing time (less than 1 h)</td><td>Low cost specimens</td></tr>
<tr><td>Test simulates dry and wet low stress abrasion conditions</td><td>Specimens are able to be immersed in a slurry mix</td><td rowspan="2">Wear measurement on certain materials can be difficult</td></tr>
<tr><td colspan="2">Test data available on reference materials</td></tr>
<tr><td>Controlled environment</td><td>Test helps assessing erosion and corrosion effects</td><td rowspan="2">Water and sand mixing rates might be a problem</td></tr>
<tr><td>Test uses mass loss as a test metric (gravimetric)</td><td>Test rig is commercially available</td></tr>
<tr><td>Wear can be optically assessed</td><td>Test setup easy to modify</td><td rowspan="2">Noisy when testing certain materials</td></tr>
<tr><td>Fixed speed and load</td><td>Test consumables are readily available</td></tr>
<tr><td>Test conforms to consensus standard</td><td>Test does not require an operator present at all times</td><td rowspan="3">Different testing wheels might produce different desired results</td></tr>
<tr><td>Test can be conducted by anybody with minimal training</td><td>Testing with different wheel diameters will not be a concern</td></tr>
<tr><td>Constant specimen contact</td><td>Abrasive material is used only once</td></tr>
</table>

3.2. Evolution of the ASTM G65 Apparatus

When studying the development and evolution of the DSRW apparatus in the wear assessment and characterization field, many researchers have paid great attention to experimental setup conditions that are still under study and actively being modified to fulfill particular needs. Most of the modifications introduced to the original G65 setup were based on experimental performance and the advantages and disadvantages of this particular abrasion test method. Among the advantages highlighted by Ma et al. (2000) are the good correlations that can be found between laboratory test results and actual field tests. This method allows to perform testing with fixed loads and sliding speeds, facilitating the process of evaluating the scratching abrasion resistance of different materials under the same testing conditions. A desirable advantage of this test method is having the abrasive material circulate through the specimen only once per test cycle. However, these two experimental variables are key elements in the variation of wear behavior among materials. Some materials have excellent wear resistance under low loads or sliding speeds, but have poor wear performance under higher loads and/or sliding speeds, and vice-versa. Due to the sensitivity of these two factors, the focus of the present research is based on evaluating 6 different materials under same loads and sliding speeds as per suggested by the ASTM G65 methodology.

According to the literature, two disadvantages of the G65 test are ineffective control of the rate of feed of the abrasive (Gant and Gee. 2001), and the inability to simulate wet conditions.

When considering the evolution of the G65 testing method, the most popular modifications made to the DSRW have been those dealing with the sand feeding system and the capability of performing dry and wet abrasive tests on the apparatus. Other additional changes had been made to the lever arm mechanism in order to manage where the dead weights should be added as part of the lateral load that is pending at the other end of the arm mechanism holding the testing specimen. Also, the location of the specimen with respect to the rubber wheel has been part of the modifications introduced to the G65 testing method by various authors. Stevenson and Hutchings developed a modified version of the G65 machine in which the test specimen was being held horizontally as opposed to the original vertical G65 setup; and they applied the weights directly above the specimen (Stevenson and Hutchings. 1996). Wirojanupatump and Shipway modified the G65 by having the specimen held with a certain inclination angle with respect to the rubber wheel and the vertical component of the lever arm. They also added a lateral load and counterbalance load to the pivot arm mechanism (Wirojanupatump 2000). These particular changes contributed in gathering more consistent results, as the applied load over the specimen was not affected by frictional forces present in the traditional apparatus set up.

The G65 tester was chosen as the experimental methodology to use in the present research based on a set of desired characteristics, experimental data availability on reference materials, controlled testing environment; ability to introduce modifications to the experimental rig for allowing dry and wet abrasion testing of several materials in the same machine and with the same experimental conditions; and capability of assessing wear optically and by gravimetric methods. Moreover, with this research, there is an initial interest in studying common wear mechanisms that might be present in a standard test method such us ASTM G65 and, a slurry pipeline application.

3.3. The Wet Sand Rubber/Steel Wheel Abrasion Apparatus

The wet G65 machine was developed based on the original concept of the dry sand rubber wheel apparatus (DSRW) according to the ASTM G65 standard. Some modifications were introduced to the apparatus in order to address the experimental needs of allowing the use of both a dry abrasive and an abrasive slurry for practical demonstration of abrasive wear mechanisms and for their comparison in a different set of polyurethane particulate reinforced materials and X-70 grade alloy steel samples.

3.3.1. Original Conceptual Design

The main objective in the conceptual design of the Wet G65 was to allow the capability of using abrasive particles in both dry conditions and in a slurry, and allowing the passing of abrasive material over the testing specimen only once, maintaining the abrasiveness quality of the silica sand used in the G65 once-through test method. As previously explained in chapter 2, similar wet abrasion techniques such as the ASTM B611 and the ASTM G105 simulate erosive slurry conditions on a specimen being exposed to a water and abrasive mix that is forced to pass between the gap of the specimen's face and the rotating steel wheel. However, the downturn of these setups is the fact that the slurry is not "fresh" due to the continuous recirculation of water and solids, becoming ablated in the process and losing their sharpness (and abrasiveness).

The Wet G65 apparatus used in the present study is schematically illustrated in figure 6. It was inspired by the (DSRW), introducing some modifications that makes it a hybrid abrasion rig for conducting controlled lab-scaled dry and wet abrasive tests. The rig consists of a 203.6 mm in diameter steel wheel with a 12.7 mm rubber rimmed mounted on the wheel. The wheel rotates counterclockwise when viewed from the front, in the same direction in which silica sand particles fall from a nozzle located above and between the gap of the testing specimen and the rubber wheel (commonly referred to as "the contact

zone"). The motor drive allows the wheel to rotate at different speeds and two movement sensors record the wheel's sliding speed and number of revolutions. A stainless steel lever arm mechanism holds the test specimen and locates it against the rubber wheel. Two water nozzles were added to the dynamics of the wear rig: one for mixing with the sand and creating slurry flows in the contact zone, and the second for cleaning the wheel from slurry residues. The latter was required to prevent buildup of sand at the specimen. The design, construction and commissioning of the apparatus followed the ASTM G65 standard specifications, however, some modifications regarding positioning of the water nozzles and adjustments made to the sand nozzle were introduced as part of a trial and error approach during commissioning and preliminary experimentation. More design detailed information is given in Appendix I.

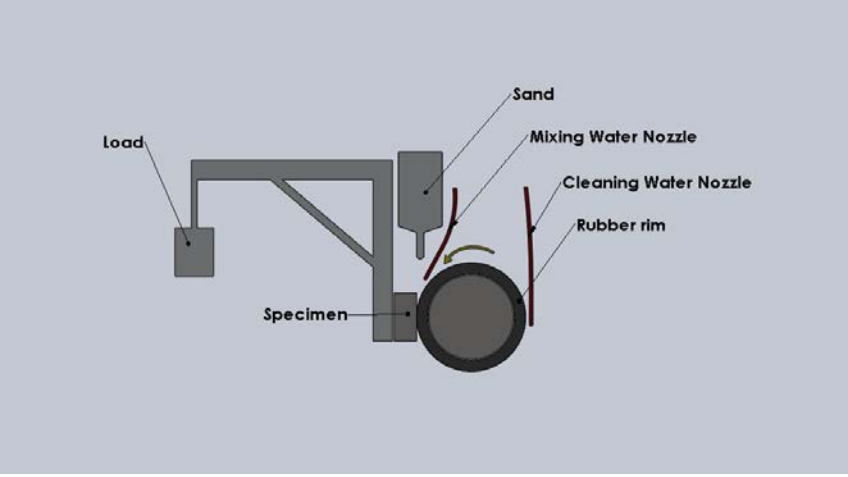

Figure 6- Wet G65 apparatus schematic

When running tests in wet conditions, water is circulated through two hoses which transport water to flexible nozzles. The water flow rate is controlled through a series of parallel ball valves installed at the front panel of the test apparatus (figure 7). The direction of these nozzles can be adjusted to optimize the water flow performance. This way, the nozzle can rotate with respect to the surface of the specimen, allowing alignment of the sand curtain against the specimen's surface. A transparent acrylic lid encloses the wheel, specimen, and nozzles to reduce splashing , and clogging of the sand nozzle is controlled by two small aluminum films that work as protective screens.

The new system also was developed to control the level of dissolved oxygen in the slurry. Dissolved oxygen (DO), is an important parameter which has been observed to accelerate wear rates in carbon steel slurry pipelines.

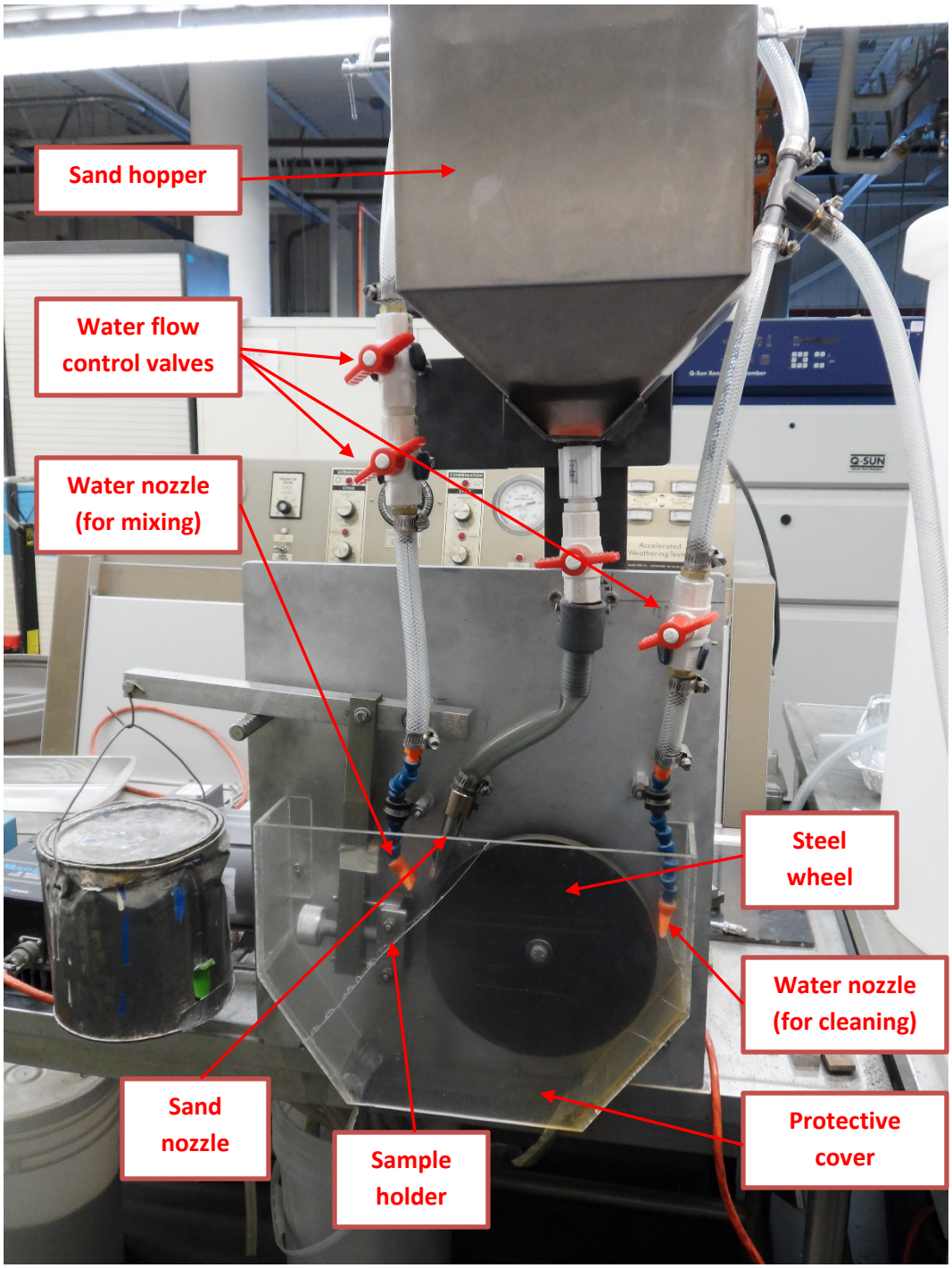

Figure 7 - The wet G65 apparatus

For adding DO capabilities to the modified G65 tester (second stage of tests), the initial water supply (from the tap) was replaced by a 270 liter tank. The contained water was de-aerated before use in experiments. This experimental configuration had the following components:

1) Three 0.9 m long copper tubes of 6 mm outer diameter, were connected to a nitrogen gas cylinder to supply a set of gas dispersion tubes (spargers) shown in Figure 10. 2) A 190 lph submersible portable pump was installed inside the tank to pump the water to the wet G65 machine once treated for de-aeration (not shown in figure 8). 3) Two ball valves were set in the lower end of the tank for transporting water to the tester machine and for allowing the collection of water samples for dissolved oxygen readings. 4) A portable Oakton Acorn DO-6 dissolved oxygen meter was used for tracking and recording dissolved oxygen levels in water in ppm before and after the tests.

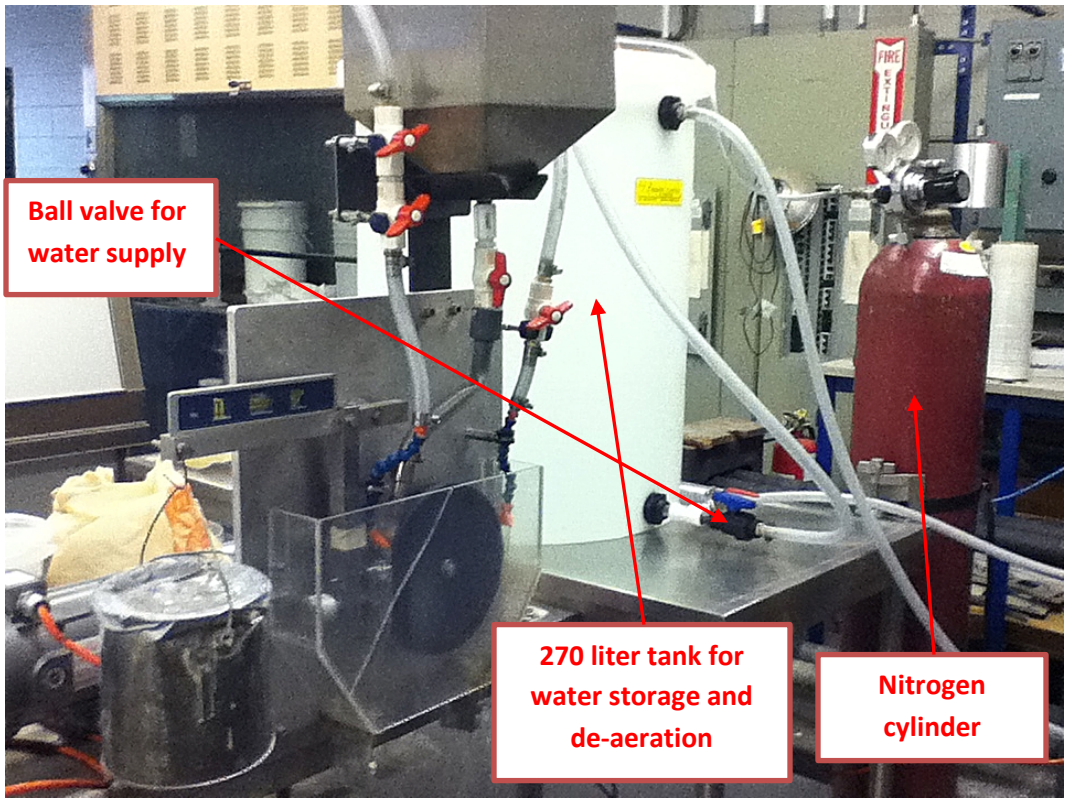

Figure 8 - Modifications made to wet G65 machine for low oxygen abrasion testing

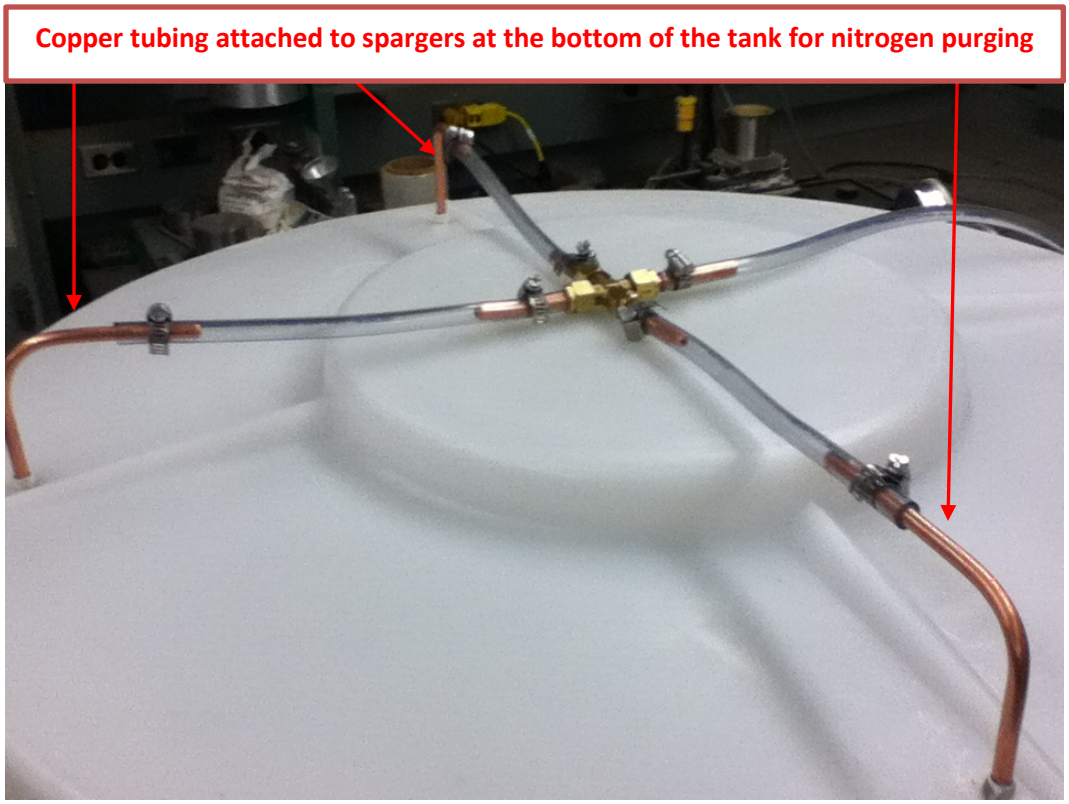

Figure 9 -Tubing for nitrogen purging in water

Figure 10 - Gas dispersion tube (sparger)

As previously stated, the aim of the present study is to develop a novel testing method that helps understanding the wear mechanisms present in slurry pipeline applications.

3.4. Slurry Pipeline Loop Development

A pipeline loop rig was designed and developed as part of a larger research program intended to study the damage mechanisms present in different pipeline slurry transport applications at a laboratory scale. This experimental apparatus was used in the present research project for comparative purposes only and no experimental data was collected from the rig.

3.4.1. Motivation

As previously mentioned, slurry pipelines in the oil sands industry are subjected to high levels of erosion, corrosion, a mixture of both, and blockage of pipes or other degradation processes, according to the system operating conditions. All of these degradation processes occur as a consequence of the abrasive action of slurry flow mixtures being pumped through the pipeline. This results in costly shutdowns due to repair and replacement of sections of pipe (Paterson. 2011). As a result, current research is focused on understanding and

modeling the variables that are involved in damage accumulation in these pipeline systems (Lipsett 2004).

3.4.2. Conceptual Design

The apparatus consists of a 50.8 mm (2 in) diameter pipeline system in an indoor, controlled environment. This loop was designed to carry a water-sand slurry pumped continuously within the system at different flow velocities, sand concentrations, and a range of particle types. The pipeline slurry loop was intended to be operated in dense bed two-layer conditions. The apparatus allows for control of manipulated variables and measurement of responding variables related to impact and erosive wear in pipes, such as: slurry flow rate, sand concentration in the slurry, pressure drops, particle type, temperature, and granularity.

With this experimental design in mind, the pipeline loop was developed with the following components:

- Approximately 18 meters of 50-mm inner diameter carbon-steel pipe.
- 6 meters of 75 mm rubber suction hose.

- Approximately 25 meters of 50 mm discharge hose for drainage.
- A 7.5 Hp slurry centrifugal pump with variable frequency motor drive.
- A 2 Hp gear drive mixer.
- Two 450 litre cone bottom tanks: one for preparing the slurry mix and another for drainage purposes.
- A straight line coriolis flow-meter.
- Three pressure transducers.
- Two testing replaceable spool sections: one of 1 meter long and inclined (approximately 10 degrees) and another horizontal 0.5 meter long intended to be replaced by a particle floating element when required.
- Two sight glass sections for observation of slurry regimes during the tests (one located before the particle floating element and another after it).
- Three designated draining points: one by the drainage tank with a metallic container for sand filtering placed inside a plastic tray underneath it, a second drain valve attached to a hose run to the drainage system, and a third valve located in the inclined section of pipeline for sample taking purposes. A schematic of the pipeline loop is provided in Figure 11.

This system was designed with three different elevations from the floor. The discharge section of the loop is elevated 1.3 meters from the floor, while the section following after the second elbow has approx. 15 degrees of inclination and 1.5 meters from the floor. The third section of pipeline is 1.0 meter from the floor before returning to the tanks.

Details and design calculations of the slurry pipeline loop are provided in Appendix II of this thesis.

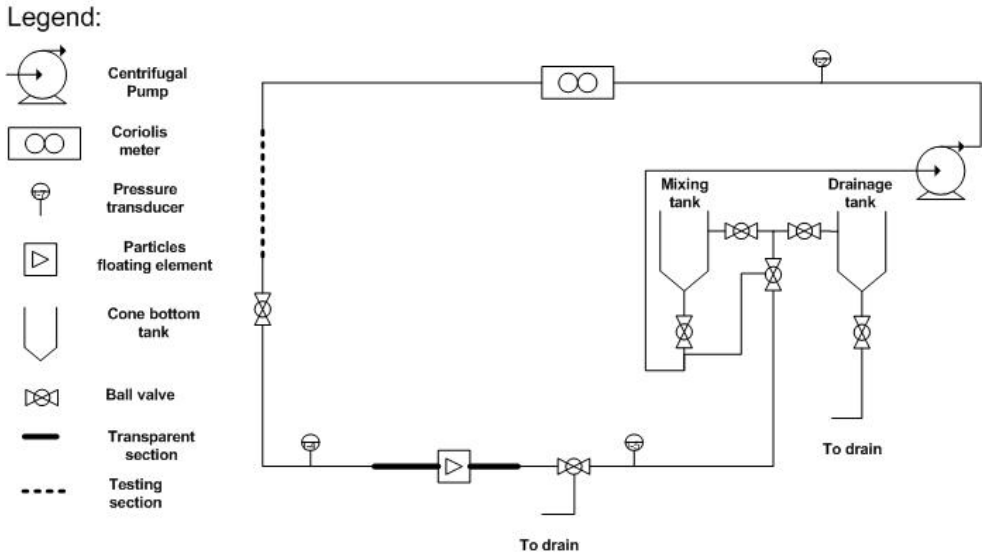

Figure 11 - Slurry pipeline loop lay-out schematic

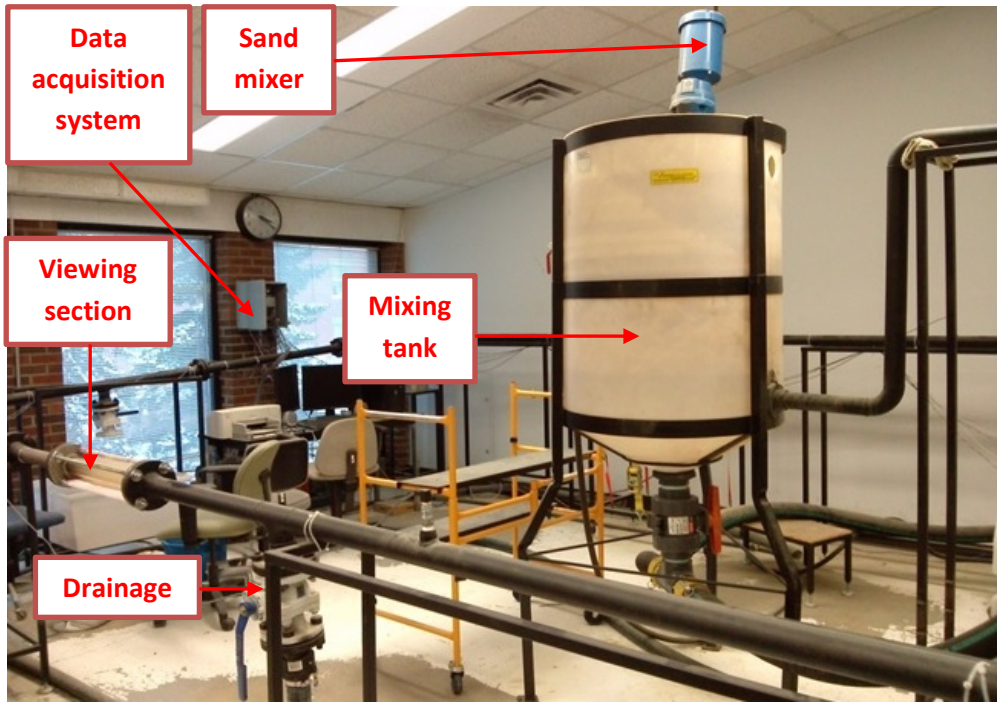

Figure 12 - Slurry pipeline loop elements (tank and mixer)

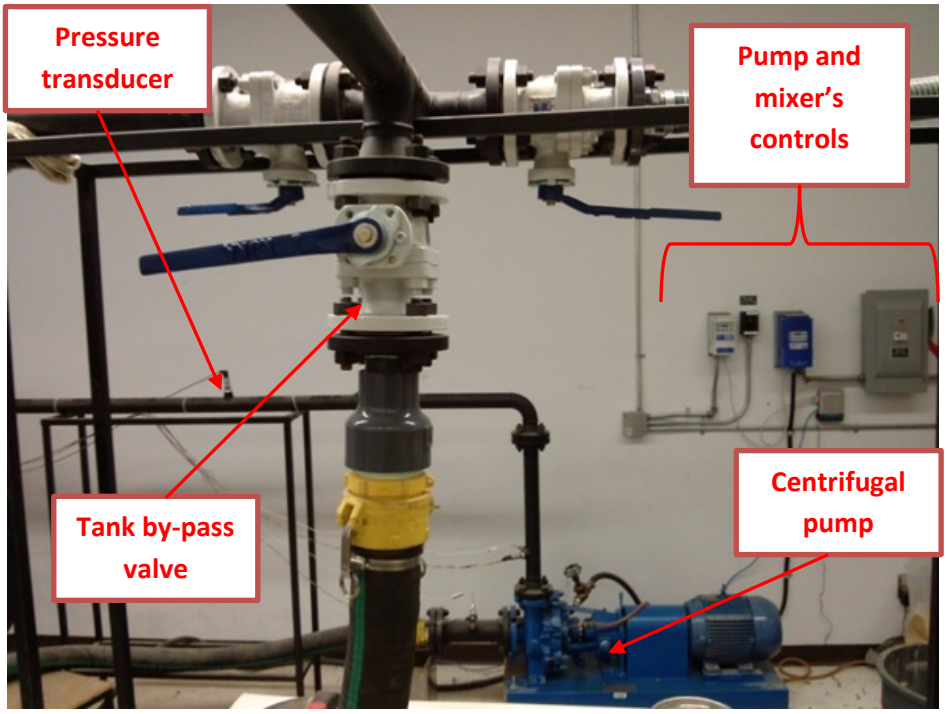

Figure 13 – Slurry pipeline loop elements (pump and controls)

3.5. Wet G65 Apparatus and Slurry Pipeline Loop Common Mechanisms

The flow conditions taking place in a slurry pipeline transport application has been studied extensively over the past few decades through the two layer model developed by Wilson in 1970 and 1972 (Gillies 2000). This model highlights the heterogeneous nature of both layers and flow regimes: a top fast moving layer with fine particles in suspension being carried by water in a turbulent fashion, and a bottom sliding layer also known as a "sliding bed" with a more laminar flow at the bottom of the pipeline (El Sayed 2009). This second layer is the consequence of gravitational forces acting over bigger particles in suspension in the slurry and the reduction of the mean velocity in the flow (Doron et al. 1987). As this mean velocity is decreased, the particles tend to deposit at the bottom creating what is understood as the "sliding bed or slurry bed" (Doron et al. 1987). The upper layer flows at an average velocity V_u, and has a low concentration of solids C_u, while the lower bed layer is a dense fluid with high concentration of solids C_l with a low average or mean velocity V_l . The two layer model is illustrated in the following figure (Lipsett 2012).

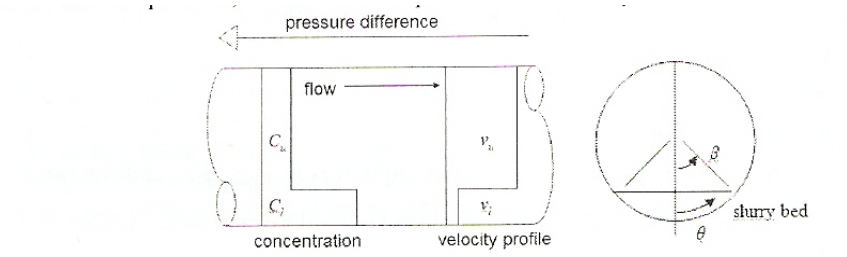

Figure 14 - The two layer model schematic.

(Source: Lipsett. 2012)

For the bottom layer, the friction of the bed against the pipeline wall is represented by F_l in the following equation:

$$F_l = \frac{1}{2} g D^2 n_s (\rho_s - \rho_f)(C_l - C_u)(sin\beta - \beta cos\beta) \qquad (4)$$

(Source: Roco 1987)

where:

n_s is the sliding friction coefficient (assumed to be 0.5 for sand particles).

ρ_s is the density of the solids.

ρ_f is the density of the fluid.

C_l is the concentration of the bed.

C_u is the bulk concentration.

D represents the pipe diameter.

g is gravity acceleration.

β is the subtended angle in radians that defines the interface between the bed layer and the bulk fluid layer (Roco 1987).

In the two layer model, it is assumed that most of the energy dissipated by friction is lost in the form of heat raising the slurry temperature, but not causing damage to the inner wall of pipe (Lipsett 2012). However, there may be a fraction of this friction energy which causes damage to the pipe if the energy transfer threshold is exceeded. Part of the lost energy in suspending the slurry particles for the top layer causes the exit of some particles from the stream flow, impacting randomly on the inner pipeline walls. A fraction of the energy transmitted to the inner pipe walls from these random impacts eventually causes damage to the pipeline (El Sayed 2009). A similar process occurs in the bottom layer or sliding bed; however, the energy lost due to friction is divided into kinematic and Coulombic friction (El Sayed 2009).

The wear rate at the pipeline wall for a water and sand slurry can be expressed by the following equation:

$$d = \alpha^{*}\lceil V^{*}\,(\tau - \tau_0)\rceil \qquad (5)$$

(Roco. 1987)

where:

d is the wear rate expressed in mass units.

τ is the shear stress due to the contact of precipitated particles scratching along the pipe wall resulting in wear in units of force per area.

τ_0 is a parameter that represents the threshold of wall damage

α^* is an experimental proportional constant

V^* is the corresponding velocity to the wear component (particles in the sliding bed), in units of length/time. It is assumed in this model that $V^* = V_l$ (Lipsett 2012).

Using the two-layer model as the conceptual premise, the damage mechanism can be analyzed experimentally by the use of the ASTM G65 testing machine. This standard testing method is widely used in research due to its convenience and repeatability assessing scratching abrasion on a variety of testing materials used in many industries.

The experimental conditions present in a slurry pipeline application can be imitated on this standard test, providing that the effect of the population of solid particles used in a test exhibits similarities to that which would be observed in pipeline flow conditions. Besides, the normal force of the particles and the

tangential speed of the rubber wheel are close to how particles slide in the actual pipe walls (El Sayed. 2009). By this means, if the suspended weight in the lever arm is known, the sliding friction shear stress can be calculated by multiplying the normal force by the dynamic friction factor n_s. The average velocity of the flowing sand particles is assumed to be the same as the sliding velocity of the rubber wheel, and the wear rate for the sliding bed of particles can be calculated for the slurry/testing material combination, since the wear rate obtained in the testing specimen can be measured on the testing specimen (El Sayed 2009).

Chapter 4

4. Experimental Method and System Commissioning

This chapter describes the methodology for the development of a novel G65 apparatus to better simulate slurry wear under both, dry and wet conditions. The commissioning and preliminary testing phase of the test rig, and the monitoring and adjustment of testing parameters is described in detail in this chapter.

4.1. Materials and Methods

The experimental plan for the new G65 apparatus was developed in two main phases: commissioning (preliminary testing) on the apparatus, and actual tests X-70 steel and Polyurethane composites. The first stage after getting the apparatus operational was to perform a calibration in dry conditions according to the G65 ASTM standard. This was followed by preliminary tests to monitor testing factors and their impact on the materials in this study.

4.1.1. Materials

Six different materials were assessed according to their abrasive wear resistance in the wet G65 apparatus. Tests were performed on X70 steel, un-reinforced polyurethane (PU), and on four types of reinforced PU composites mainly based on Titanium carbide (TiC) particles.

Titanium carbide (TiC) is a material with extremely high hardness and light refractory qualities, and has high thermal shock and abrasion resistance. This material is commonly used for powder metallurgical parts such as: cutting tools, dies, and wear-resistant parts. It is also found as an additive to plastic and rubber parts to make them more wear resistant (Pacific Particulate Materials Ltd., 2012). In addition , titanium carbide has very high hardness (Moh +9), and density between 4,900 and 5,200 kg/m^3. (Pacific Particulate Materials Ltd., 2012)

Two of the five PU particulate composites were reinforced with 5 micron and 0.6 micron particles of TiC, respectively. A set of samples were un-reinforced PU, and two other groups of materials were special combinations added to the base PU. The main characteristics of these two materials are described in the following table:

Table 1 - Particulate composite PU materials

(Pacific Particulate Materials, 2012)

Material	Properties	Comments
PU TiCM2201 (PUTI)	Hardness: 2470 Knoop/Mohs +9 Average particle size: FSSS APS 1.2 – 1.6µ Density: 4.85 – 5.0 g/ml Chemically inert and oxidation resistant	Surface modified TiC fine particles to broaden the endurance of polymeric compounds designated to extend service life of non-metallic machine parts.
PU MP8828 (PUMP)	TiC hardness: 3,400 VHN Average particle size: 63u TiC grain size: 1.6 u Bulk density: 2.07 g/ml	Ideal TiC polymer alloy consisting of spherically shaped TiC micro grains chemically bonded to surface activated ultra-high molecular weight Polyethylene (UHMW PE) particles. Ideal for machinery parts and mechanical components under severe service mechanical or chemical environments.

Abrasive Material

AFS Silica sand with quartz particles was chosen as the abrading medium (50 – 70 US Mesh size) for the experimental trials. This type of particle has a hardness and angularity similar to the solids found in actual oil sand slurries (Clark and Llewellyn 2001).

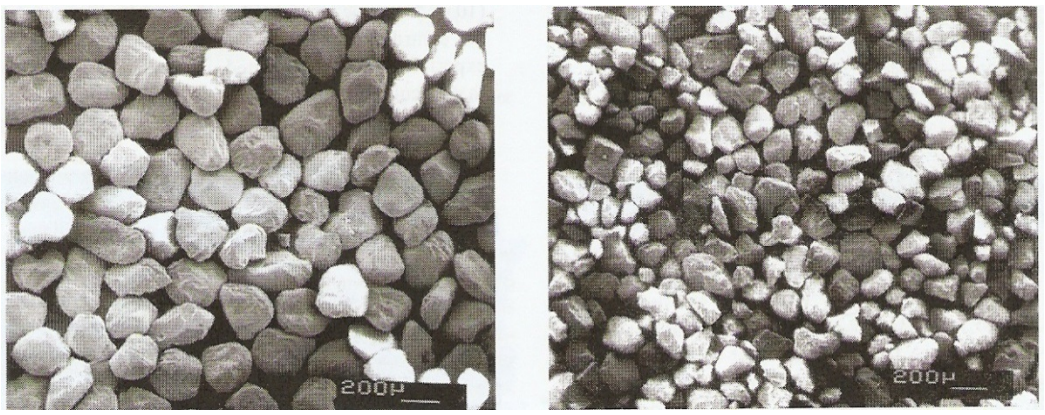

Figure 15- Silica sand particles

Silica sand particles used in experiments (left), Silica particles in slurries in pipelines (right). (Source: Clark and Llewellyn. 2001)

4.2. Experimental Variables

The new G65 test system was developed based on an analysis of key variables. These were classified in three major groups:

Responding Variables: These variables identify the main measurable parameters in this research including: volume loss of material, wear scar patterns, and dissolved oxygen levels in water.

Manipulated Variables: These variables correspond to the group of experimental conditions that may be altered during the experiments and are later identified as sensitivity factors.

Controlled Variables: Include those experimental conditions that will not change during the experimentation, and that are identified as standard for testing and comparison purposes.

Table 2 – Experimental variables

Experimental Variables		
Responding Variables	**Manipulated Variables**	**Controlled Variables**
Sand particle roughness before and after tests in microns.	Wheel type: Rubber wheel for steel samples and steel wheel for plastic composite specimens.	Lateral load: 120 N (30 lbf).
Volume loss of material in mm^3 as reported by the ASTM G65 standard.	Environment: dry, wet and wet with reduced oxygen contents in water.	Sand Flow rate: 315 – 350 g/min
Wear scars characterization through scanning electron microscopy.	Rubber wheel diameter: 228.6 – 217 mm.	Water Flow rate: 1.2 – 1.4 l/min.
Oxygen Levels in water in ppm	Steel wheel surface roughness	Rotating speed: 200 +/- 3 rpm.
		Abrasive: Angular Silica Sand (50-70 US Mesh distribution size)
		Test duration: 6,000 rpm

4.3. Experimental Matrix

In this study, experiments were conducted on six different materials, two types of wheels and two different environmental conditions. A minimum of three tests per trial were performed for statistical purposes. This made a total of 42 tests to be conducted on the six materials in this study, without repeats. The preliminary tests conducted on the materials studied provided initial insight into the definition of the experimental matrix. Moreover, the wet testing condition

included two variations. These variations included two new testing scenarios that helped to provide further information regarding two variables under observation: Moisture content in polyurethane composites when exposed to water for long periods of time, and low levels of dissolved oxygen in water as a measure intended to reduce corrosion effects in X-70 steel specimens. With the extra experimental conditions, the total amount of tests conducted on the wet G65 apparatus increased to 48. Table 3 illustrates the experimental matrix.

Table 3 – Experimental matrix

Material	Number of Samples	Manipulated Variables				
		Type of wheel	**Dry environment**	**Wet Environment**	**Low dissolved oxygen**	**Pre-soaked samples**
X70 steel	12	steel	3	3	3	
		rubber	3	3	-	
Unreinforced polyurethane	6	steel	3	3		
		rubber	-	-		
PU micro TiC composite	6	steel	3	3		
		rubber	-	-		
PU nano TiC composite	6	steel	3	3		
		rubber	-	-		
PU-TiCM 2201 (PUTI)	6	steel	3	3		3
		rubber	-	-		-
PU-MP 8828 (PUMP)	6	steel	3	3		
		rubber	-	-		
Sub-total	**42**					
	6				**3**	**3**
Total	**48**					

The following table summarizes the experimental conditions tested during the commissioning process for the dry environment according to ASTM G65 standard.

Table 4 – Experimental conditions according to ASTM G65

Testing Parameter	ASTM Standard	Actual Testing
Lateral Load	130 N (30 lbf)	130 N (30 lbf)
Sliding Speed	(200 +/- 10) rpm	(200 +/- 3) rpm
Sand Flow	(300 – 400) g/min	(315 – 350) g/min
Rubber wheel hardness	A58 – A62	A59 –A61
Rubber wheel diameter	228.6 – 215.9 mm	225 – 218 mm
Abrasive Material	AFS 50/70 Silica sand	AFS 50/70 Silica sand
Reference Material for procedure A	AISI D-2 tool steel	AISI D-2 tool steel
Specimen Size	Rectangular shape 25mm (w) x 76mm (l) x 3.2 – 12.7 mm (d)	Rectangular shape 25mm (w) x 76mm (l) x 7 – 10 mm (d)
Testing Time	30 min for procedure A	(30 +/- ½ to ¾) min

Only procedure A of the G65 standard was performed in present study for comparison purposes. For procedure A, tests are conducted for a duration of 6,000 wheel revolutions at a load of 130 N. The commissioning procedure used in this study was based on replicating these conditions as accurately as possible. Moreover, certain testing parameters were continuously monitored during the experiments in order to guarantee a successful calibration of the apparatus. Calibration was performed using AISI D-2 tool steel. The target volume loss

range of the material was (35.6 +/- 5.2 mm^3) for AISI D-2 tool steel as per procedure A of the G65 standard.

Overall, the system required some care during set up. One of the main physical parameters was maintaining a good alignment of the gap between specimen and rubber wheel, which allowed consistent flow of sand particles between the specimen and the rubber wheel. If this gap was not consistently maintained, a buildup of sand would occur, or an uneven wear pattern would result.

The commissioning process of the machine was divided into two steps: dry sand and wet sand procedures.

4.4. Commissioning and Preliminary Testing of New Test Rig

In the first step, the commissioning of the Wet G65 machine was carried out as suggested by the ASTM G65 standard for the dry sand rubber wheel set up. Once the experimental conditions were set and the testing rig provided reliable and repeatable results in the dry environment, the commissioning process continued on wet abrasion testing conditions. The preliminary testing phase

confirmed the performance of the new abrasion tester and contributed to the experimental development process.

4.4.1. General Dry Commissioning Testing Procedure

The standard G65 experimental procedure was followed during the commissioning process and subsequently for all the tests performed on the abrasion rig in dry conditions. This procedure is outlined below:

a) Specimens were cut and machined as per the ASTM G65 standard. Before each test, samples were cleaned with a cloth and demagnetized.

b) Before each test, each specimen was weighted on a BL-150 Sartorious digital scale with three digit resolution.

c) The sand flow rate was checked before each set of three tests. This was based on an average of three readings of sand flow rate.

d) The wheel sliding speed and the revolution counter was checked prior to the start of a test trial.

e) The test specimen was loaded in the sample holder and aligned against the center of the rubber wheel. The level arm mechanism was adjusted accordingly in order to level the load with respect to the specimen-rubber wheel contact area.

f) The sand valve was opened to allow silica sand to flow into the gap between the rubber wheel and the specimen, and then the motor drive was turned on to start the abrasion test.

g) Once the number of wheel revolutions was completed, the test was stopped. This was done by closing the valve to the sand flow, and stopping the motor. The specimen was then taken from the sample holder for final measurements.

h) The obtained wear scar on the specimen's face was inspected, and the specimen was weighted again to determine the amount of mass lost.

Steps "a" to "h" are repeated for each test and data is recorded for further analysis. For all tests conducted on the AISI D-2 tool steel, recycled 50/70 US mesh silica sand was used for convenience and cost reduction during commissioning.

4.4.2. Dry Sand Rubber Wheel Commissioning Results

In total, 11 test trials were performed during dry sand rubber wheel commissioning to achieve the optimal performance of the system.

Table 5 describes the results obtained from these first commissioning tests and the corresponding actions to improve the performance of the system. . In the dry environment commissioning process, the important testing parameters for measurement were: sand flow rate and sand curtain alignment.

Table 5 – Dry abrasion testing parameters

Test #	Testing Parameter	Outputs	Correcting Action
1	Sand nozzle location	• Some problem occurred with buildup of sand on top of the sample holder. • Uneven wear scars on specimens, probably improper alignment of sand curtain with the specimen.	• Sand flow rate was checked. • Sand nozzle was relocated at 24.5 mm of vertical distance from contact zone. • Specimen holder alignment with rubber wheel was checked.
2			
3			
4	Sand flow curtain	• Uneven wear scars still showing in the results.	• Sand nozzle angle with respect to specimen's faces was checked and adjusted by rotating the sand nozzle.
5			
6			
7	Wear scars on specimens and volume loss of material	• Wear scars were more evenly shaped after sand nozzle adjustment in these trials, and the volume loss was within the expected range.	No modifications made.
8			
9			
10			
11			

As can be seen in the graph in figure 16, the volume loss of material varied from 32.86 to 41.56 mm^3 for the AISI D-2 tool steel in 11 test trials period while performing set up modifications on the tests. After these changes, the system operated as a conventional G65 apparatus.

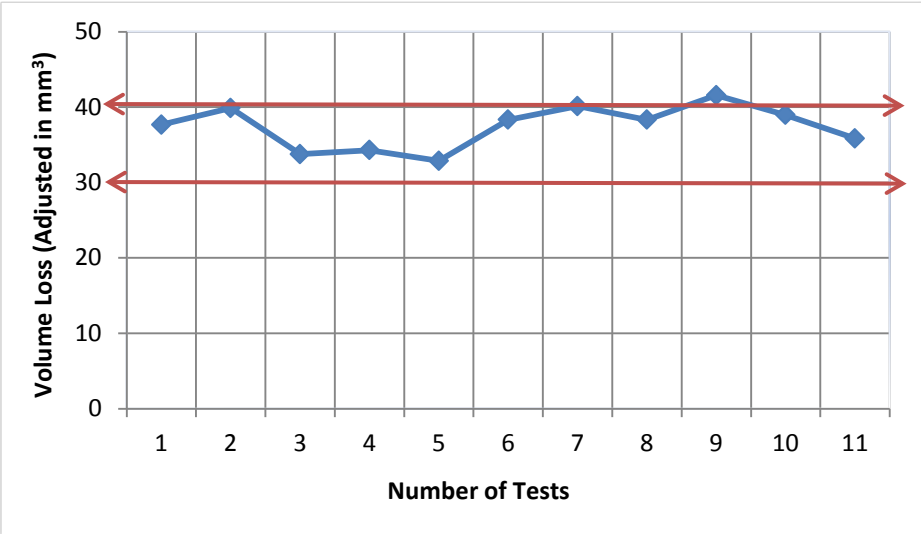

Figure 16 - Dry sand rubber wheel commissioning results.

The desire range of volume loss results (30 – 40 mm^3) per ASTM G65 was achieved in most tests.

4.4.3. Wet Sand Rubber Wheel Commissioning Results

Commissioning of the wet sand rubber wheel tester was conducted in conditions similar to the dry environment, with the addition of two more nozzles. One water nozzle was incorporated for mixing water and sand, and a second for washing out the slurry residue on the wheel once it had passed through the contact zone. This ensures the “one pass through” characteristics of the G65 tester.

A detailed description of the commissioning process and its outputs and correcting actions is provided in Table 6.

Table 6 – Wet abrasion testing parameters

st #	Testing Parameter	Output	Correcting Action
1 2 3 4 5	Water nozzle location	• Water nozzle was improperly located with respect to the sand nozzle and, as a consequence, partial clogging of sand nozzle occurred before completing the tests.	• The mixing water nozzle was relocated allowing a reasonable gap between it and the sand nozzle for facilitating the slurry mixing.
6 7 8 9 10 11	Water flow rate & sand accumulation on top of specimen holder	• At the beginning of the wet commissioning process, the water flow rate was too slow producing excessive accumulation of sand over the sample holder, which eventually tended to clog the sand nozzle over time. At other occasions, the water flow rate was too fast resulting in accelerated wear rates of the D-2 tool samples.	• An admissible water flow range was defined for the tests by performing repeated flow rate readings before and after each test and comparing wear results. An average value from three consecutive readings was adopted.
12 13 14 15	Water flow rate & water nozzle shape	• The stream of water was not uniform at the contact zone due to the shape of the nozzle.	• A flat shaped water nozzle was used instead of the original circular nozzle. • Wear results on specimens were compared, and the water flow rate was kept between 1.2 – 1.4 l/min. This was the “admissible water flow rate” which allowed optimal performance (i.e. avoided the wash away of sand particles from the specimens surfaces, and the accumulation of sand at the top of sample holder blocking the natural flow of the slurry).

The graph in Figure 17 summarizes the entire calibration process for the wet environment with silica sand on AISI D-2 tool steel as the reference material. After 24 trials, it was deemed that the variability between trials was acceptable, at less than +/- 2 mm^3. The graph illustrates a great variability in volume loss at the beginning of commissioning as a consequence of manipulating set up conditions to optimize the testing procedure. However, after trial number 15 the variability tendency started to narrow down depicting more controlled and repeatable results.

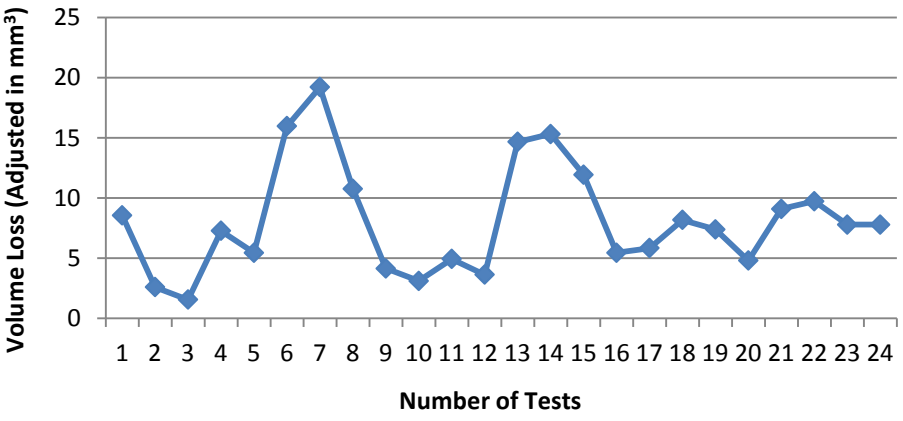

Figure 17- Wet sand rubber wheel commissioning results

The wet sand commissioning process required further system adjustments for dry sand conditions. The addition of water to the tribological dynamics of the machine introduced another challenge, establishing a mixing flow rate at which water and sand continuously flow through the contact zone without causing any stoppages to the testing process (that is, without splashing or losing particles from the contact zone).

4.4.4. Preliminary Testing on Polyurethane Composites

This phase in the experimental methodology played a very important role in the direction of the present study. It provided insight regarding two main aspects of the research: (1) The experimental procedures to follow when conducting wet abrasion tests on plastic composites, and (2) whether it would be possible to effectively conduct wet abrasion tests on plastic composites with a rubber rimmed wheel on the G65 set up.

To address these concerns, tests were conducted on unreinforced polyurethane composite samples in wet conditions, firstly with a rubber wheel, and secondly with a steel wheel. The results obtained with the rubber wheel were convincing in the fact that it is not possible to run tests on plastic composite materials in the G65 set up for wet conditions. Due to the nature of the materials involved (wheel & specimen) and the frictional forces acting in the rubbing process against each other, the level of damage on both was severe and highly variable, and thus not useful at all for the objectives of this study. Figures 18 and 19 show typical wear scars, which include gouging and apparent tears, not typical of rubber or polyurethane in abrasive sand conditions. For this reason, testing the polyurethane composites in wet abrasion conditions was done with the steel wheel and not with the rubber wheel.

Figure 18 - Wear scar on PU sample tested with rubber wheel

Figure 19 - Worn rubber wheel after wet test with PU

Preliminary tests were also run with a steel wheel under wet conditions. During the initial part of the test it was observed that the steel wheel lost its surface roughness due to abrasion of the sand. This left the wheel with a very smooth surface which reduced its ability to direct the sand towards the specimen contact surface. This was evident when running the second or third test in a row with the same wheel and noticing that the wear pattern on the plastic composites and wheel was uneven. This suggests that the steel wheel will need to be roughened prior to any subsequent test. This is possible by running the steel wheel against a harder material (D-2 tool steel) in dry conditions for a period of 1,000 rpm until its surface was even (roughness is visually and tactilely noticeable).

4.4.5. Volume Loss Sensitive Factors in X -70 steel and PU Composite Tests

Tests results on X-70 steel and PU composites were found to be directly affected by these two experimental factors:

Steel wheel roughness: As previously mentioned in the preliminary tests section, when testing in both conditions, dry and wet environments, the wheel surface played an important role in helping in the adherence of sand particles to the contact zone. Moreover, it was observed that whenever the wheel's surface was rough (control condition), more sand particles were able to penetrate in the

contact zone and consistently abrade the specimen surface than when the steel wheel surface was very smooth. This was observed in all tests conducted on both types of materials, X-70 steel and polyurethane composites. For the polyurethane specimens, a more defined texture and deeper wear scar was observed as a result of using a rough steel wheel compared to a smooth surface wheel.

Water and sand flow rate: According to the literature review, this experimental factor can impact in wear rates results. Increase in flow rate of the slurry can produce the specimen's contact area to wear at a higher rate. However, manipulation of higher volume rates of slurry flows is subjected to a limit at which the slurry does not go between the sample and the wheel. Moreover, experimental issues arise as a consequence of this condition (i.e. a dense slurry mix that causes the sand nozzle to clog, or the water to completely wash away the sand from the gap between the sample and the wheel). For this reason, and due to the experimental need to reproduce dense slurry flows in the testing apparatus, the low slurry flow rate was considered the control testing condition.

After many attempts during the commissioning of the test rig, it was determined that the appropriate sand flow rate was between 315 and 350 g/min and between 1.20 – 1.40 l/min for the water flow.

4.4.6. Low Dissolved Oxygen Tests on X-70 steel

Once the testing rig was adapted for running wet abrasion tests with de-aerated water instead of tap water, a set of trials was conducted using water with low dissolved oxygen (DO). The intent was to determine the effect of oxygen on the results of wear and corrosion interaction. The modifications and experimental considerations included for these tests are described below:

Water was collected in a 270 liter cylindrical tank prior to being used for the tests.

De-aeration or reduction of dissolved content of oxygen in water was achieved by purging nitrogen gas into the water for a period of approximately 1.5 hours.

Once ready, the de-aerated water was pumped to the wet G65 machine by a small submersible pump located inside the tank.

Dissolved oxygen content was measured before and after the de-aeration process (see figure 20), and right after each abrasion test with a portable dissolved oxygen probe.

Nitrogen purging rate was kept constant (20 psi) during the water de-aeration process and then reduced to maintain a nitrogen blanket over the water and to compensate air mixing with water during the pumping process.

Volume loss results on X-70 steel samples were recorded for further analysis and comparison with previous wet abrasion tests performed with non-de-aerated water.

During water de-aeration process, it was observed to have initial values of dissolved oxygen (DO) in water inside the tank of about 6.84 ppm. After 1.5 hours of de-aeration with N^2 the dissolved oxygen dropped to 0.51 ppm. Once the water was used for making the slurry and passed the contact zone it was collected in a container and the O^2 content raised up to a level of 3.72 ppm.

Figure 20 - Readings for dissolved oxygen content in water

4.5. Reporting of Test Results

The abrasion test results were reported as volume loss of material for all the different six materials covered in this study. The determination of density values for the polyurethane (PU) composite samples was done following the procedure described in the "Standard Test Methods for Density and Specific Gravity (Relative Density) of Plastics by Displacement," according to ASTM D792-08 standard (ASTM. 2008). The conversion of mass loss to volume loss was done by the following equation:

$$Vol\ loss\ (mm3) = \frac{Mass\ loss\ (g)}{density\ (\frac{g}{cm3})}\ \text{x}\ 1000 \qquad (6)$$

After each test, in both dry and wet conditions, the wheels were inspected for wear damage. Four points along their outer diameter surface were defined for

measurement. The differences on wheel diameter before and after a test was recorded and included for reporting volume loss results of material.

After a series of tests, the testing wheels decrease in their diameter. As such, the scratching abrasion developed in the experiments will also reduce accordingly, which will provide an inaccurate volume loss value of material produced by the smaller wheels. The adjusted volume loss (AVL) equation was used for reporting final test results:

$$AVL = Measured\ volume\ loss\ x\ \frac{228.6\ mm\ (9\ in)}{wheel\ diameter\ after\ use} \qquad (7)$$

(Source: ASTM. 2001)

Chapter 5

5. Testing Results

The following chapter presents abrasive wear results obtained in the new G65 test rig with both, rubber and steel wheel. Comparisons between both testing conditions (dry and wet) are also presented, including some sensitivity testing factors (steel wheel roughness, sand and water flow rates) considered before the testing phase. Wear characterization analysis of the test pieces is carried out through Scanning Electron Microscopy (SEM), and mass loss measurement of coupons after testing

5.1. X-70 Steel Alloy Wear Testing

Once the commissioning process of the wet G65 apparatus was completed, the first set of actual tests were conducted on X-70 grade alloy steel (reference material). This material was chosen for this study as it is the most common material used in slurry pipeline transport systems in the Alberta oil sands industry.

The assessment of abrasive wear on the X-70 samples was carried out in both dry and wet environments with both rubber wheel (RW) and steel wheel

(SW) on the modified G65 apparatus. Figure 21 illustrates the wear results for the X-70 alloy steel.

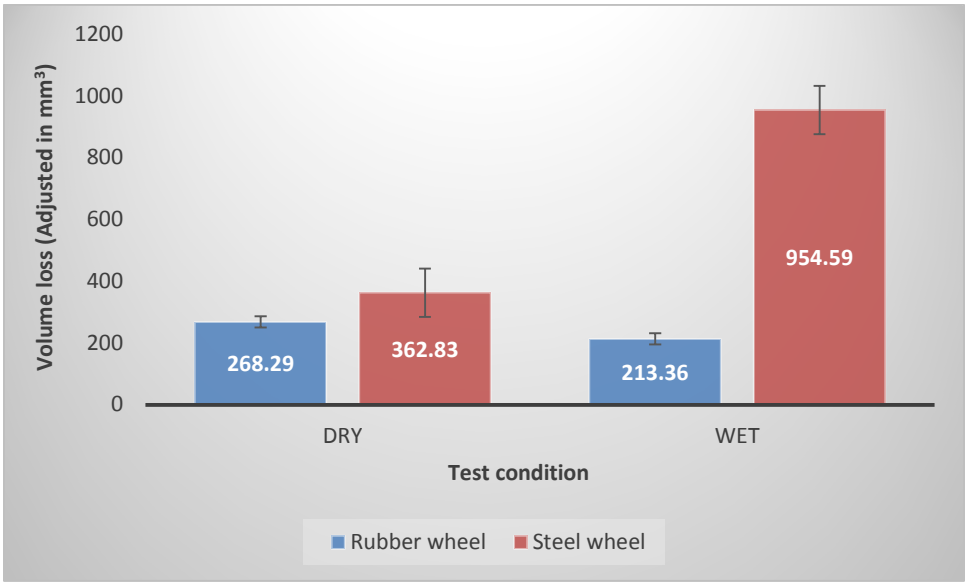

Figure 21- Dry and wet abrasion testing on X-70 steel.

Error bars in graph were determined by the standard error, calculated from dividing the standard deviation of the set of test trials by the square root of the number of tests conducted for each test condition.

In general terms, higher volume loss was observed in dry conditions on the X-70 samples than in wet, when the rubber wheel was used. It seems to be a lubricating action of the water that contributes to lower the wear rate of the material in the wet condition.. However, the completely opposite tendency occurred when comparing dry and wet wear results on the X-70 samples with the steel wheel. For the steel wheel, wet conditions always resulted in noticeable higher volume loss of material, in fact, it was the highest wear rate obtained out of the four case scenarios studied.

The results also showed distinctive wear patterns for each of the four combinations studied. Clean and smooth wear scars were observed on X-70 specimens tested in dry conditions with the rubber wheel (see Figure 22). However, for the steel wheel, some asperities were noticeable on the specimen surfaces when tested in dry conditions, showing roughness on both the specimen surfaces and the steel wheel after each test (Figure 24). Moreover, the surface texture was smoother on specimens tested on dry conditions, with both rubber and steel wheels, compared to those specimens tested with these same wheels in wet conditions.

Wear tests conducted in wet conditions with the rubber wheel show a different wear pattern on the specimen surfaces. Wear furrows were observed on X-70 steel specimens (and were repeatable), as can be seen in Figure 23. Less loss of material was observed in the lower center area of the specimens, resulting in a distinctive “peak”.

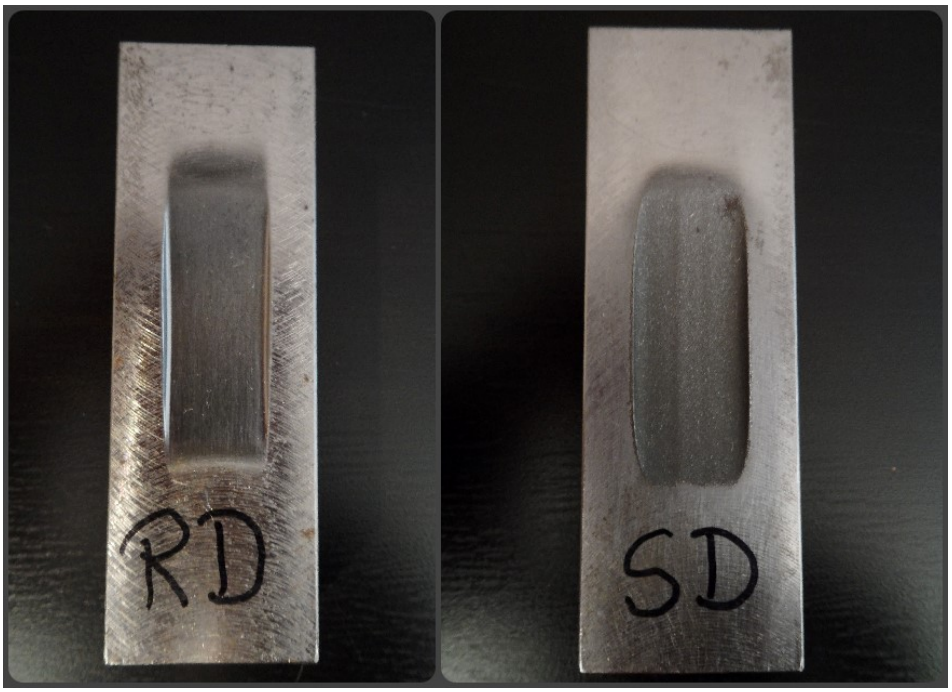

Figure 22 - Wear scars on X-70 steel samples (RD) and (SD)

From left to right: (RD) rubber wheel in dry conditions, (SD) steel wheel in dry conditions.

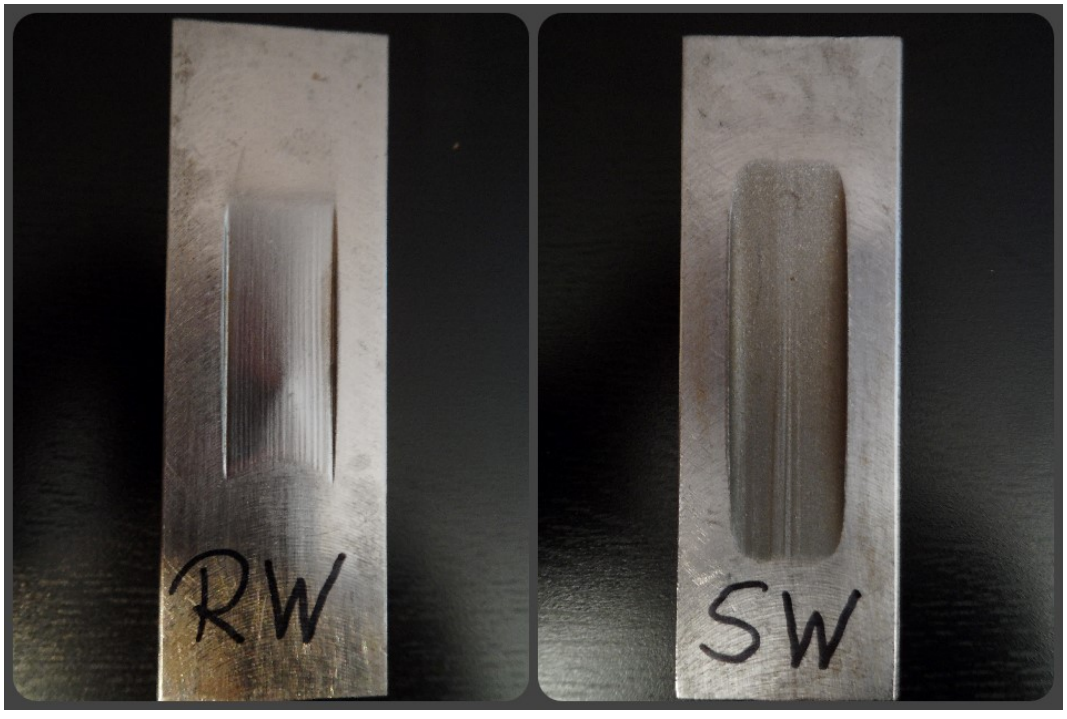

Figure 23 - Wear scars on X-70 steel samples (RW) and (SW)

From left to right: (RW) rubber wheel in wet conditions, (SW) steel wheel in wet conditions.

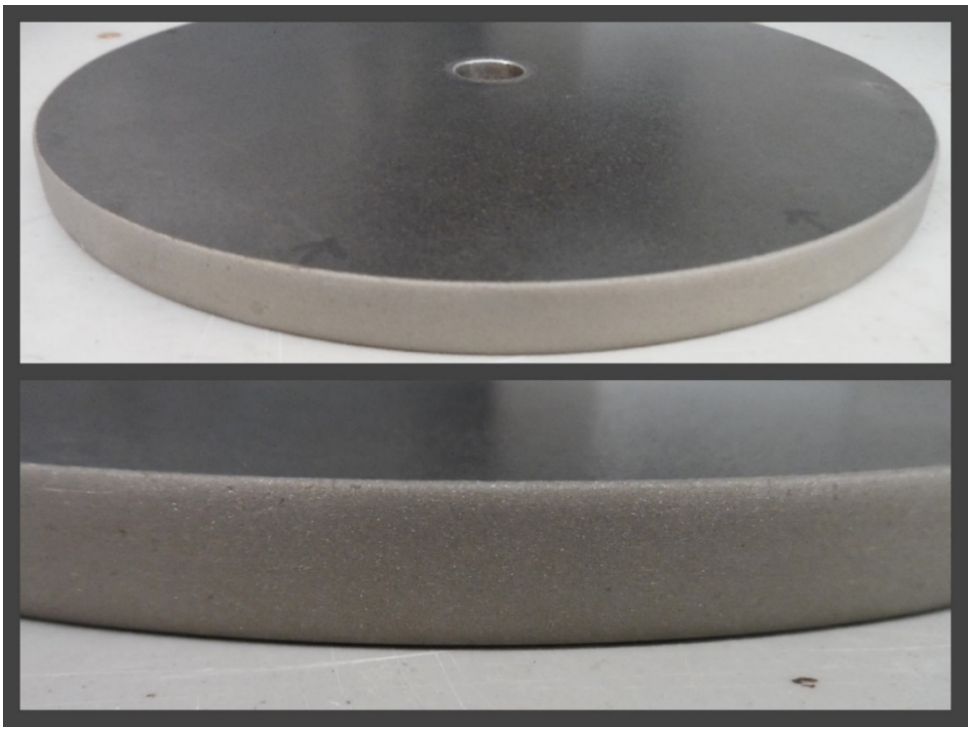

Figure 24 – Steel wheel surface roughness after tested on X-70 steel samples in dry condition.

As previously mentioned, the most severe wear was evident on the X-70 steel samples tested in wet conditions with the steel wheel. For this tests condition, the wear scars were remarkably deeper compared to all other three cases in this study. In these tests, the steel wheel wore out at a faster rate than in the dry condition tests. Wet abrasion tests also showed a well-defined wear pattern on the scar surfaces. Significant material removal, in the form of deep indentations and furrows, was observed longitudinally on the specimen surface.

5.2. Titanium Carbide (Ti-C) Reinforced Particulate PU Composite Wear Testing.

5.2.1. Testing Procedure: All tests conducted on the PU composites followed these steps:

a) The specimens were cleaned and weighted in a three figure scale.

b) For dry testing condition, the sand flow rate was checked before each set of three tests in the same material. Three readings of sand flow rate were taken and averaged for experimental results.

c) For wet testing condition, first the sand flow rate was checked as per the procedure in (b). Next, the water flow rate was adjusted to avoid clogging of the sand nozzle and washing away the sand from the contact zone. Water flow readings were taken and averaged.

d) The steel wheel was run against D2 tool steel samples at 200 rpm for a duration of 1,000 rpm in order to roughen the surface. This process was repeated right after each test conducted on PU samples.

e) The wheel diameter was measured after testing and used to adjust the calculated volume loss (see section 4.4.1).

f) Steps “a” to “e” are repeated for each test and data was recorded for further analysis.

5.2.2. Polyurethane Samples - Dry Abrasion Results

Tests were conducted on the five different PU particulate composites following the same parameters and conditions considered for the X-70 steel; however, only the steel wheel was used for all the tests. Wear rate results are shown in Figure 25.

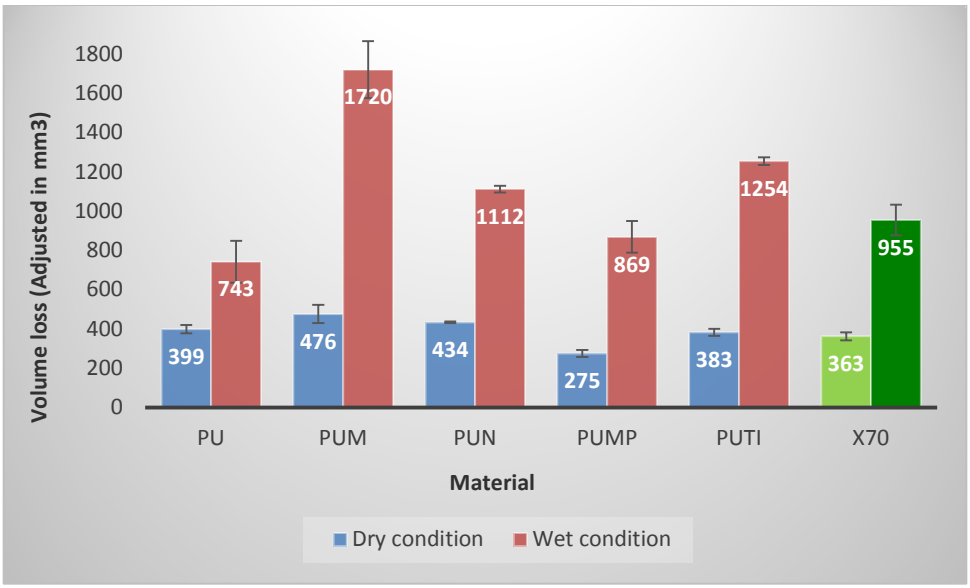

Figure 25- Dry and wet abrasion of PU composites compared to X-70 steel.

Error bars in graph were determined by the standard error, calculated from dividing the standard deviation of the set of test trials by the square root of the number of tests conducted for each test condition.

Wear results shown in figure 25 illustrated a remarkable wear resistance of polyurethane PUMP over all other materials tested in dry conditions (this includes the control material X-70 steel). It is important to highlight that un-reinforced PU had a relatively good wear performance in dry conditions among all test materials. It ranked third best option, after PUMP and X-70 steel. The PUMP is a titanium carbide polymer alloy spherically shaped, with a 1.6 micron ultra-high molecular weight polyethylene grains (UHMW PE) chemically bonded (Table 1). It`s a product designed for alloying with various polymer materials forming a very good abrasion resistant material, with good wear performance that can improve metal wear performance (Pacific Particulate Materials, 2012).

Wear on scars depicted a consistent wear pattern among all the materials tested. No considerable differences in texture of wear scars were found, as shown in Figures 26, and 27. Only the reinforced polyurethane with 5 micron particles showed slightly higher wear rate on average compared to the other four.

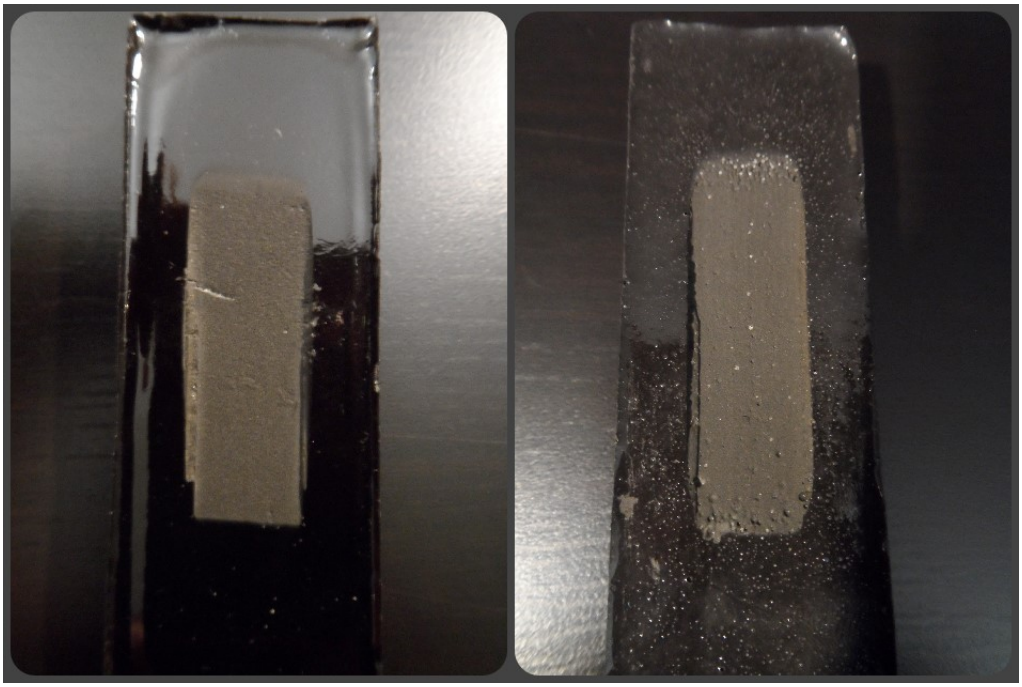

Figure 26 - Wear scars on un-reinforced PU (left) and PUM (right) samples in dry conditions.

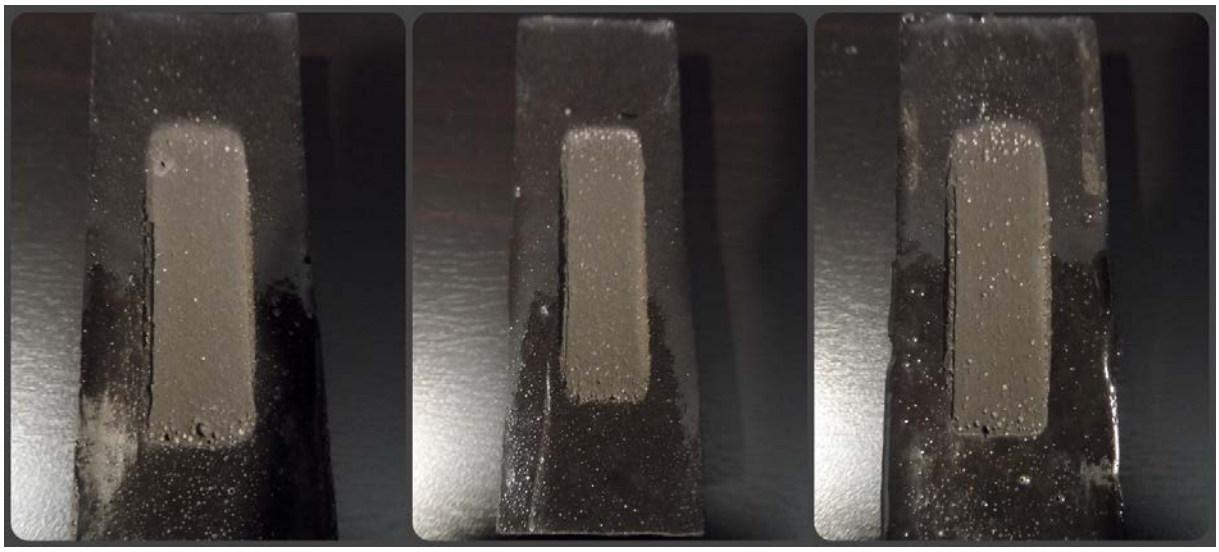

Figure 27 - Wear scars on PUTI (left), PUN (middle), and PUMP (right) samples in dry conditions.

5.2.3. Polyurethane Samples - Wet Abrasion Results

Wear rates obtained from test conducted on polyurethane samples in wet conditions are shown in Figure 25. Similar to the tests conducted in wet conditions on the X70 steel samples (section 5.1), all the tests conducted on polyurethane composites in wet conditions resulted in higher volume loss of material and more defined and deeper wear scars on the specimens compared to their dry counterparts (Figures 28, and 29). The reinforced PU with 5 micron TiC particles (PUM) was the material with the highest volume loss recorded for both testing conditions (dry and wet), while the reinforced PU with 0.6 micron TiC particles (PUN) had a more consistent pattern as for the volume loss values and performed better than PUM. This suggested that smaller particle sizes (Nano) in the re-enforced polyurethane samples did contribute in increasing cohesion among

particles in the material and as such, improve the wear resistance of this particular PU, with respect to the micro version of this material. The reference material (X-70 steel) had a slightly better performance than PU un-reinforced in dry conditions. However, in wet conditions the superior performance of the un-reinforced PU was evident, not only compared to X-70 steel, but also to all the other four re-enforced polyurethane materials. X-70 steel performed as second best option in dry environment, after PUMP, and third best option in wet environment, after PU and PUMP respectively. Between the two chemically re-enforced polyurethanes, PUMP performed better than PUTI in both testing environments.

In all samples, except PUMP, a repeatable wear pattern was observed (Figures 28, and 29). For PUM, deeper and longer wear scars were observed in the specimens as evidence of the steel wheel penetrating more into the specimen surface and consequently generating more severe wear. For the PUMP, the wear scar features were distinct.

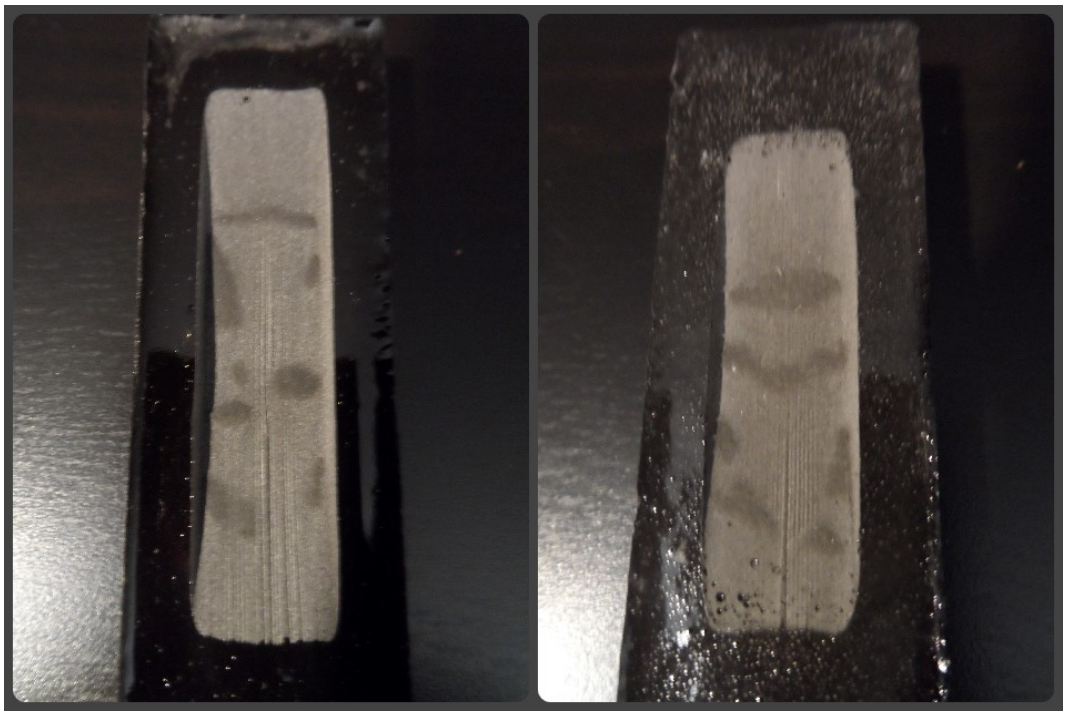

Figure 28 - Wear scars on un-reinforced PU and PUM composite samples in wet conditions

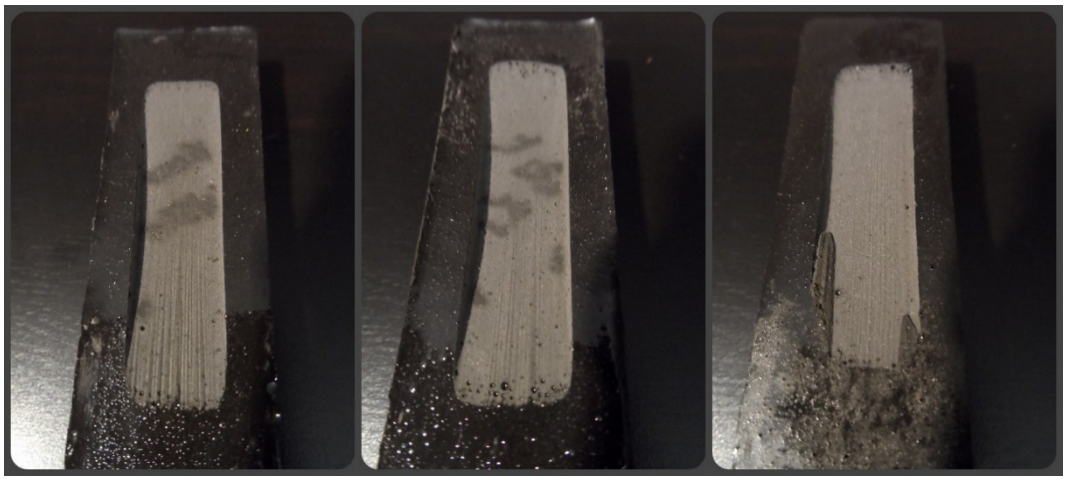

Figure 29 - Wear scars on PUTI (left), PUN (middle), and PUMP (right) samples in wet conditions.

5.3. Extra Wet Abrasive Testing

In order to study the effect of pre-conditioning factors of the testing materials (i.e. effect of polyurethanes exposed to moisture prior wear testing), and the synergistic effect that corrosion may have with slurry abrasion of X-70 steel samples, two additional set of tests were conducted in the apparatus.

5.3.1. Pre-soaked PUTI sample Test

Test were conducted on PUTI samples immersed in water for three periods of time: 1 week, 2 weeks and 3 weeks. The samples were weighted on a digital scale before and after being immersed in water. Their dimensions were also taken before and after being in contact with water. Due to the flexible nature of the PU composites and their irregular cutting, many dimensions were taken and averaged for the records.

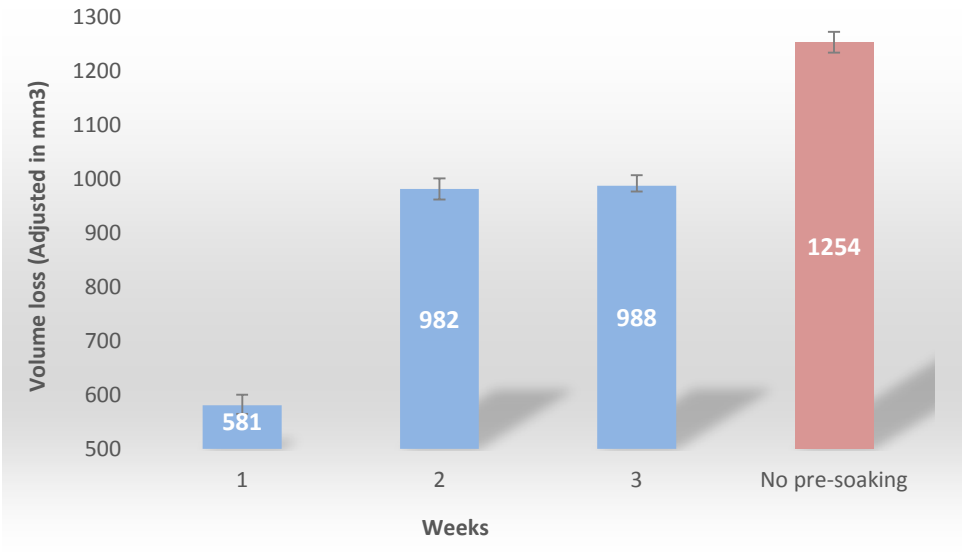

Figure 30 - Pre-soaked in water PUTI wet abrasion tests.

Error bars in graph were determined by the standard error, calculated from dividing the standard deviation of the set of test trials by the square root of the number of tests conducted for each test condition.

The results obtained from the pre-soaked of PUTI samples prior to abrasion testing are shown in Figure 30. It was observed a considerable variability in volume loss of material compared to the controlled test condition (no pre-soaking of specimen) on the same material. Wear rate differences were very evident after pre-soaking the PUTI specimen for one week. However, for the two and three weeks groups of tests, the tendency of higher wear rate results close to the control condition was observed. The number of specimens available for testing was very limited, therefore, only one specimen per time frame was used for the experiments. These results show an unexpected tendency of increase of wear rate as the polymer stays for longer periods of time immersed in water. The type of sample used for this experiment was a reinforced polyurethane with surface modified structure. This PU material is formed by TiC particles with an

average size of 1.2 to 1.6 micron that are part of a bonded chemically reactive layer forming a sheath around the organic polymer matrix resin. This being said suggests that more tests should be conducted in order to have a better understanding of this particular polyurethane structure and its effects over moisture absorption, hardness and wear resistance (Pacific Particulate Materials, 2012).

5.3.2. Low Oxygen Wear Tests Results

Low dissolved oxygen (DO) wear tests were conducted on X-70 steel samples and the results are shown in Figure 31. Additionally, results of testing with the two sensitivity factors previously mentioned (wheel roughness and water flow rate) in section 4.4.5 are also illustrated.

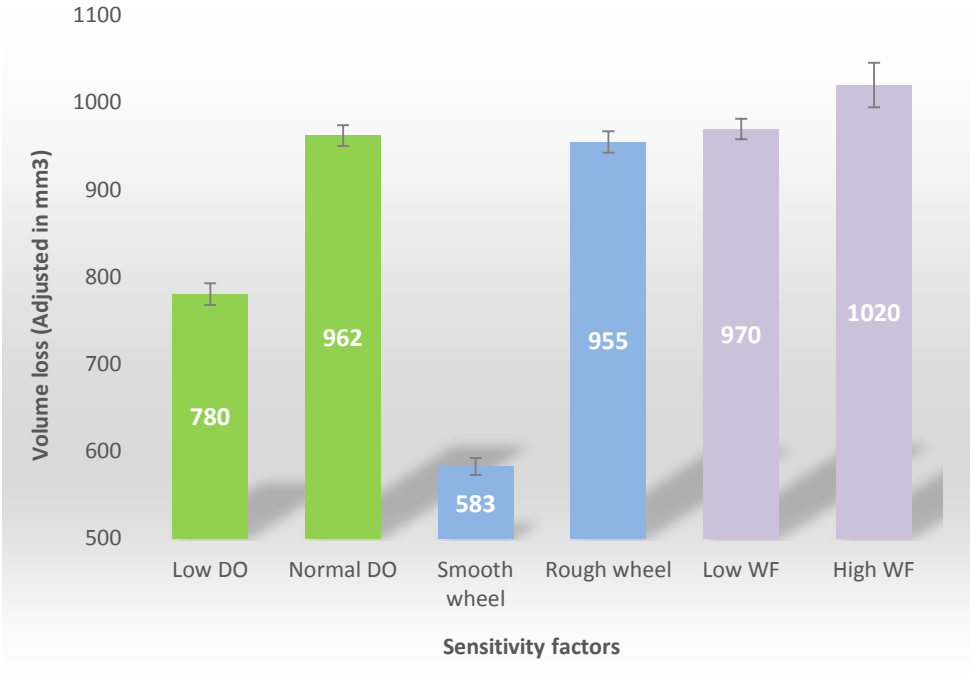

Figure 31 - Sensitivity factors in wear rate results on X-70 steel.

Error bars in graph were determined by the standard error, calculated from dividing the standard deviation of the set of test trials by the square root of the number of tests conducted for each test condition.

The abrasion tests conducted on X-70 steel samples under low dissolved oxygen conditions confirm the tendency of obtaining higher volume loss values in the testing material when erosion and corrosion are acting together in a synergistic effect. The volume loss results obtained on samples with 0.5 ppm of dissolved oxygen in water were slightly lower (approximately 18% lower) in comparison to the results obtained for volume loss on the same material with the same testing conditions, with non-de-aerated water (6.54 – 7.15 ppm range of dissolved oxygen). The wear scars obtained were very similar to naked eye observation. This suggests that besides the presence of corrosion in the tap water sample group, the wear pattern mechanism was the same as in the low oxygen test group

and the damage magnitude did not increase considerably. Indentations were not observed on the worn surfaces.

It was also evident in the wet abrasion tests results shown in Figure 31 that from all three sensitivity factors previously discussed, the steel wheel surface roughness had an outstanding impact in volume loss results by reducing them by more than half when the steel wheel surface was smooth and not able to retain enough sand particles towards the contact zone. The second sensitivity factor considered in these results was the levels of dissolved oxygen in water prior testing. It is important to highlight that normal dissolved oxygen in water (Normal DO), a rough steel wheel, and low water flow (Low WF) were the control conditions set for the testing apparatus when commissioning and preliminary testing. Finally, the third sensitivity factor considered, water flow rate, showed evidence that can also affect wear rate results. However, due to the complexity of water and sand mixture in the experiments this variable can be only manipulated within certain limits without generating experimental inconveniences due to the experimental apparatus design and limitations (i.e. clogging the sand nozzle, due to its location and opening, or washing away the sand before it reaches the contact zone), and consequently the variation in terms of impacting volume loss results were low compared to the other two factors analyzed.

5.4. Wear Characterization by Scanning Electron Microscope Imaging (SEM).

Qualitative wear characterization for the scars obtained in the different coupons was done using a Zeiss EVO SEM with LaB6 crystal source, providing images in a magnification range of 20x to 100,000x, with a resolution of ~5 nm at the highest magnification.

The following figures present the wear tracks found in the X-70 steel samples (use as a reference material), after the abrasion tests conducted in dry and wet conditions with either the rubber or steel wheel. For all SEM images the direction of motion of the abradant and the wheels is from right to left. An arbitrary magnification of 1,000x was chosen in all SEM images for comparative purposes of the wear mechanism present in the test coupons.

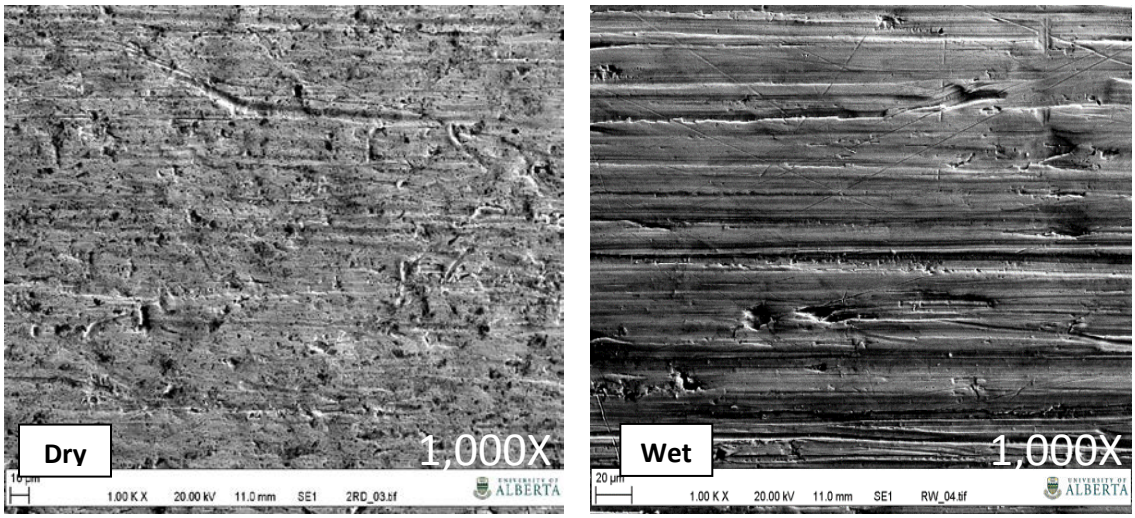

Figure 32 - SEM images of X-70 steel wear scars

Images resolution: 1,000x on left, dry abrasion scar with the rubber wheel. On right, wet abrasion scar with the rubber wheel.

These images show evidence of contrasting wear mechanisms observed on X-70 samples under dry and wet abrasion conditions. The dry abrasion figure illustrates a relatively smooth worn surface with very shallow grooves and several indentations parallel to the sand flow (right to left), possibly suggesting a three-body behavior since the sand particles were able to rotate freely when passing through the contact zone (Wirojanupatump 1999).

In contrast, the wet abrasion scar appears to show two-body behavior, possibly because sand particles adhered to the rubber wheel surface causing well defined and deeper furrows parallel to the sand particle motion on the specimen surface. There are clear indications of a ploughing damage mechanism. Indentations were less evident, however, there appeared to be some evidence of

cutting of small particles out of the material, leaving small, round holes behind. Major cracking of material was not observed in these conditions as appeared in the wear scars obtained with the steel wheel in dry and wet environments. Wear rates for wet abrasion testing on X-70 was observed to be considerably more severe, than for dry testing conditions. The two body wear mechanism appears to have a deeper impact in material removal from the specimen's surface, than the observed for the three body mechanism. Moreover, the dynamic system water-sand plays an important role in abrading metal compared to only sand. The effects of water in an abrasive slurry mix are still under extensive research and are not part of the experimental objectives covered in the present research.

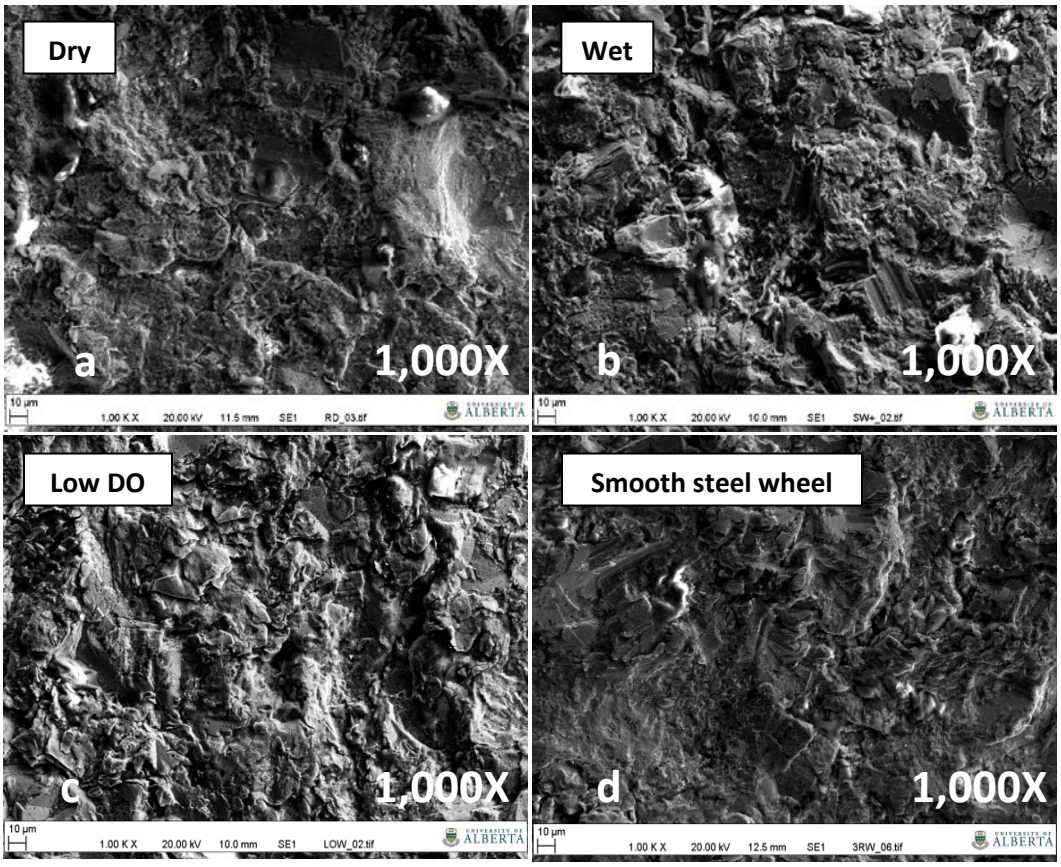

Figure 33 - SEM images of X-70 steel wear scars with a steel wheel

Images resolution: 1,000x a)dry abrasion condition. b)wet abrasion condition. c)low oxygen in wet abrasion condition. d)wet abrasion with steel wheel's roughness sensitivity (smooth wheel surface) testing.

As observed in the previous figures, the most noticeable wear mechanisms present on the X-70 samples worn in both dry and wet conditions with the steel wheel appear to be fracture and pluck-out of material. This gave a repeated damage pattern in all the four cases analyzed, but a little less severe in the dry abrasion condition. By contrary, in wet abrasion condition, (the most severe case of wear), it was observed in the SEM picture that very few micro grains of material (polyurethane sample) were left on the specimen's surface as a sign of a more severe material degradation and removal mechanism. When observing the

resulting wear scar of this case, sign of severe damage condition was evident with a deeper wear scar on the specimen surface compared to the other cases studied. Wear rates for this set of tests showed its highest values for wet condition, followed by wet condition testing with low dissolved oxygen, and finally by dry condition (in decreasing order). Two body wear mechanism was evident for the tests conducted in wet environment, however, the synergistic effect of erosion-corrosion showed some variability in wear rates for the same material, with the same damaging mechanism occurring in both tests conducted in wet environment. In both cases, the wear rates were higher than the observed in dry testing environment, in which the three body wear mechanism was present.

The test conducted with a smooth wheel surface (roughness sensitivity) showed less evidence of damage on the specimen's wear scar to the naked eye observation. However, it was difficult to distinguish remarkable differences (at a microscopic level) to the other test cases analyzed.

The particulate-reinforced polymer samples showed a similar wear behavior to that observed on the X-70 steel samples, in terms of some evidence of embedding of particles and little grooving on the specimen surface. However, a particular wear pattern arose in these tests and it was clearly noticeable the formation of small raised areas, as seen in Figure 34. These appear towards the center and lower centered sections of the wear scars on all the polyurethane

specimens, except for the polyurethane PUMP samples. This particular wear pattern was repeated with more or less severity in the four types of polymer materials tested in wet abrasion conditions with the steel wheel.

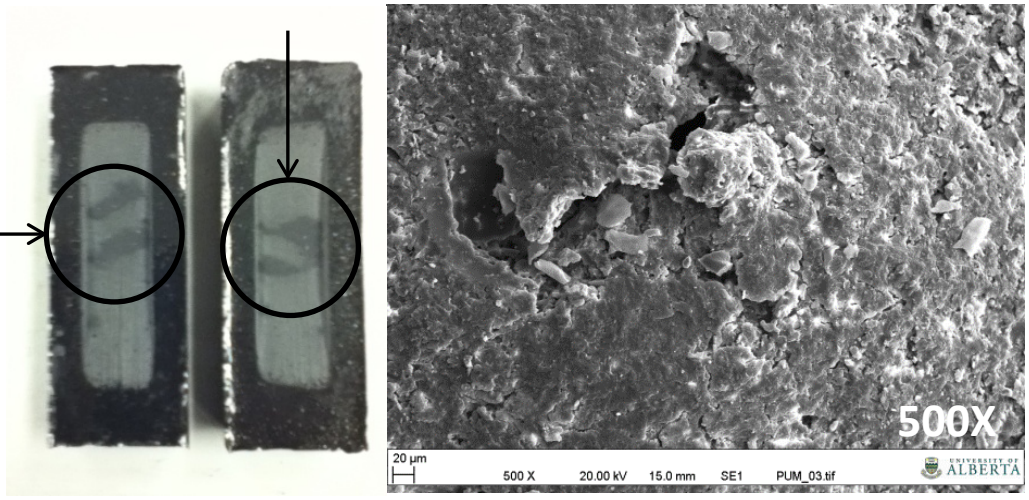

Figure 34 - PU 5 micron TiC (PUM) and SEM raised scar area image.

SEM image resolution: 500X. On left, PU 5 micron TiC (PUM) with raised wear area on scar. On right, SEM image of raised wear area on scar of (PUM) 5 micron TiC.

The raised area pattern on the wear scars might suggest more accumulation of sand particles towards the center of the specimen surface than the top or lower areas during the abrasion testing process. This could possibly be due to the adhering action of the steel wheel surface over the sand particles at the beginning and during one third of the duration of the test (2,000 rpm of testing). It has been observed that around this point in the testing process the steel wheel loses roughness on its surface due to the continuous friction with the sand particles that are adhered to the polymer material; and in order to conduct another test on a PU sample the wheel needs to be rubbed against hard steel material in

dry conditions in order to recover its roughness again. Another factor that might interfere in the wear patterns observed in the polymer samples could be the material properties associated with each group of PU samples in particular. This might be of interest when comparing wear scars on PUMP and not finding raised worn surfaces as in the other four PU specimens. The PUMP samples were chemically treated polymers with ultrahigh molecular weight polyethylene for improvement of abrasion resistance, corrosion resistance and high mechanical performance. This suggests a different structure of this particular polyurethane in comparison to the other four polyurethanes under study. Further structure analysis of this material should be conducted in order to determine effectively the elements that impact in material degradation and wear mechanism present in this type of polyurethane.

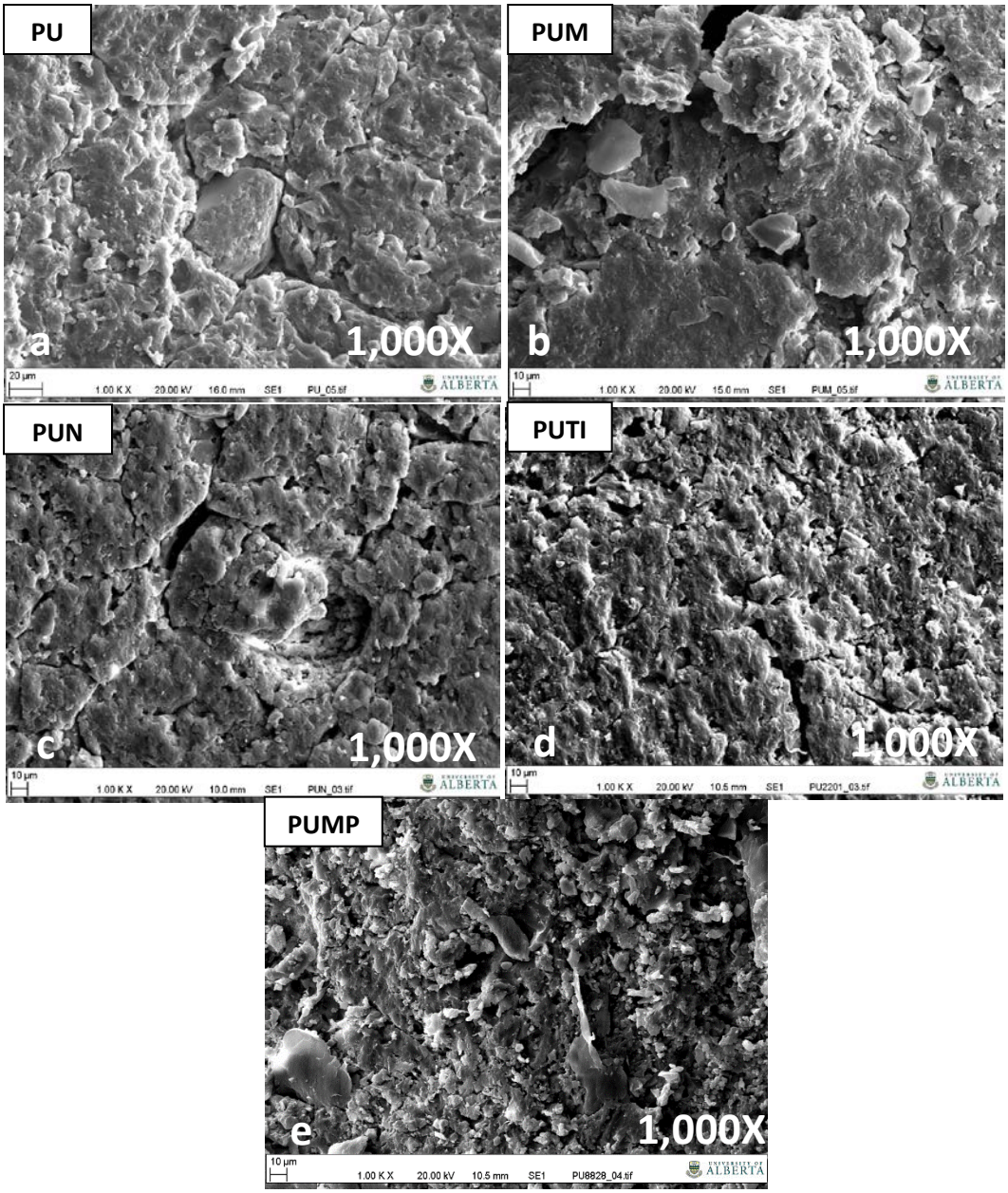

Figure 35 - Wear scars of PU composites tested in wet conditions

Images resolution: 1,000X. a)unreinforced polyurethane (PU); b)5 micron TiC (PUM), c) 0.6 micron TiC (PUN), d)PUTI (1.2-1.6 micron); e)PUMP (63 micron).

Among the four types of PU specimens in which a worn raised area was observed, a very particular case was observed on the PUM specimens (as previously mentioned and illustrated on Figure 34). The PUMP samples, by contrary, did not show this type of worn scar textures on the specimen's surfaces. This suggests that the reinforced chemically structure of this polymer affects the mechanical deterioration of the material when exposed to abrasion wear. However, more studies should be conducted in order to investigate the structure and chemical behavior of this particular polymer.

The SEM image of the PUM sample shows more material removal due to cracking and pluck-out than in the rest of the PU samples tested in the same conditions. These wear mechanisms were observed in the PUN and the un-reinforced PU samples, but with milder intensity. It is important to highlight the better performance of PUN compared to PUM. This clearly suggests that the grain size of particles did play an important role in increasing the cohesion among particles in the polyurethane nano, and thus increasing its wear resistance. The PUTI SEM image illustrates evidence of indentations of sand particles over the specimen, but very little signs of material removal by cracking or pluck-out, just like in the previous three PU materials mentioned. This chemically re-enforced polyurethane presented a lower wear performance compared to its similar, the PUMP polyurethane. Finally, the PUMP shows indentations with shallow holes on the specimen surface similar to the ones observed on the X-70 steel sample tested in dry abrasion conditions. Generally, the wear acting mechanisms were

repeated in all the polyurethane specimens studied, with more or less severity in some cases, as previously indicated. The wear rates for four PU showed a slightly variability among them, however, a remarkable difference was observed for the PUM in which the highest wear rate was recorded. It is very important to highlight the outstanding performance of the un-reinforced polyurethane in wet conditions, compared to the rest of reinforced polyurethanes and the X-70 steel. This material alone, without any particle size or chemical reinforcement showed better wear resistance in a slurry testing condition, suggesting that it might be a good option to consider when choosing materials for lining a slurry pipeline application operating under similar conditions.

Chapter 6

6. Conclusions and Recommendations for Future Work

The main objective of this experimental research was to obtain a better understanding of the wear mechanisms present in slurry erosive wear for pipeline applications. In order to achieve this purpose a modified version of the dry sand rubber wheel apparatus (also known as the ASTM G65) was designed and built for conducting dry and wet scratching abrasion testing on six different types of materials: X70 steel, un-reinforced polyurethane particulate samples and 4 different types of polyurethane reinforced composite based on titanium carbide particles (TiC).

6.1. Conclusions

The following conclusions were derived from this study:

- The standard G65 test method can be used to assess the scratching abrasion in dry and wet conditions of different types of materials. However, in this particular study, the rubber wheel incompatibility with

the polyurethane specimens analyzed, limited the tests to use only steel wheel in both testing conditions (dry and wet).

- During commissioning the wet G65 apparatus, adjustments were made during preliminary testing and final setup for low dissolved oxygen abrasion testing with X-70 steel samples. Sensitivity factors such as slurry rate and steel wheel roughness were also investigated as part of the elements that might affect wear rate results.

- In general, results showed higher wear rates in dry conditions than when water was involved for the classic rubber wheel tests on the G65 apparatus. Whereas, wear rates were considerably higher in wet conditions on the X-70 steel when a steel wheel was used instead of the rubber wheel.

- The X-70 steel samples were assessed for dry and wet abrasion with both rubber and steel wheel. When testing X-70 steel in dry and wet conditions with the rubber wheel, contrasting wear mechanisms were observed on the SEM images. Three-body abrasion and several indentations with very smooth wear scars were obtained on the dry abrasion conditions. On the other hand, deeper furrows depicting a ploughing damage mechanism were evident on the wet abrasion condition. This particular case suggested a two-body abrasion dynamic instead of a three-body wear mechanism. Wear rates for wet abrasion testing on X-70 steel was more severe than for

dry testing conditions. The two body wear mechanism appears to have a deeper impact in material removal from the specimen's surface, than the observed for the three body mechanism. In addition, the role of water in the abrasive slurry mix is still under extensive research and is part of a complex dynamic that might impact wear rate and damaging mechanisms. This was beyond the objectives of the present research.

- The X-70 steel samples had a more consistent wear behavior when tested with the steel wheel in dry and wet conditions. Evidence of fracture and pluck-out of material was found in all cases analyzed with this material; however, the mildest wear condition was observed in the dry abrasion case, and the most severe in wet abrasion condition.

- As part of a sensitivity factor study on wear rate on the polyurethane samples, a set of tests were conducted with steel surface sensitivity roughness (a smooth wheel surface was used). This resulted in considerable less wear rates compared to a rough wheel surface. This sensitivity factor ranked first among the three considered in this research (Steel surface roughness, low levels of dissolved oxygen in water, and water flow rate). Results showed that the steel wheel surface was not capable of retaining sand particles and lead them to the contact zone in order to abrade the polymer under study.

- Another sensitivity factor studied for wear rate was the effect of moisture on PUTI samples prior to abrasive testing. For this set of tests PUTI samples were pre-soak in water for one, two and three weeks respectively. Generally, volume loss was always lower when the specimens were pre-soaked in water prior testing. It was observed a considerable difference in wear rate for the first week pre-soak PUTI sample, with respect to a not pre-soak specimen (controlled condition). About half of volume loss was recorded for wear rate results. However, this tendency was not repeatable in the other two time groups, an increase of wear rates was observed for two and three weeks of pre-soaking the PUTI samples in water before the tests. Factors such as the chemically reinforcement of the PUTI samples with a bonded chemically reactive layer forming a sheath around the organic polymer matrix resin suggests this particular polymer should be subjected to further structure analysis.

- A group of X-70 steel samples were tested with low dissolved oxygen levels (about 0.5 ppm, compared to almost 7 ppm in regular tap water) in an effort to investigate erosion-corrosion synergy in wear rate results. For this set up water was previously de-aerated by purging nitrogen gas on it for a certain time prior to running the tests. This confirmed the hypothesis of synergism between erosion and corrosion processes in this experimental setting. Wear rate results were slightly lower in comparison to the ones obtained with non-de-aerated water.

- The Polyurethane particulate samples were tested for dry and wet conditions like with the X-70 steel, but only the steel wheel was used due to the incompatibility between the rubber wheel and the PU specimens. Main attention was given to the wet abrasion testing results, in which the wear mechanisms analyzed on the SEM showed evidence of embedment of particles and little grooving over the test pieces. In general, wear mechanisms such as cracking, pluck-out, and indentations were repeated in all the polyurethane specimens studied, with more or less severity. The un-reinforced PU showed the best wear performance for slurry test conditions, when compared to the rest of the polyurethanes and the X-70 steel. This material had lower volume loss results when compared to the particle size and chemical re-enforced polyurethanes, suggesting that this material alone without any structure or chemical modification, might be a good option for pipelining when the set of operating conditions are similar to the ones considered in this experimental research work.

- Particle size reinforcement played a considerable role in wear rate resistance in this experiments, as the polyurethane nano (PUN) generally performed better than polyurethane micro (PUM) in both testing conditions (dry and wet). This suggested a better cohesion among particles in the polymer that increased its wear resistance as these particles were smaller.

- A repeated raised wear scar was observed as a pattern on four of the five PU groups of samples. This was not present in PUMP specimens, which were specimens chemically treated with ultrahigh molecular weight polyethylene for improvement of abrasion resistance, corrosion resistance and high mechanical performance. This suggests a different structure of this particular polyurethane in comparison to the other four polyurethanes under study.

6.2. Recommendations for Future Work

The design and development of a laboratory scaled pipeline loop used for reference purposes in this particular study opens the door for more research on erosive wear mechanisms in slurry transport applications. More erosion-corrosion research should be done in order to accurately identify their particular damaging mechanisms and how they work together in a synergetic manner for slurry transport applications. Some research has been conducted previously on erosion-corrosion assessment in pipeline loops by (Ratnam Sankaran, 2004). However, uniformity in experimental concepts and methodology followed in the complex tribological world of dry and wet abrasion testing has not yet been achieved.

Some important recommendations are as follows:

- Further analysis on worn scar surfaces product of wear abrasion testing is suggested. Methods such as profilometry analysis of the worn surfaces obtained in this study should be conducted in order to clearly identify (by more than one characterization method), and predict wear abrasive behavior of X-70 steel and diverse reinforced polyurethane materials, intended to be used in slurry transport applications.

- New research should be conducted to better understand the role of water as a lubricant agent in the slurry mix dynamic, and how this impact two and three body wear mechanisms, and its effects in wear rate results.

- A structural and chemical analysis should be conducted of bonded TiC micro grain with active organic coating in the polymer matrix of polymers such as PUTI and PUMP. These formulas were introduced for the improvement of mechanical and physical properties of these materials. This showed differences in wear rates with respect to the other materials not chemically treated, and suggests that more testing and research should be done in order to better understand the effects of these structures on the wear mechanisms present and their wear rate results.

- More experimental work on assessing slurry testing conditions on different materials should be continuing this work, including scanning electron microscopy analysis, as efforts to identify stresses in different structure composition of a test material at a microscopic level. This will provide better understanding of the wear resistance behavior of chemical re-enforced polymers, as the non-re-enforced counterparts.

- More research should be conducted on phenomenological modeling of wear in slurry pipelines, so that the testing variables can be tuned to emulate the process conditions as much as possible. The concentration and velocity vectors of particles in the transition zone between the dense bed and the top layer should be examined.

References

1. ASTM B611-85: Standard test method for abrasive wear resistance of cemented carbides, in: ASTM standards, 2005. ASTM International, West Conshohoken, PA, USA.

2. ASTM D792-08: Standard test methods for density and specific gravity (relative density) of plastics by displacement, in: ASTM standards, 2008. ASTM International, West Conshohoken, PA, USA.

3. ASTM G105-02: Standard test method for conducting wet sand/rubber wheel abrasion tests, in: ASTM standards, 2002. ASTM International, West Conshohoken, PA, USA.

4. ASTM G65-04: Standard test method for measuring abrasion using the dry sand/rubber wheel apparatus, in: ASTM standards, 2004. ASTM International, West Conshohoken, PA, USA.

5. Andrews, P., Illson, T.F., and Matthews, S.J. (1999). Erosion–corrosion studies on 13 Cr steel in gas well environments by liquid jet impingement. Wear (233-235), pp 568-574.

6. Bartenev, G.M., and Laurentev,V.V. (1981). Friction and wear of polymers. Elsevier, Amsterdam.

7. Bharat, B. (2001). Modern Tribology Handbook, Vol 1 (pp. 276 - 296). Columbus , Ohio: CRC Press.

8. Bhushan, B. (2002). Introduction to Tribology, John Wiley & Sons, Inc. (pp 640-656), New York, USA.

9. Bourithis, G., and Papadimitriou, G. (2005). Three body abrasion wear of low carbon steel modified surfaces. Wear (258), 1775-1786.

10. Budinski, K. G. (1997). Resistance to particle abrasion of selected plastics. Wear, 203, 302-309.

11. Budinski, K. G. (2007). Guide to Friction, Wear, and Erosion Testing. Mayfield: ASTM International.

12. Brent W. Madsen, Measurement of erosion-corrosion synergism with a slurry wear test apparatus, Wear, Volume 123, Issue 2, 15 April 1988, Pages 127-142

13. Chen, H. Hutchings, I. M. (1998). Abrasive wear resistance of plasma sprayed tungsten carbide cobalt coatings. Surface Coating Technologies, (107), 106-114.

14. Clark, H. M., & Llewellyn, R. . (2001). Assessment of the erosion resistance of steels used for slurry handling and transport in mineral processing applications. Wear, 250(1-12), 32-44.

15. Davim, P. J., (2011). Tribology for engineers: a practical guide. (46-51 pp), Cambridge-U.K, WP woodhead publishing.

16. Doron, P., Granica, D., & Barnea, D. (1987). Slurry flow in horizontal pipes-experimental and modeling. Multiphase Flow, 13(4), 535-547.

17. Deuis, R.L., Subramanian, C., & Yellup, J.M. (1998). Three body abrasive wear of composite coatings in dry and wet environments. Wear, (214), 112-130.

18. Elalem, K., and Li, D.Y. (2001). Variations in wear loss with respect to load and sliding speed under dry sand/rubber-wheel abrasion condition: a modeling study. Wear, (250), 59-65.

19. Elalem, K. and Li, D.Y. (1999). Dynamic simulation of an abrasive wear process. Journal of Computer Aided Materials Design. (6), 185-193.

20. El Sayed, S., and Lipsett, M.G. (2009). Parametric modelling of wear in a slurry pipeline with bed flow. Department of Mechanical Engineering, University of Alberta.

21. El Sayed, S. MSc thesis, University of Alberta. Measuring Wall Forces in a Slurry Pipeline. Fall 2010.

22. Eskin, D., Leonenko, Y. and Vinogradov, O. (2004). On a turbulence model for slurry flow in pipelines. Chemical Engineering Science. (59), 557-565.

23. Evans, A. G., and Lancaster, J. K. (1979). Treatise on materials science and technology. Treatise on Materials Science and Technology, 16.

24. Finnie, I. (1995). Some reflections on the past and future of erosion. Wear (186-187). 1-10.

25. Gant, A.J., Gee, M., & Roebuck, B. (2005). Rotating wheel abrasion of WC/Co hardmetals. Wear, 258(1-4), 178-188.

26. Gant, A.J., and Gee, M. G. (2001). Wear of tungsten carbide–cobalt hardmetals and hot isostatically pressed high speed steels under dry abrasive conditions. Wear, 251(1-12), 908-915.

27. Gant, A.J., and Gee, M.G. (2006). Abrasion of tungsten carbide hardmetals using hard counterfaces. Refractory metals & hard materials journal. (24), 189-198.

28. Gant, A.J. and Gee, M.G. (2005). Effect of abrasive type and size in high-stress abrasion of hardmetals. National Physical Laboratory. (12), 1-11.

29. Ghabchi, A. et all. (2009). behaviour of HVOF WC-10Co4Cr coatings with different carbide size in fine and coarse particle abrasion. Journal of Thermal Spray Technology. Vol 19 (1-2), 368-377.

30. Giguere, R., Fradette, L., Mignon, D., and Tanguy, P.A. (2008). Characterization of slurry flow regime transitions by ERT. The Institution of Chemical Engineers. (10) 8-15.

31. Gillies, R.G. (2000). Modelling high concentration settling slurry flows. Canadian Journal of Chemical Engineering, 709-716.

32. Goodwing, J.E., Sage, W., and Tilly, G.P. (1970). Study of Erosion by solid particles. Proc. Institute of Mechanical Engineers, Vol. 184, 1969-1970, pp. 279-289.

33. Grigoroudis, K., and Stephenson, D.J. (1997). Modelling low stress abrasive wear. Wear. (213), 103-111.

34. Gupta, R., Singh, S.N., and Seshadri, V. (1995). Study on the uneven wear rate in a slurry pipeline. Bulk Solids Handling, 15(4), pp 603-607.

35. Hocke, H. and Wilkinson, H.N. (1978). Abrasive resistance of slurry pipeline materials. Tribology International, Vol. 11, 289-294 pp.

36. Hutchings, I.M. (1992). Tribology; friction and wear of engineering materials. (78-79; 98-101; 166-168; 192-194) pp; Boca Raton, Florida . CRC Press.

37. Jones, A.H., and Roffey, P. (2009). The improvement of hard facing coatings for ground engaging applications by the addition of tungsten carbide. Wear. (267), 925-933.

38. Kajdas, C., Harvey, S.S.K., and Wilusz, E. (1990). Enciclopedia of Tribology. New York - USA, Elsevier.

39. Kasparova Michaela, Zahalka Frantisek and Sarka Houdkova. (2010). WC-Co and Cr3C2-NiCr Coatings in Low- and High-Stress Abrasive Conditions. Journal of Thermal Spray Technology. (12), 412-424

40. Knuuttila Jari, Ahmaniemi Samppa and Mantyla Tapio. (1999). Wet abrasion and slurry erosion resistance of thermally sprayed oxide coatings. Wear. (232), 207-212

41. Levy, A.N., and Hickey, G. (1987). Liquid-solid particle slurry erosion of steels. Wear, Vol. 117, 129-158 pp.

42. Levy, A.N., Jee, N., and Yau, P. (1987). Erosion of steels in coal-solvent slurries. Wear, Vol.117, 115-127 pp.

43. Lipsett, M.G. (2004). Oil Sands Extraction Research Needs and Opportunities. The Canadian Journal of Chemical Engineering, 82(4), 626-627.

44. Lipsett, M.G. and Brushan V. (2011). Modeling erosion wear rates in slurry flotation cells. Springer, (12), 51-65.

45. Lipsett, M.G. (2012). Using parametric dynamic models to determine observability requirements for condition monitoring systems. University of Alberta, Department of Mechanical Engineering, 1-9.

46. Ludema, Kenneth C. (1996). Friction, wear, lubrication; A textbook in tribology. (127-138 pp),Boca Raton - Florida, CRC Press.

47. Luke, Jason. MSc thesis, University of Alberta. Pipeline Transport of Straw Slurry. Fall 2010.

48. Ma, X., Liu, R., & Li, D. Y. (2000). Abrasive wear behavior of D2 tool steel with respect to load and sliding speed under dry sandrrubber wheel abrasion condition. Wear, 79-85.

49. McI, H., and Llewellyn, R.J. (2001). Assessment of the erosion resistance of steels used for slurry handling and transport in mineral processing applications. Wear, (250), 32-44.

50. Nahvi, S.M., Shipway, P.H. and McCartney, D.G. (2009). Particle motion and modes of wear in the dry sand-rubber wheel abrasion test. Wear, (267), 2083-2091.

51. Neale, M.J., Gee, M. (2001). Guide to Wear Problems and Testing for Industry (pp. 3-6, 88-118). New York, USA.

52. Ness, E. Zibbell, R. (1996). Abrasion and erosion of hard materials related to wear in the abrasive waterjet. Wear, 120-125.

53. Particulate Materials Ltd. (2012). Carbide Metal Powder Products. Retrieved from http://www.ppm.bc.ca/Cermet_Carbide_Nitride_Powder_Products.html#TiC

54. Paterson, A. J. C. (2011). Pipeline transport of high density slurries: a historical review of past mistakes, lessons learned and current technologies, 121(1), 37-45.

55. Ratnam Sankaran, S. MSc thesis, University of Alberta. Erosion Corrosion in simulated oil sand slurry transportation. Spring 2004.

56. Ravi Kumar, B.N., Suresha, B. and Venkataramareddy, M. (2010). Effect of abrasives on three-body abrasive wear behaviour of particulate-filled Polymide66/polypropylene. Composites Interfaces, (17), 113-126.

57. Ravi Kumar, B.N, Suresha, B., Sailaja, R.R.N., and Venkataramareddy, M. (2010). Experimental investigation on the abrasive wear behavior of nanoclay-filled EVA/LDPE composites. Society of Plastics Engineers, 426-432.

58. Roco, M.C, and Addie, G.R.. (1987). Erosion wear in slurry pumps and pipes. Powder Technology, 50(1), 35-46 pp.

59. Ruff, A. W., and Bayer, Raymond G. (1993). Tribology; wear test selection for design and application. (45-59; 113-128 pp), Philadelphia, PA, ASTM International.

60. Safaei M., Hossein. MSc thesis, University of Alberta. Characterization and pipelining of biomass slurries. Spring 2009.

61. Salama, M. (2000). An alternative to API 14E erosional velocity limits for sand-landen fluids. Journal of Energy Resour. Technol. Trans. ASME 122(2), (71-77) pp.

62. Sanders, R. Sean, Schaan Jason, Hughes Roxby and Shook Clifton. (2004). Performance of sand slurry pipelines in the oil sands industry. The Canadian Journal of Chemical Engineering, Vol. 82, 850-857.

63. Sarka, Houdkova, Zahalka, Frantisek and Kasparova, Michaela. (2008). The influence of thermally sprayed coatings microstructure on their mechanical and tribological characteristics. Materials Science Forums, Vols 567-568, 229-232.

64. Shida, Y., and Fujikawa, H. (1985). Particle erosion behaviour of boiler tube materials at elevated temperature, Wear, Vol. 103, pp. 281-296.

65. Sasada, T., Oike, M. and Emori, N. (1984). The effects of abrasive grain size on the transition between abrasive and adhesive wear, Wear, Vol. 97, 291-302 pp.

66. Stachowiak, G.W., (2005). Wear, Materials, Mechanisms and Practice. (pp. 9 - 17; 269-286). England. John Wiley & Sons Ltd.

67. Stachowiak, G.W., and Batchelor, A.W., (1988). Predicting synergism between corrosion and abrasive wear, Wear, Vol. 123, 281-291 pp.

68. Stachowiak, G.W., and Batchelor, A.W. (2005). Engineering Tribology. 3rd edition. (502-505; 527-533; 580 pp), Elsevier.

69. Stephen, H., Scott, M. ASCE, & Steven, R. (2002). Hydraulic transport of fine and coarse sediment mixtures in pipelines. Journal of Transportation Engineering. (128), 1-8.

70. Stevenson, A.N.J., and Hutchings, I.M. (1996). Development of the dry sand/rubber wheel abrasion test. Wear, 195, 232-240.

71. Takadoum, Jamal. (2008). Materials and surface engineering in tribology. (66-67 pp), U.K, Willey.

72. Terva, Juuso et all. (2009). Abrasive wear of steel against gravel with different rock-steel combinations. Wear, 267, 1821-1831.

73. University of Calgary. How to write a literature review. (2011). Retrieved from http://pages.cpsc.ucalgary.ca/~saul/wiki/pmwiki.php/Chapter1/HowToWriteALiteratureReview

74. Vite, M., Castillo, M., Hernandez, L., Villa, G., Cruz, I., & Stephane, D. (2005). Dry and wet abrasive resistance of Inconel 600 and stellite. Wear, 258(1-4), 70-76. doi:10.1016/j.wear.2003.12.018

75. Vite, M., Carillo, J.N., Agiular, J., and Hilerio, I. (2003). Aqueous Abrasive Wear of 8620 Borided Steel. Materials Science Forum, 426(2), 1343 - 1348.

76. Wirojanupatump, S. (1999). A direct comparison of wet and dry abrasion behaviour of mild steel. Wear, 233-235(1-2), 655-665.

77. Wirojanupatump, S. (2000). Abrasion of mild steel in wet and dry conditions with the rubber and steel wheel abrasion apparatus. Wear, 239(1), 91-101.

78. Zhang, G.A., Xu, L.Y & Cheng, Y.F. (2009). Investigation of erosion-corrosion of 3003 aluminum alloy in ethylene glycol-water solution by impingement jet system. Corrosion science, 283-290.

79. Zhang, Y., Reuterfors, B.S., McLaury, S.A., Shirazi, E.F. Rybicki. (2007). Comparison of computed and measured particle velocities and erosion in water and air flows. Wear, 263, 330-338.

Appendix I: Wet G65 Design

This appendix provides the CAD drawings for the development of the Wet G65 experimental apparatus.

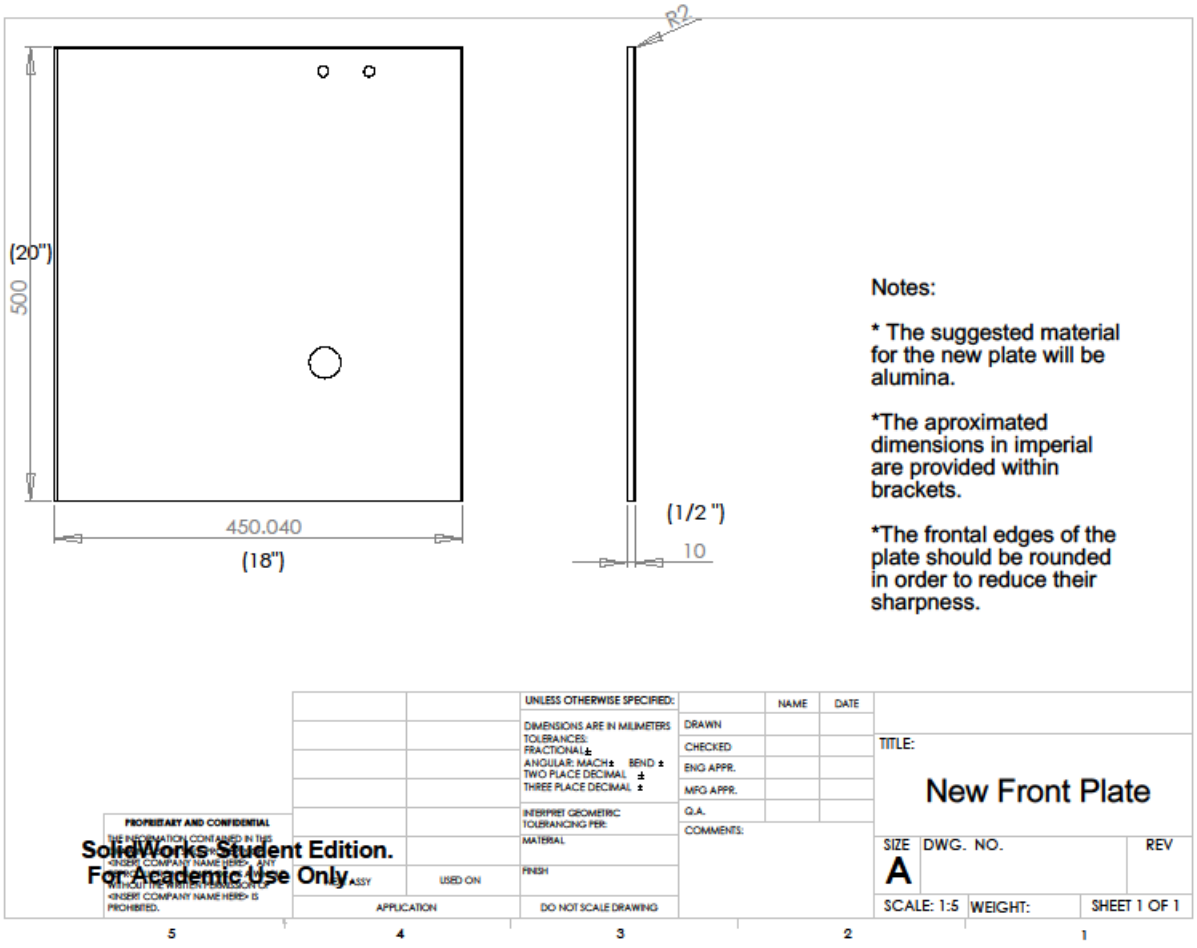

Figure 36 -The Wet G65 apparatus (front plate)

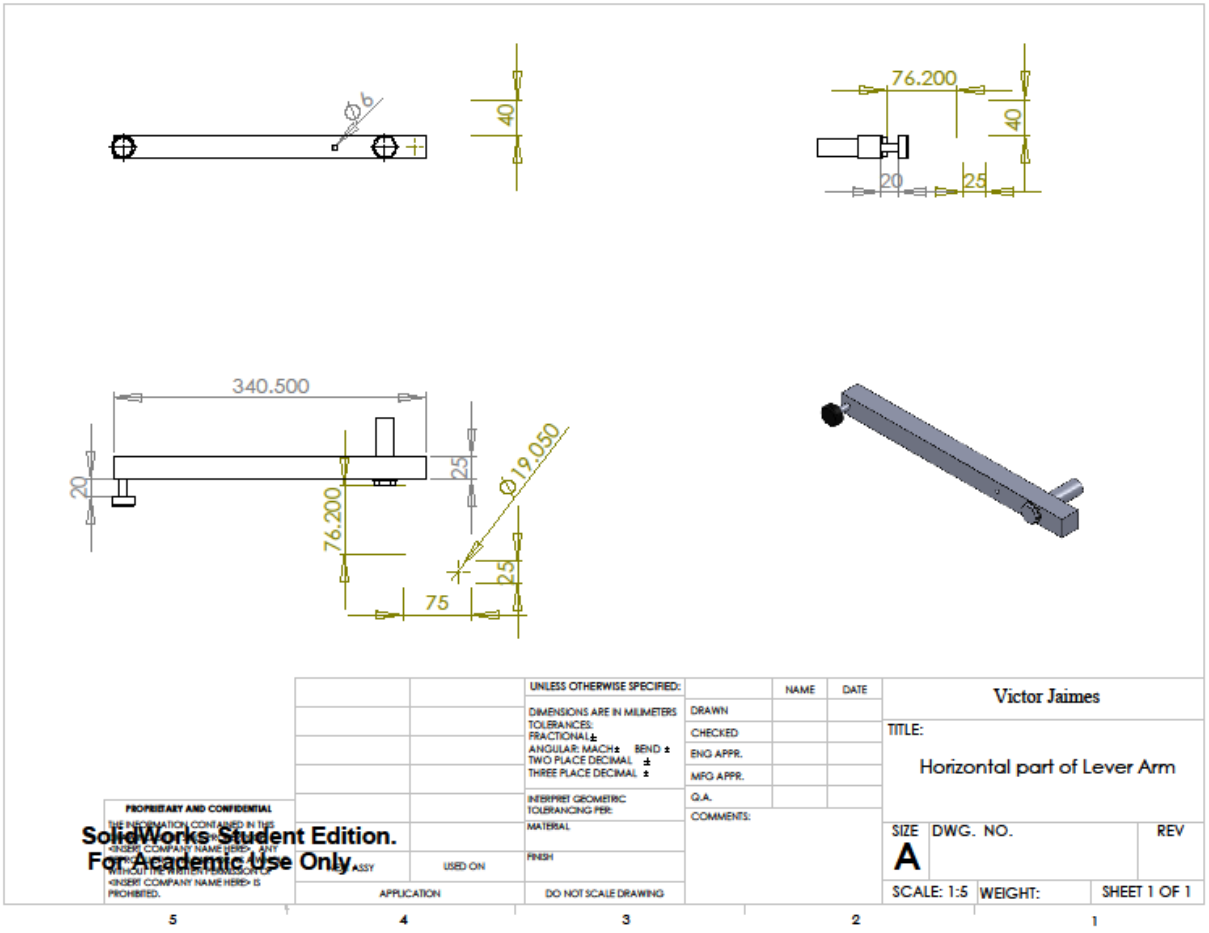

Figure 37 - The Wet G65 apparatus (horizontal component of lever arm)

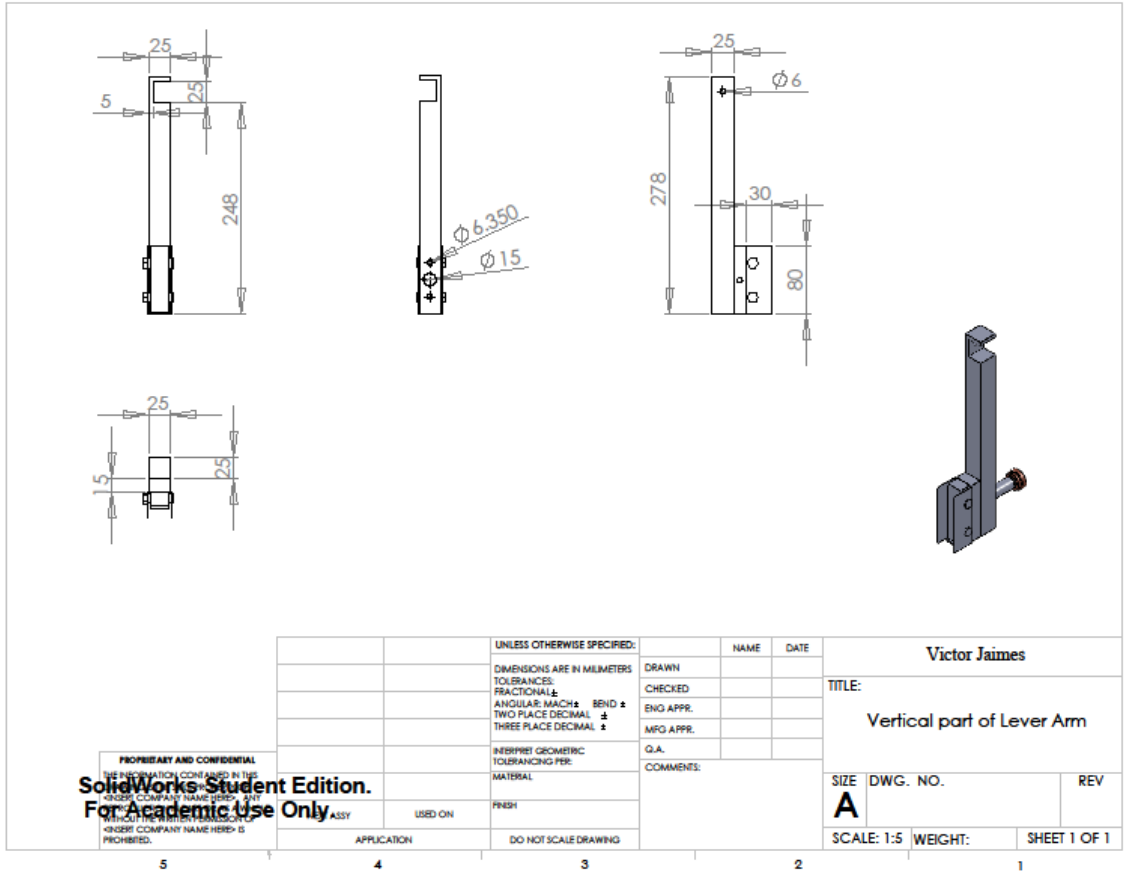

Figure 38 - The Wet G65 apparatus (vertical component of lever arm)

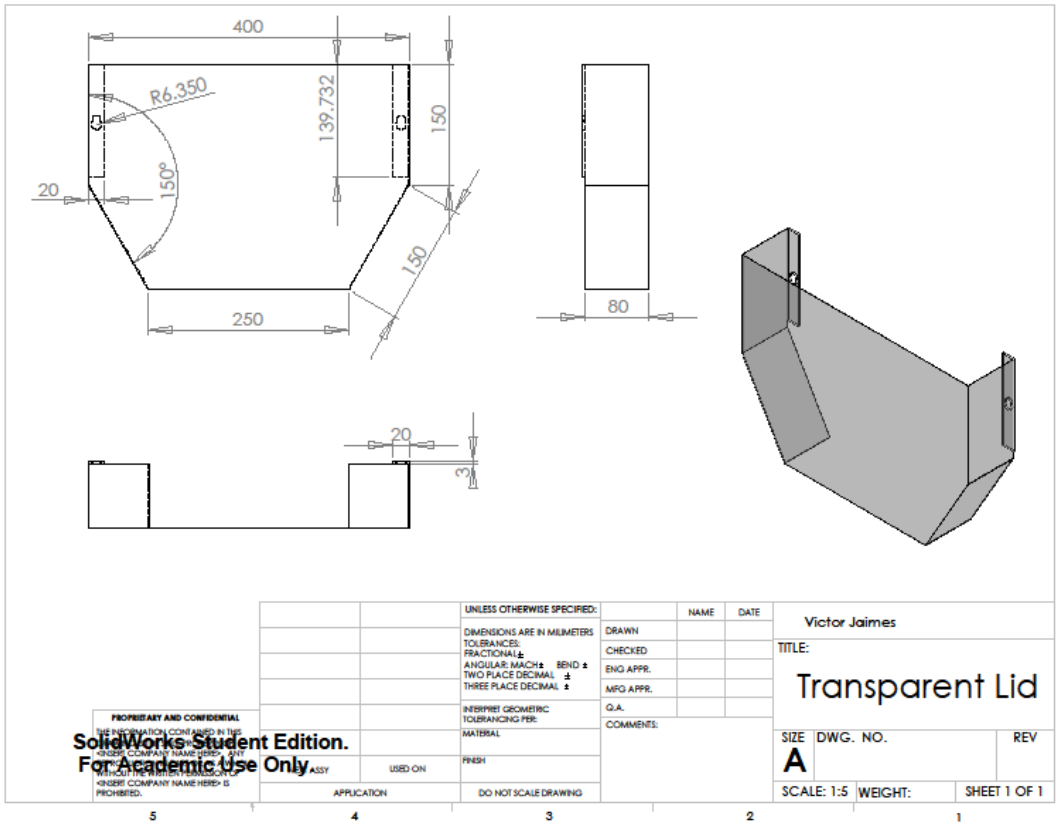

Figure 39 -The Wet G65 apparatus (transparent cover lid)

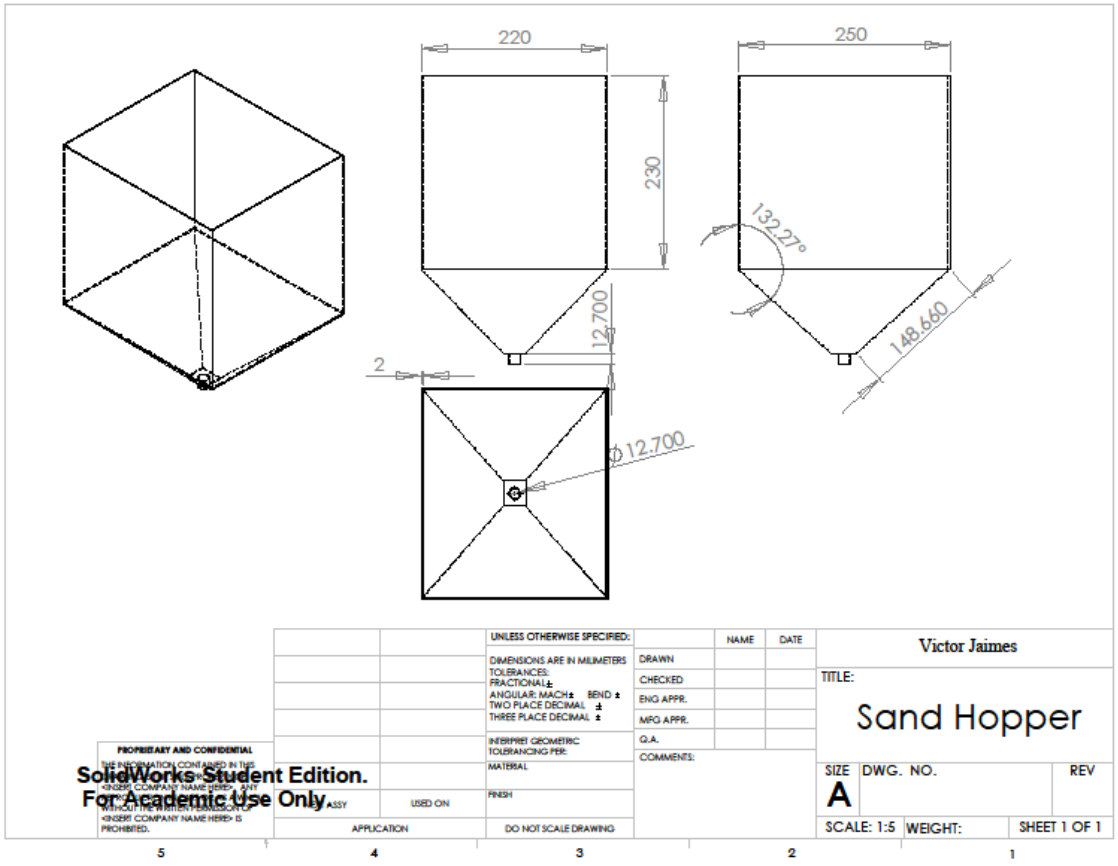

Figure 40 - The Wet G65 apparatus (sand hopper)

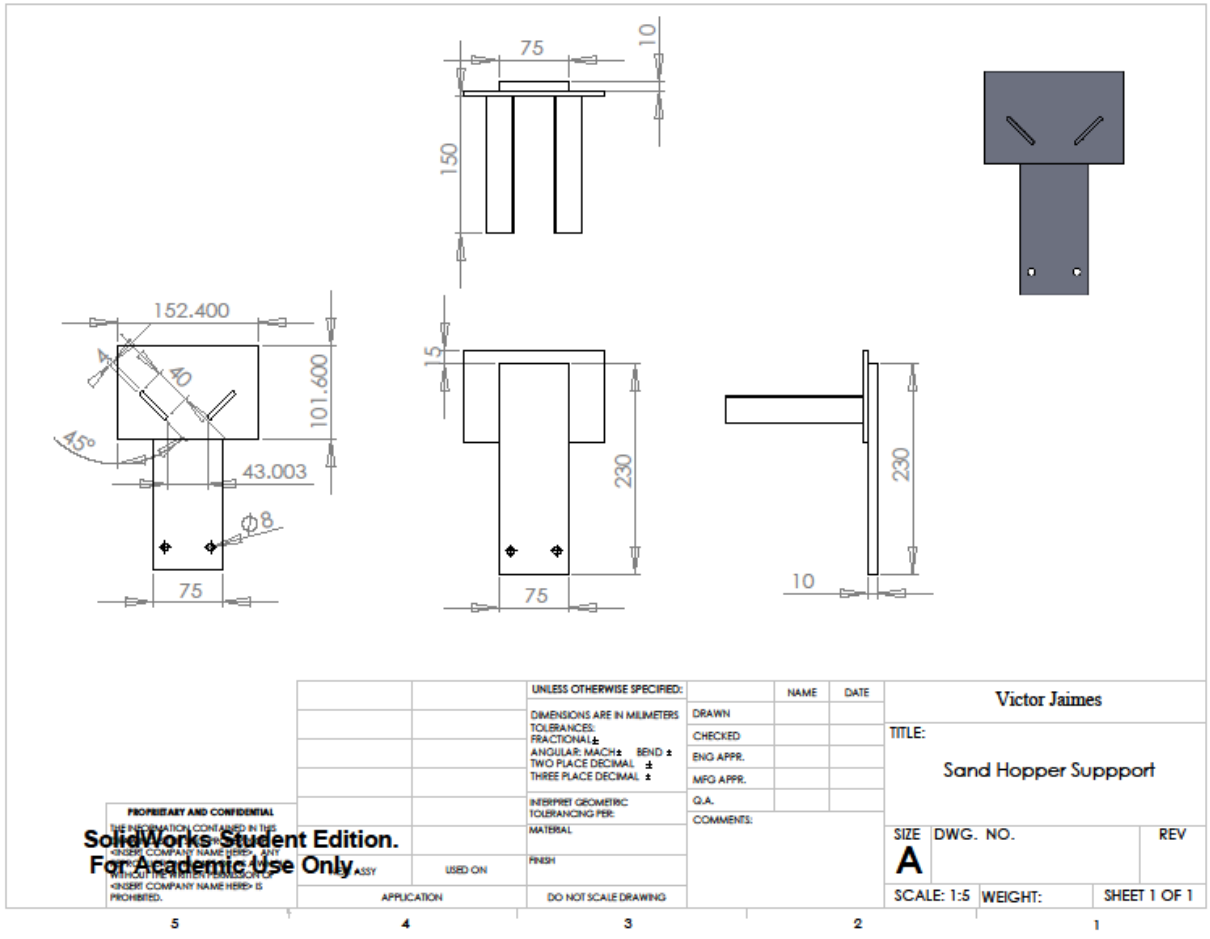

Figure 41 - The Wet G65 apparatus (sand hopper support)

Appendix II: Slurry Pipeline Loop Design

This appendix provides design calculations and considerations taken in the development of the slurry pipeline loop apparatus.

Design Calculations and Assumptions

The slurry pipeline loop was designed and built according to the space availability constraints (laboratory room with 32.48 m^2 area), pipeline diameter of 2 inches (50.8 mm) permissible for simulating a two layer model slurry in the loop for the length of 21 m of pipe, and the rheological parameters that define the slurry transport system behavior.

The carrying fluid of the slurry pipeline loop will be normal tap water at ambient temperature. However, according to the energy dissipated within the system, it is expected to have water circulating at around a temperature of 40C. The rheological characteristics of water of interest for this project are shown in table 7.

Table 7 – Water properties

(Source: Wilson 2006)

Temperature (C)	Density (kg/m^3) ρ	Viscosity μ x 10^{-3} (Pa.s)
40	992.2	0.653

The solids in the slurry system are defined as silica sand Sil 4 medium coarseness. This is blasting sand with sub angular grain shape, hardness of 6.5 in Mohr's scale, and a particle size distribution of 40-50 US Mesh size (420 to 297 microns). The correspondent particle size analysis for this type of sand is shown in table 8:

Table 8 – Particle size distribution from silica sand sample (Sil4)

Diameter (mm)	**Weight % (Cw)**	**Cvi**	**Cdi**
1.190	0.0	0.00	**$1.24*10^{-4}$**
0.840	0.3	0.00	
0.590	5.0	0.02	
0.420	51.1	0.24	
0.297	38.9	0.18	
0.250	3.6	0.02	
0.177	0.8	0.00	
0.074	0.3	0.00	
0.479	**100.0**	**0.06**	

In the above table, the sand particle size distribution is presented for the different types of particles sizes, its correspondents percentages in the sample of sand, the volume fractions per particle size (Cvi) and the average drag coefficient value (Cdi) for the range of pipeline velocities that are considered in the slurry pipeline system (see table 9).

The pipeline system was built of carbon steel 2 inches diameter (inner diameter of 52.57 mm), schedule 40 standard.

Slurry System Calculations

In order to determine the system's curve and size the centrifugal pump for the experimental loop, the following initial assumptions were made:

-2 inches steel schedule 40 pipe inner diameter = 2.07 inches (52.57 mm)

-Minimum slurry velocity is determined according to the deposition velocity in order to avoid blockages within the system

-Concentration of solids by weight of 30%.

-Relative roughness for steel pipe of 0.045 mm.

-Density of sand = 2,650 kg/m^3

-Concentration of solids by weight = 30%

-Average sand particles diameter = 0.47975 mm

-Water is assumed to be circulating at 40C while the system is in operation.

Following the methodology described in the Saskatchewan Research Council slurry pipeline course for heterogeneous flows setting slurries, the deposition velocity was calculated for the type of sand previously describe according to the following formula:

Deposition Velocity:

$$Vc = FL\left[2gD(S-1)\right]^{0.5} \qquad (8)$$

where:

S = (ρ s/ ρ l)

Vc = deposition velocity

D = pipeline inner diameter

FL = Froude number

g = gravity acceleration

$$FL = \frac{F}{\sqrt{2}} \qquad (9)$$

where:

$$F = aAr^{b} \qquad (10)$$

And:

$$Ar = \frac{4gd^3 \rho s(\rho s - \rho f)}{3\mu f^2} \qquad (11)$$

If:

Ar > 540: a = 1.78; b = -0.019

160 < Ar > 540: a = 1.19; b = 0.045

80 < Ar > 160: a = 0.197; b = 0.4

Deposition velocity calculation:

$$Ar = \frac{4 * 9.81 * (0.00047975)^3 * 992.2 * (2650 - 992.2)}{3 * (0.653x10^{-3})^2} = 5{,}571.31 \qquad (12)$$

$$F = (1.78) * (5571.31)^{-0.019} = 1.51 \qquad (13)$$

$$FL = \frac{1.51}{\sqrt{2}} = 1.06 \qquad (14)$$

$$Vc = 1.06 * \left[2 * 9.81 * 0.052578 * (2.67 - 1)\right]^{0.5} = 1.39 \frac{m}{s} \qquad (15)$$

Reynolds Number:

$$\mathrm{Re} = \frac{VD\rho}{\mu} = \frac{1.56 * 0.052578 * 992.2}{0.653x10^{-3}} = 1.25 * 10^5 \qquad (16)$$

The Reynolds number was calculated for all the rest of velocities considered in the pipeline system (see table 9).

Churchill's Equation:

By using this set of equations, the Darcy-Weisbach friction factor is calculated for each velocity considered in the pipeline system.

$$f = 8\left[\left(\frac{8}{\mathrm{Re}}\right)^{12} + (A+B)^{-1.5}\right]^{1/12} \qquad (17)$$

where:

$$A = \left(-2.457 Ln\left[\left(\frac{7}{\mathrm{Re}}\right)^{0.9} + 0.27(rr)\right]\right)^{16} \qquad (18)$$

$$rr = \frac{k}{D} \qquad (19)$$

$$B = \left(\frac{37530}{\mathrm{Re}}\right)^{16} \qquad (20)$$

Drag Coefficient for Turbulent Flows: (Reynolds number greater than 1000)

$$C_D \, \mathrm{Re}^2 = \frac{4gD^3(\rho s - \rho l)}{3\mu^2 gc^2} \quad (21)$$

Note: gc is a unit multiplication factor equal to $32.2 lbm * ft / lbf * s^2$ but it is assumed to be 1 for SI units.

Density of the slurry:

Assuming the initial values for water and sand densities, and the concentration of the sand-water mixture, the density of the slurry was calculated as follows:

$$\rho m = \frac{100}{Cw/\rho s + (100 - Cw)/\rho l} = \frac{100}{30/2650 + (100-30)/992.2} = 1221.43 \frac{Kg}{m^3}$$

(A-22)

Volume fraction of solids in the Slurry:

$$Cv = Cw \frac{\rho m}{100 \rho s} = 30 \frac{1221.43}{100 * 2650} = 0.138 \quad (23)$$

Friction loss for water (iw): (Assuming that length of pipe is still unknown)

$$iw = f\frac{V^2}{D2g} \qquad (24)$$

The friction loss for water is calculated for each velocity of flow in the pipeline system (see table 9).

Friction loss for Heterogeneous Flow-Horizontal –Pipes:

$$\frac{i-iw}{iw} = 81\left[\frac{V^2}{(S-1)gD}\right]^{-1.5} CvC_D{}^{-0.75} \qquad (25)$$

Head calculated Through Bernoulli's Equation:

$$h = i + \frac{V^2}{2g} + \frac{P}{\rho g} \qquad (26)$$

where:

i = friction losses in the system.

P= pressure gradient

V = velocity of the flow

ρ = density of slurry

g = gravity acceleration

However, there are a couple of practical assumptions to take into account in our pipeline system:

a) It is assumed that only the losses within the system will come due to friction of the slurry with the pipe walls. Hence, pressure gradient in the system will be equal to cero.

b) There won't be a change in velocities between two points in the system, so our velocity term also will be cero.

As a consequence of the previous assumptions, the head of the system (H) will be equal to the friction losses of the slurry (i):

$$h = i + \cancel{\frac{V^2}{2g}} + \cancel{\frac{P}{\rho g}} \qquad (27)$$

Pump Power:

$$Wp = \frac{\rho Q h g}{\mathrm{n}\rho} \qquad (28)$$

where:

h = head

Q = flow rate

$\eta\rho$ = efficiency of the pump (It is assumed that the efficiency of the pump has a theoretical value of 60%)

ρ = density of the slurry

g = gravity acceleration

The average values for pipeline velocity and drag coefficient were calculated in table 9 at the bottom of their correspondent column, in order to facilitate the estimations of the system's curve average values and hence, determine the sizing of the centrifugal pump for the system.

All the parameters shown in table 9 were calculated using IS units and based on the previous mention methodology and calculations. However, the resulting head and slurry flow rate are shown in imperial units in the system curve in order to facilitate plotting of these values.

Table 9 - Slurry pipeline system parameters calculations

Slurry Flow Rate (Q) (m3/s)	Pipeline Velocity (m/s)	Re Number	A	B	Friction Factor (f)	Drag Coefficient C_D	Friction Loss of Water (iw)	Friction Loss of Slurry (i)	Head (H)	Pump Power (Wp)
0.0034	1.56	$1.25*10^{5}$	$3.85*10^{20}$	$4.57*10^{-9}$	0.0214	$4.76*10^{-4}$	0.0504	0.056	0.056	3.763
0.0046	2.10	$1.68*10^{5}$	$4.68*10^{20}$	$3.93*10^{-11}$	0.0209	$2.63*10^{-4}$	0.089	0.093	0.093	8.463
0.0055	2.53	$2.02*10^{5}$	$5.20*10^{20}$	$2*10^{-12}$	0.0206	$1.81*10^{-4}$	0.128	0.131	0.131	14.353
0.0064	2.95	$2.36*10^{5}$	$5.62*10^{20}$	$1.71*10^{-13}$	0.0204	$1.33*10^{-4}$	0.172	0.175	0.175	22.337
0.0073	3.37	$2.69*10^{5}$	$5.97*10^{20}$	$2.03*10^{-14}$	0.0202	$1.02*10^{-4}$	0.223	0.225	0.225	32.886
0.0082	3.79	$3.03*10^{5}$	$6.27*10^{20}$	$3.10*10^{-15}$	0.0201	$8.06*10^{-5}$	0.280	0.282	0.282	46.352
0.0091	4.21	$3.36*10^{5}$	$6.53*10^{20}$	$5.78*10^{-16}$	0.0200	$6.53*10^{-5}$	0.344	0.346	0.346	63.090
0.0101	4.63	$3.70*10^{5}$	$6.75*10^{20}$	$1.26*10^{-16}$	0.0199	$5.40*10^{-5}$	0.414	0.416	0.416	83.454
0.0110	5.05	$4.03*10^{5}$	$6.95*10^{20}$	$3.14*10^{-17}$	0.0199	$4.54*10^{-5}$	0.491	0.492	0.492	107.797
0.0119	5.47	$4.37*10^{5}$	$7.13*10^{20}$	$8.76*10^{-18}$	0.0198	$3.87*10^{-5}$	0.574	0.575	0.575	136.475
0.0128	5.89	$4.71*10^{5}$	$7.29*10^{20}$	$2.68*10^{-18}$	0.0197	$3.34*10^{-5}$	0.664	0.665	0.665	169.841
0.0183	8.42	$6.73*10^{5}$	$7.97*10^{20}$	$8.81*10^{-21}$	0.0195	$1.63*10^{-5}$	1.341	1.342	1.342	490.026
0.0090	**4.16**					**$1.24*10^{-4}$**				
143 gpm	**13.6 ft/s**									

Given all the values previously calculated in order to determine the system's pump power in table 9. Finally, the head of the system was calculated and compared to the slurry flow rate, in order to plot the system's curve. These values are shown in table 10.

Table 10 - Slurry flow rates and system's head calculations

Slurry flow Rate (Q) m^3/s	Slurry Flow Rate (Q) gpm	Head (h) m	Head (h) ft
0.0034	53.90	1.11	3.65
0.0046	73.00	1.86	6.10
0.0055	87.00	2.62	8.58
0.0064	101.00	3.49	11.46
0.0073	116.00	4.50	14.77
0.0082	130.00	5.64	18.51
0.0091	144.00	6.91	22.68
0.0101	160.00	8.31	27.28
0.0110	174.00	9.85	32.30
0.0119	189.00	11.51	37.76
0.0128	203.00	13.30	43.64
0.0183	290.00	26.84	88.07
0.0091	**143.408**	7.995	**26.233**

The bold values shown at the bottom of table 10 represent the average of flow rate and head for the designing point of the system plotted in the following graph as shown in figure 40.

As can be observed in the graph, the behavior of the slurry system is considerably stable, showing a gentle increase in head as long as the flow rate increments. This indicates that the system`s head performs in a steady manner,

changing gradually as long as the flow rate increases accordingly. However, when considering a jump in the flow rate, as appreciate it in the last value in the table, the head tends to increase in the same manner.

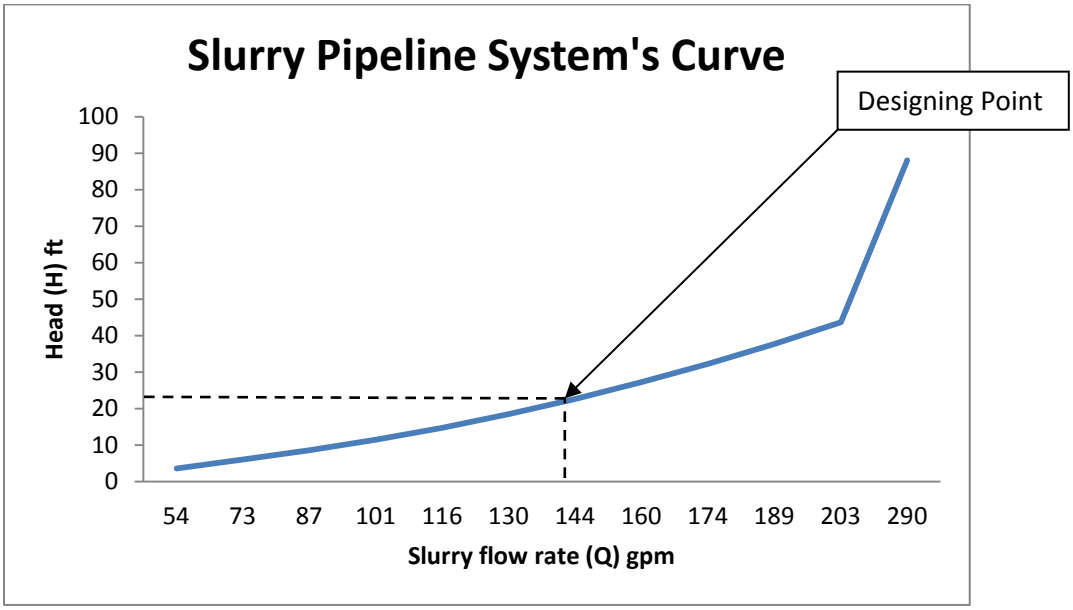

Figure 42 - Slurry pipeline system's curve

Based on all previous calculations and considerations the centrifugal pump was determined, taking in consideration the following:

A velocity of the bulk within the system between 1.5 and 8.4 m/s.

Capacity average flow rate around the 0.090 m^3/s of water (143 US gpm).

Specific gravity of 1.22

Head power average of 12 m of water (40 ft)

Solid concentration in slurry of 30% by weight

Following this reasoning and matching the pump performance graph provided by the supplier with the slurry system curve (see designing point in figure 40), a good option pump suggested for the system was a Tourus Recessed XR 2-7 with 3” x 2” and a 6.5” diameter impeller able to operate at 7.5 Hp and 1,800 rpm. Having a direct drive configuration and being able work properly in an abrasive medium.